UNIVERSITY OF NAPLES FEDERICO II
Department of Pharmacy

Ph.D. Thesis
26th Cycle

NON-PSYCHOTROPIC PHYTOCANNABINOIDS IN INTESTINAL INFLAMMATION AND COLON CANCER

Barbara Romano

TUTOR: Prof. Angelo A. Izzo

COORDINATOR : Prof. Maria V. D'Auria

Ph.D. Programme in Pharmaceutical Sciences 2011-2014

TABLE OF CONTENTS **Page**

ABBREVIATION LIST

2-AG	2-arachidonoylglycerol
5-HT$_{1A}$	5-hydroxytryptamine subtype 1A receptor
ACEA	arachidonyl-2'-chloroethylamide
ACF	aberrant crypt foci
AM251	N-(Piperidin-1-yl)-5-(4-iodophenyl)-1-(2,4-dichlorophenyl)-4-methyl-1H-pyrazole-3-carboxamide
AM630	6-Iodo-2-methyl-1-[2-(4-morpholinyl)ethyl]-1H-indol-3-yl](4-methoxyphenyl)methanone
AMTB	N-(3-Aminopropyl)-2-[(3-methylphenyl)methoxy]-N-(2-thienylmethyl)benzamide hydrochloride
AOM	azoxymethane
BSA	bovine serum albumin
CB$_1$	cannabinoid receptor type 1
CB$_2$	cannabinoid receptor type 2
CBC	cannabichromene
CBD	cannabidiol
CBD BDS	*Cannabis* extract with high content in cannabidiol
CBDA	cannabidiolic acid
CBDV	cannabidivarin
CBG	cannabigerol
CBN	cannabinol
CD	Crohn's disease
CHO	chinese hamster ovarian cells
CPM	count *per* minute
CRC	colorectal cancer
DAGL	diacylglycerol lipase
DAN	2,3-diaminonaphtalene
DCFH-DA	2′,7′-dichlorofluorescin diacetate
DMSO	dimethyl sulfoxide
DNBS	dinitrobenzenesulfonic acid
DTT	dithiothreitol
EDTA	ethylenediaminetetraacetic acid
EGTA	ethylene glycol tetraacetic acid
ELISA	enzyme-linked immunosorbent assay
FAAH	fatty acid amide hydrolase
FBS	foetal bovine serum
FITC	fluorescein isothiocyanate -conjugated dextran
GPR55	G protein-coupled receptor 55
H_2O_2	hydrogen peroxide
HBSS	Hanks' Balanced Salt solution
HCEC	human colonic epithelial cells
HEPES	(4-(2-hydroxyethyl)-1-piperazineethanesulfonic acid)
HPLC	high-performance liquid chromatography

HTAB	hexa-1,6-bisdecyltrimethylammonium bromide
IBD	inflammatory bowel disease
ICR	imprinting Control Region
IFN-γ	interferon- γ
IL-1β	interleukin-1β
IL-2	interleukin-2
IL-10	interleukin-10
IL-12	interleukin-12
ip	intraperitoneal administration
JWH133	(6aR,10aR)-3-(1,1-Dimethylbutyl)-6a,7,10,10a-tetrahydro-6,6,9-trimethyl-6H-dibenzo[b,d]pyran
LPS	lipopolysaccharide
MAGL	monoglyceride lipase
MAPK	mitogen-activated protein kinase
MOPS	3-(N-morpholino)propanesulfonic acid
MPO	myeloperoxidase
MTT	3-(4,5-dimethylthiazol- 2-yl)-2,5-diphenyltetrazolium bromide
NAPE-PLD	*N*-acyl-phosphatidylethanolamine selective phospholipase D
NaPP	sodium phosphate buffer
NBT	nitro blue tetrazolium
OEA	oleoylethanolamide
PBS	phosphate buffer saline
pCBs	phytocannabinoids
PEA	palmitoylethanolamide
PI3K	phosphoinositide3-kinase
PMSF	phenylmethanesulfonyl fluoride
PPARs	peroxisome proliferator-activated receptors
PPARγ	peroxisome proliferator-activated receptors type γ
SR 141716A	rimonabant hydrochloride
ROS	ontracellular reactive oxygen species
SDS	sodium dodecyl sulphate
SOD	superoxide dismutase
SR144528	5-(4-chloro-3-methylphenyl)-1-[(4-methylphenyl)methyl]-N-[(1S,2S, 4R)-1,3,3-trimethylbicyclo[2.2.1]hept-2-yl]-1H-pyrazole-3-carboxamide
THC BDS	*Cannabis* extract with high content in Δ^9-tetrahydrocannabinol
TNF-α	tumor necrosis factor-α
TRP	transient receptor potential
TRPA	transient receptor potential ankyrin
TRPA1	transient receptor potential ankyrin type 1
TRPC	transient receptor potential canonical
TRPM	transient receptor potential melastatin
TRPM8	transient receptor potential melastatin type 8
TRPML1	transient receptor potential mucolipin
TRPN	transient receptor potential NompC-like
TRPP	transient receptor potential polycistyn
TRPV	transient receptor potential vanilloid

TRPV1	transient receptor potential vanilloid type 1
UC	ulcerative colitis
Δ^9-THC	Δ^9-tetrahydrocannabinol
Δ^9-THCA	Δ^9-tetrahydrocannabinolic acid
Δ^9-THCV	Δ^9-tetrahydrocannabivarin

1.0 INTRODUCTION

1.1 Inflammatory bowel disease (IBD)

Inflammatory bowel disease (IBD) is a global healthcare problem with a sustained increasing incidence (Ko *et al.*, 2014) (Figure 1). Accumulating evidence suggests that IBD results from an inappropriate inflammatory response to intestinal microbes in a genetically susceptible host. Although the etiology of IBD remains largely unknown, recent research indicated that the individual genetic susceptibility, intestinal microbial flora and immune responses are all involved and functionally integrated in the pathogenesis of IBD (Danese and Fiocchi, 2006; Podolsky, 2002). It is of interest that in several countries with historically low rates of IBD, a pattern of rising incidence in the past one to two decades, particularly for Crohn's disease (CD), has occurred, suggesting that environmental factors are also involved (Ko *et al.*, 2014). The idiopathic inflammatory bowel diseases comprise two types of chronic intestinal disorders: Crohn's disease (CD) and ulcerative colitis (UC) which are distinct chronic bowel-relapsing inflammatory disorders. CD can cause transmural inflammation and affect any part of the gastrointestinal tract (most commonly, the terminal ileum or the perianal region) in a non-continuous type. Unlike UC, CD is commonly associated with complications such as abscesses, fistulas and strictures. In contrast, UC is typified by mucosal inflammation and limited to the colon (Abraham and Cho, 2009). While CD and UC involve different genetic vulnerabilities, pathological abnormalities, and different regions of involvement in the intestinal tract, both are characterized by gastrointestinal symptoms such as bloody diarrhea, weight loss, and abdominal pain, as well as extra-intestinal manifestations such as joint pain, uveitis, and erythema nodosum. Their etiologies are unknown, but they are characterized by an imbalanced production of pro-inflammatory mediators, *e.g.*, tumor necrosis factor (TNF)-α, as well as increased recruitment of leukocytes to the site of inflammation. Advantages in understanding

the role of the inflammatory pathways in IBD and an inadequate response to conventional therapy in a large portion of patients, has over the last two decades lead to new therapies which includes, for example, the TNF-α inhibitors, designed to target and neutralize the effect of TNF-α. However, convenient alternative therapeutics targeting other immune pathways are needed not only for patients with IBD refractory to conventional therapy, that traditionally includes steroids and 5-ASA treatments (Sewell *et al.*, 2010; Jones *et al.*, 2011) but even because, although these drugs may be effective, their long-term use can induce severe side effects that have detrimental impact on life quality of patients (Blonski *et al.*, 2011). For this purpose, experimental models have proven to be important tools for detecting potential therapeutic agents and for investigating the mechanisms of IBD pathogenesis.

In the present work, the experimental model of colitis induced by dinitrobenzenesulfonic acid (DNBS) has been used (Hibi *et al.*, 2002). Granulomas with infiltration of inflammatory cells in all layers were seen in the intestine of this model. The isolated macrophages produced large amounts of interleukin-12 (IL-12), and the lymphocytes produced large amounts of interferon-γ (IFN-γ) and interleukin-2 (IL-2). This evidence suggests that the colitis seen in this model was induced by a Th type-1 response (Neurath *et al.*, 1995). It has been noted that water absorption in the inflamed mucosa is markedly diminished in this model and this effect would be expected to contribute to the diarrhea that occurs not only in this animal model but also in human IBD. The DNBS model serves in clinical investigations for the development and testing of new therapeutic molecules that have the potential to enter into the clinic.

Finally, it is noteworthy that there is a link connection between IBD and colorectal cancer (CRC), highlighted by the observation that patients with IBD has an increased risk for CRC (Burisch and Munkholm, 2013). The risk is related to the duration and the anatomic extent of the disease (Ekbom *et al.*, 1990).

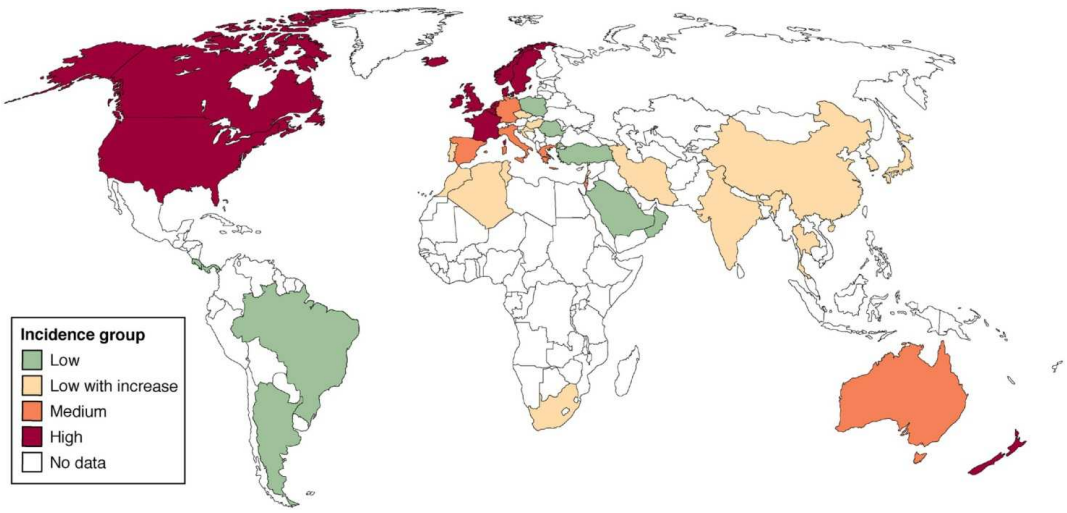

Figure 1. Epidemiology and Natural History of Inflammatory Bowel Diseases (IBD): the global map of IBD: red refers to annual incidence greater than $10/10^5$, orange to incidence of $5–10/10^5$, green to incidence less than $4/10^5$, yellow to low incidence that is continuously increasing. Absence of color indicates absence of data (**From:** Cosnes *et at., Gastroenterolgy* 2011;140:1785-1794).

1.2 Colorectal cancer (CRC)

Colorectal cancer (CRC) is an important health problem across the world. In Europe each year approximately 435,000 people are newly diagnosed with CRC (Ferlay *et al.,* 2008); about half of these patients die of the disease making CRC the second leading cause of cancer deaths in Europe. Similarly, in 2014, an estimated 136,830 new cases of CRC were diagnosed in the USA, with 50,310 estimated deaths (Siegel *at al.*, 2014) (Figure 2). CRC is thought to arise as the result of a series of histopathologic and molecular changes that transform normal colonic epithelial cells into a colorectal carcinoma, with aberrant crypt foci (ACF) and polyps as intermediate steps in this process (Markowitz and Bertagnolli, 2009). This multi-step process spans 10 to 15 years, thereby providing an opportunity for prevention (Half and Arber, 2009). Surgery is the cornerstone for cure in localized colorectal cancer (Sargent *et al.,* 2007). Chemotherapy after surgery (adjuvant chemotherapy, in high risk stage II and stage III CRC patients) *vs* surgery alone reduced the risk of cancer relapse (Cunningham *et al.*, 2010; Wolpin and Meyer, 2008). Drugs used in colorectal cancer chemotherapy include fluorouracil, irinotecan, oxaliplatin, angiogenesis inhibitors (i.e. bevacizumab) and epidermal growth factor receptor inhibitors (*i.e.* cetuximab and and panitumumab) (Wolpin and Meyer, 2008). Despite many progresses, and improvement of overall survival to nearly 2 years for non-resectable disease, cures for this kind of neoplasia remain unsatisfactory (Cunningham *et al.*, 2010). Also, the new chemotherapeutic agents (*i.e.* the biologicals cetuximab, panitumumab and bevacizumab) have not come without a significant cost to the health care system (Wolpin and Meyer, 2008).

In the present work we used to different models of colon cancer, *i.e* the azoxymethane (AOM) model, which is particularly appropriate for testing compounds with putative chemopreventive action and the xenograft model, which is used to verify possible curative (therapeutic) effects.

The AOM colon cancer model is extensively used in the study of the underlying mechanisms of human sporadic colon cancer. AOM is a potent carcinogen causing a high incidence of colon cancer in rodents. Development of this cancer closely mirrors the pattern seen in humans. Repetitive intra-peritoneal treatment of rodents with AOM causes tumours specifically in the distal colon. Following AOM treatment, the epithelial cells undergo pathogenesis from minor lesion ACF, to adenoma and malignant adenocarcinoma. The *in vivo* metabolite of AOM causes DNA mutations, changing the nucleotides from G:C to A:T. The duration of AOM-induced colon cancer takes 14 weeks in mice or rats (Takahashi and Wakabayashi, 2004). In the xenograft model, human tumor cells are implanted into recipient mice. To prevent xenograft rejection, nude mice are used, in which the *nu* gene is knocked out, resulting in hairless thymus-less mice which cannot generate T lymphocytes. The accessibility of these subcutaneous tumors is tremendous advantageous for monitoring tumor progression and for assessing the effects of therapeutic intervention (Voskoglou-Nomikos *et al.*, 2003).

Estimated New Cases*

Males				Females		
Prostate	233,000	27%		Breast	232,670	29%
Lung & bronchus	116,000	14%		Lung & bronchus	108,210	13%
Colorectum	71,830	8%		Colorectum	65,000	8%
Urinary bladder	56,390	7%		Uterine corpus	52,630	6%
Melanoma of the skin	43,890	5%		Thyroid	47,790	6%
Kidney & renal pelvis	39,140	5%		Non-Hodgkin lymphoma	32,530	4%
Non-Hodgkin lymphoma	38,270	4%		Melanoma of the skin	32,210	4%
Oral cavity & pharynx	30,220	4%		Kidney & renal pelvis	24,780	3%
Leukemia	30,100	4%		Pancreas	22,890	3%
Liver & intrahepatic bile duct	24,600	3%		Leukemia	22,280	3%
All Sites	**855,220**	**100%**		**All Sites**	**810,320**	**100%**

Estimated Deaths

Males				Females		
Lung & bronchus	86,930	28%		Lung & bronchus	72,330	26%
Prostate	29,480	10%		Breast	40,000	15%
Colorectum	26,270	8%		Colorectum	24,040	9%
Pancreas	20,170	7%		Pancreas	19,420	7%
Liver & intrahepatic bile duct	15,870	5%		Ovary	14,270	5%
Leukemia	14,040	5%		Leukemia	10,050	4%
Esophagus	12,450	4%		Uterine corpus	8,590	3%
Urinary bladder	11,170	4%		Non-Hodgkin lymphoma	8,520	3%
Non-Hodgkin lymphoma	10,470	3%		Liver & intrahepatic bile duct	7,130	3%
Kidney & renal pelvis	8,900	3%		Brain & other nervous system	6,230	2%
All Sites	**310,010**	**100%**		**All Sites**	**275,710**	**100%**

Figure 2. Ten Leading Cancer Types for the Estimated New Cancer Cases and Deaths by Sex, United States, 2014 (**From:** Siegel *et at., CA Cancer J Clin.* 2014;64:9-29)

1.3 *Cannabis sativa*

Cannabis sativa (Family: Cannabaceae) is an annual plant, that gets erect stems growing from 1 to 3 m or more high, very slightly branched, having greyish-green hairs. The leaves are palmate, with five to seven leaflets (three on the upper leaves), numerous, on long thin petioles with acute stipules at the base, linear-lanceolate, tapering at both ends, the margins sharply serrate, smooth and dark green on the upper surface, lighter and downy on the under one. The small flowers are unisexual, the male having five almost separate, downy, pale yellowish segments, and the female a single, hairy, glandular, five-veined leaf enclosing the ovary in a sheath. The ovary is smooth, one-celled, with one hanging ovule and two long, hairy thread-like stigmas extending beyond the flower for more than its own length. The fruit is small, smooth, light brownish-grey in colour, and completely filled by the seed (Quimby, 1974) (Figure 3). *Cannabis* has a long history of use both as a medicine and as a recreational drug, the written records of its use span more than five millennia. During the last century C*annabis* moved from being a frequently prescribed item for a variety of therapeutic conditions, through a period of increasing opposition to its use because of its potential for abuse, to the point where its use was completely withdrawn in the mid-twentieth century. Recently, there has been a resurgence of interest in *Cannabis* as a medicine for the treatment of conditions unresponsive to other types of therapy. In the last 20 years an increasing number of patients with severely debilitating diseases such as multiple sclerosis have used it to obtain relief.

Figure 3. *Cannabis sativa*, leaves

1.4 Phytocannabinoids

The limitation of the therapeutic utility of *Cannabi*s is its assigned psychoactive effects. *Cannabis sativa* produces over 421 chemical compounds, including about 100 terpeno-phenol compounds named phytocannabinoids (pCBs) that have not been detected in any other plant. pCBs are lipid-soluble chemicals present in the resin secreted from trichomes that are abundantly produced by female plants of the *Cannabis sativa* herb (Hill *et al.*, 2012). The plant can be genetically manipulated to alter the relative *ratios* of the pCBs produced and this approach has been successfully used to develop a legitimate medicinal product. Thus, it is possible to use solely horticultural techniques to produce cloned plants which are uniformly enriched in different, specific pCB and/or to transform a raw material into a botanical drug substance as an active pharmaceutical ingredient, which can then be formulated into a botanical drug product (de Meijer *et al.*, 2003).

Historically, among the phytocannabinoids, most attention has been paid to Δ^9-tetrahydrocannabinol (Δ^9-THC), which is the most psychotropic component and binds specific G protein-coupled receptors named cannabinoid (CB_1 and CB_2) receptors. The discovery of a specific cell membrane receptor for Δ^9-THC was followed by isolation and identification of endogenous (animal) ligands termed endocannabinoids. The two main endocannabinoids are anandamide [which is metabolized mostly by fatty acid amide hydrolase (FAAH)] and 2-arachidonoylglycerol (2-AG which is mostly degraded by monoglyceride lipase (MAGL)]. Cannabinoid receptors, endogenous ligands that activate them, and the mechanisms for endocannabinoid biosynthesis and inactivation constitute the ‘‘endocannabinoid system’’. With its ability to modulate several physiological and pathophysiological processes the endocannabinoid system represents a potential target for pharmacotherapy (Di Marzo, 2008).

In addition to pharmacological modulation of the endocannabinoid system, a different approach to minimize the well-known psychotropic side effects of *Cannabis* is the use of pCBs with very

weak or no psychotropic effects. These include cannabidiol (CBD), cannabigerol (CBG), cannabichromene (CBC), Δ^9-tetrahydrocannabivarin (Δ^9-THCV), cannabidivarin (CBDV) as well as cannabinoid acids such as Δ^9-tetrahydrocannabinolic acid (Δ^9-THCA) and cannabidiolic acid (CBDA) (Figure 4). These compounds exert multiple actions through mechanisms which are only partially related to modulation of the endocannabinoid system (Izzo *et al.*, 2009).

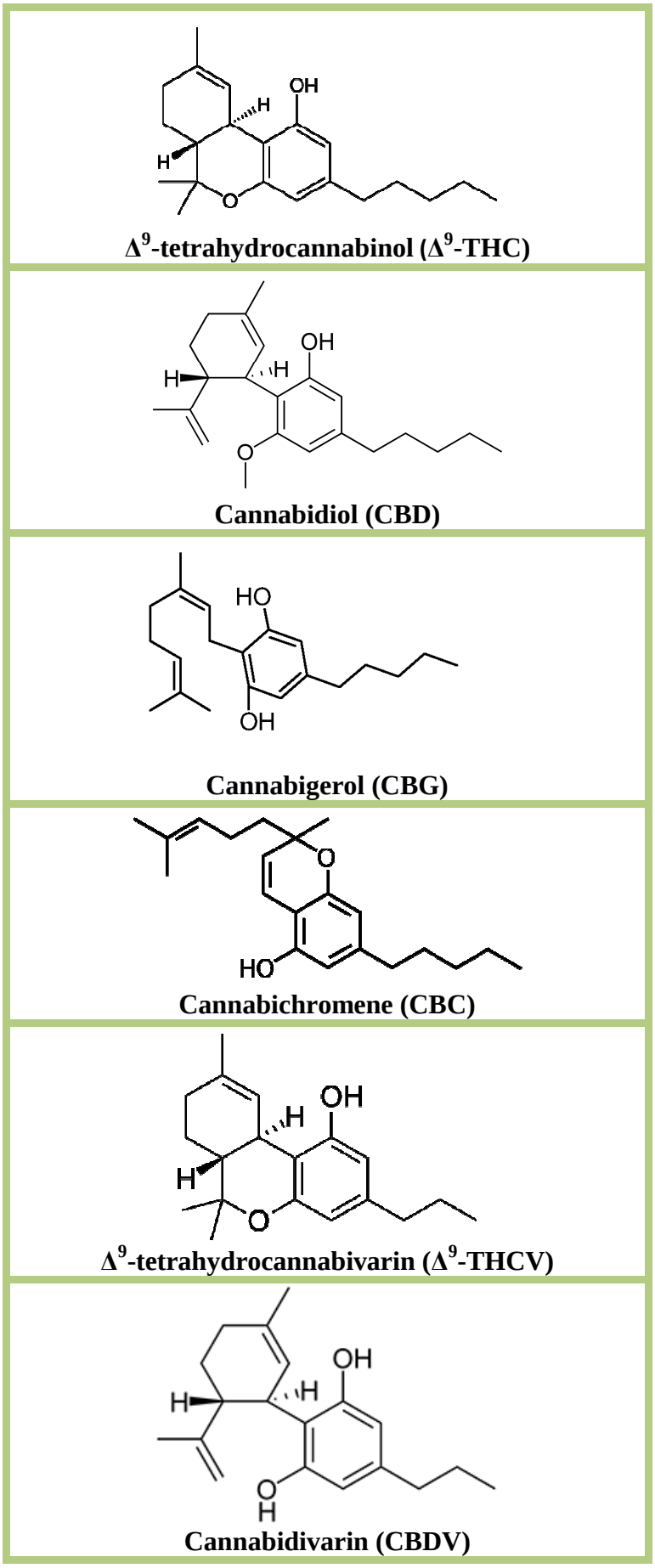

Figure 4. Chemical structures of the principals phytocannabinoids

1.4.1 Targets involved in the pharmacological action of phytocannabinoids

The main targets involved in the pCBs actions include:

The endogenous cannabinoid system: The endogenous cannabinoid system include two $G_{i/o}$ coupled membrane receptors, named CB_1 and CB_2 receptors, the endogenous ligands that activate them (*i.e.* the endocannabinoids, anandamide and 2-AG) and the proteins involved in endocannabinoid synthesis and inactivation. Endocannabinoids are biosynthesized '*on demand*' from membrane phospholipids by the action of a number of enzymes including *N*-acyl-phosphatidylethanolamine selective phospholipase D (NAPE-PLD, involved in anandamide biosynthesis) and diacylglycerol lipase (DAGL, involved in 2-AG biosynthesis), and are inactivated through a reuptake process (facilitated by a putative endocannabinoid membrane transporter), followed by enzymatic degradation catalysed by the fatty acid amide hydrolase (FAAH, in the case of anandamide and, to some extent, 2-AG) or monoacylglycerol lipase (MAGL, in the case of 2-AG) (Di Marzo, 2008).

Transient receptor potential (TRP) channels:

Transient receptor potential (TRP) channels form a large superfamily of ion channels that are important in several pathophysiological processes, which include (but are not limited to) pain, inflammation, airways hypersensitivity, cardiac hypertrophy and cell death. TRP channels have been subdivided into seven subgroups according to their sequence homology: TRP canonical (TRPC), TRP vanilloid (TRPV), TRP melastatin (TRPM), TRP mucolipin (TRPML1), TRP polycystin (TRPP), TRP ankyrin (TRPA) and TRP NompC-like (TRPN) transmembrane proteins (Kaneko and Szallasi, 2013)

Adenosine uptake: Uptake of adenosine is a primary mechanism of terminating adenosine signalling. Adenosine is a multifunctional, ubiquitous molecule that activate four known

adenosine receptors (A1, A2A, A2B and A3). Adenosine A2A receptor is an important regulator of inflammation (Izzo *et al.*, 2009).

G protein-coupled receptor 55 (GPR55): GPR55 is an orphan G-protein-coupled receptor originally identified in silico from the expressed sequence tags database. GPR55 may be activated by plant and synthetic endocannabinoids as well as by anandamide-related acylethanolamides and may be antagonized by cannabidiol (Izzo *et al.*, 2009).

Peroxisome proliferator-activated receptors (PPARs): Peroxisome proliferators- activated receptors (PPARs) belong to a family of nuclear receptors comprising three isoforms: α, β and γ. Among these, PPARγ is involved in the regulation of cellular glucose uptake, protection against atherosclerosis and control of immune reactions. Activation of PPARγ attenuates neurodegenerative and inflammatory processes (Izzo *et al.*, 2009).

5-hydroxytryptamine subtype 1A receptor (5-HT_{1A}): The 5-HT_{1A} receptor is one of the best-characterized 5-HT receptors. This G protein-coupled receptor is involved a number of physiological or pathophysiological processes, including anxiety, mood, depression, vasoreactive headache, food intake, immune regulation, and cardiovascular regulation (Izzo *et al.*, 2009).

The pCBs investigated in the present work are: cannabidiol (CBD), a *Cannabis* extract with high content in CBD (named CBD BDS, i.e. CBD botanical drug substance), cannabigerol (CBG), cannabichromene (CBC) and Δ^9-tetrahydrocannabivarin (THCV).

1.4.2 Cannabigerol (CBG)

CBG is a non-psychotropic cannabinoid obtained in 1964 by Gaoni and Mechoulam when they separated a hexane extract of hashish on Florisil (Izzo *et al.*, 2009). CBG appears as a relatively low concentration intermediate in the plant, although recent breeding works have yielded *Cannabis* chemotypes expressing 100% of their phytocannabinoid content as CBG (de Meijer

and Hammond, 2005; de Meijer *et al*., 2009). Older and recent studies support analgesic, anti-erythemic, antibacterial, antidepressant and antihyptertensive actions for this phytocannabinoid (Evans, 1991; Russo, 2011). Relevant for the present work, CBG has been proved to be cytotoxic in high dosage on human epithelioid carcinoma cells (Baek *et al*., 1998), to be effective against breast cancer (Ligresti *et al*., 2006) and to inhibit keratinocyte proliferation (Wilkinson and Williamson, 2007). Pharmacodynamic studies have shown that CBG interacts with receptors/enzymes involved both in inflammation and in carcinogenesis. Specifically, CBG is a weak partial agonist of CB_1 and CB_2 receptors (Cascio *et al*., 2010), inhibits the reuptake of endocannabinoids (De Petrocellis *et al*., 2011), is a potent 5-HT_{1A} antagonist (Cascio *et al*., 2010) and may interact with TRP channels. Among the TRP channels, CBG has been shown to be a TRPA1, TRPV1 and TRPV2 agonist and, importantly, a potent TRPM8 antagonist (De Petrocellis *et al*., 2011).

1.4.3 Cannabichromene (CBC)

The discovery of CBC, a non-psychotropic cannabinoid, was independently reported by Claussen and coworkers, and Gaoni and Mechoulam in 1966 (Izzo *et al*., 2009). CBC is one of four major cannabinoids in *Cannabis sativa* and it is known to be abundant in high-grade drug-type marijuana, with little or no CBD (Holley *et al*., 1975). CBC represents 0.3% of the constituents from confiscated *Cannabis* preparations in the USA (Mehmedic *et al*., 2010). Despite the relative abundance of this phytocannabinoid, its pharmacological activity has been hardly at all investigated. Of relevance to the topic of the present study, CBC was shown to reduce carrageenan- and lipopolysaccharide (LPS)-induced paw oedema in rodents (Wirth *et al*., 1980; Turner and Elsohly, 1981; DeLong *et al*., 2010). Pharmacodynamic studies have shown that CBC is an inhibitor of endocannabinoid cellular reuptake (Ligresti *et al*., 2006), a weak inhibitor of MAGL (*i.e.* the main enzyme involved in the inactivation of the

endocannabinoid 2-AG) and a potent activator of transient receptor potential (TRP) ankyrin 1-type (TRPA1) channels (De Petrocellis *et al.*, 2008; De Petrocellis *et al.*, 2012). Both endocannabinoids and TRPA1 are known to be involved in inflammatory processes (Burstein and Zurier, 2009; McMahon and Wood, 2006).

1.4.4 Δ^9-Tetrahydrocannabivarin (THCV)

Δ^9-THCV, the n-propyl analogue of Δ^9-THC, was detected in 1970 by Edward Gil and colleagues from a tincture of *Cannabis* BPC (then a licensed medicine in the UK). It is particularly abundant in Pakistani hashish. Δ^9-THCV at low doses (<3 mg/kg) antagonizes Δ^9-THC effects and it shares the ability of synthetic CB_1 antagonists to reduce food intake in mice (Izzo *et al.*, 2009). THCV also behaves as CB_2 partial agonist and *via* this mechanism exerts anti-inflammatory actions (Bolognini *et al.*, 2010).

1.4.5 Cannabidiol (CBD)

CBD, a major non-psycotropic cannabinoid, was first isolated in 1940 by Adams and co-workers, but its structure and stereochemistry were determined in 1963 by Mechoulam and Shvo. CBD is the most common phytocannabinoid in fibre (hemp) plants.

CBD has an extremely safe profile in humans and exerts a number of pharmacological actions (*e.g.* analgesic/anti-inflammatory, antioxidant, neuroprotective) of potential clinical interest (Izzo *et al.*, 2009). Few studies have investigated the effect of CBD in the gut. Specifically, CBD has been shown to reduce intestinal contractility (Capasso *et al.*, 2008; Cluny *et al.*, 2011) and to exert anti-inflammatory effects (Borrelli *et al.*, 2009; Jamontt *et al.*, 2010). In addition, CBD may inhibit FAAH (De Petrocellis *et al.*, 2011) and exerts antioxidant action in colorectal carcinoma cell lines (Borrelli *et al.*, 2009). Both FAAH inhibition (Izzo *et al.*, 2008; Izzo and

Sharkey, 2010) and antioxidant effects (Klauning *et al.*, 2011) are potentially beneficial for gut diseases.

1.4.6 Cannabis-extract with high content in cannabidiol (CBD BDS)

Recent progress in plant biotechnology has made possible the cultivation of *Cannabis* chemotypes rich in specific pCBs, from which standardized extracts, containing known amounts of pCBs, may be obtained (Russo, 2011). The best studied among these extracts is generally referred as CBD botanical drug substance (CBD BDS, that is a standardized *Cannabis* extract with high content of CBD). CBD BDS is a main ingredient of a *Cannabis*-derived medicine (sold under the brand name Sativex) used for the treatment of pain and spasticity associated with multiple sclerosis. Sativex is composed primarily of a 1:1 *ratio* of two *Cannabis sativa* extracts, CBD BDS and a *Cannabis sativa* extract with high content of Δ^9-THC (THC BDS). It is noteworthy that actually Sativex holds a III trials programme in cancer pain, beyond its approval for multiple sclerosis spasticity. In several pharmacological assays, CBD BDS has been shown to be more potent or efficacious than pure CBD (Comelli *et al.*, 2008; Capasso *et al.*, 2011; Russo, 2011; De Petrocellis *et al.*, 2013), suggesting that additive or synergistic interactions can occur between CBD and minor pCBs (or the non-cannabinoid fraction) contained in the extract. This observation might be useful from a therapeutic viewpoint.

1.5 Cannabinoids and intestinal inflammation

Anecdotal reports suggesting a favourable impact of *Cannabis* use in IBD patients. Such reports have recently encountered scientific evidence in a number of published clinical trials in which the effect of *Cannabis* or THC has been evaluated in IBD patients (Lal *et al.*, 2011;

Naftali *et al.,* 2011; Lahat *et al*., 2012; Naftali *et al*. 2013). In Israel, inhaled *Cannabis* has been legally registered for palliative treatment of both CD and UC.

Several studies investigating the effects of cannabinoids in rodent models of intestinal inflammation have identified a potential therapeutic role for these compounds in the treatment of IBD (for review see Wright *et al*., 2008; Izzo and Camilleri, 2009; Alhouayek and Muccioli, 2012). Protective actions have been described for non-selective CB_1 and CB_2 selective receptor agonists, FAAH or MAGL inhibitors (Izzo and Sharkey, 2010). Furthermore, endocannabinoids regulates intestinal barrier function *in vivo* through CB_1 receptor activation (Zoppi *et al.,* 2012). Conversely, experimental inflammation is aggravated in mice genetically lacking CB_1 or CB_2 receptors or in mice treated with selective CB_1 or CB_2 receptor antagonists (Massa *et al.,* 2004; Engel *et al.,* 2010).

pCBs have been also investigated in experimental models of intestinal inflammation, both *in vitro* and *in vivo*. THC and CBD have been shown to be protective in experimental models of colitis (Borrelli *et al*., 2009; Jamontt *et al*., 2010; Schicho and Storr, 2012). Additionally, THC inhibited the expression of TNF-α-induced interleukin-release from the human colonic epithelial cells (Ihenetu *et al.,* 2003) and accelerated the recovery from EDTA- or cytokine-induced increased permeability in intestinal epithelial cells (Alhamoruni *et al.,* 2010; Alhamoruni *et al.,* 2012). Finally, CBD has been shown to exert anti-inflammatory effects in human colonic cultures derived from ulcerative colitis patients (De Filippis *et al.*, 2011).

1.6 Cannabinoids and colon cancer

In addition to their palliative effects on some cancer-associated symptoms, it is now well-established that cannabinoids exert direct antitumoural actions *via* CB receptor and non-CB

receptor mediated pathways in a broad spectrum of cancer types both *in vitro* and *in vivo* (Guzman, 2003; Hermanson and Marnett, 2011).

Concerning colon cancer, it has been demonstrated that cannabinoids exert antiproliferative, antimetastatic and pro-apoptotic actions in colorectal carcinoma epithelial cells (Ligresti *et al*., 2003; Greenhough *et al*., 2007; Cianchi *et al*., 2008; Wang *et al.*, 2008; Sreevalsan *et al*., 2011) as well as antitumoural effects in experimental models of colon cancer (Izzo *et al*., 2008; Cianchi *et al.,* 2008; Wang *et al.,* 2008). The antitumour actions of cannabinoids may be mediated by activation of CB_1, CB_2 or by non-cannabinoid-mediated mechanisms. The mechanism of CB_1 receptor-mediated apoptotic effects involves: i) inhibition of RAS–MAPK and PI3K–AKT pathways (Greenhough *et al.,* 2007); ii) down-regulation of the anti-apoptotic factor survivin, mediated by a cyclic AMP-dependent protein kinase A signalling pathway (Wang *et al.,* 2008); iii) stimulation of the *de novo* synthesis of the pro-apoptotic lipid mediator ceramide. The mechanism of CB_2-receptor-mediated antitumour action involves ceramide production, with TNF-α acting as a link between cannabinoid receptor activation and ceramide biosynthesis (Izzo and Camilleri, 2009). *In vivo*, cannabinoid receptor agonists – or inhibitors of endocannabinoids inactivation - have been shown to exert protective effects against colon carcinogenesis induced by the carcinogenic substance azoxymethane, by xenografts in nude mice as well as in *Apc* mice (Izzo *et al.,* 2008; Cianchi *et al.,* 2008; Wang *et al.,* 2008). Results suggest that cannabinoids might be protective at different stages of colon cancer progression either directly, through activation of CB_1 or CB_2 receptors, or indirectly, through elevation of endocannabinoid levels.

Ligresti and colleagues have specifically demonstrated that THC and other non-psychotropic phytocannabinoid reduced colorectal cancer (Caco-2) cells growth (Ligresti *et al.,* 2006). In a more complete study, THC was shown to induce apoptosis in a number of colorectal cancer

cell lines. The mechanism of cell death was believed to involve survival signalling pathways that are frequently deregulated in colorectal tumours, *i.e.* BAD activation via CB_1-dependent RAS-MAPK and PI3K-AKT pathway inhibition (Greenhough *et al.*, 2007). However, there is a paucity of data on the effect of phytocannabinoids in experimental model of colon cancer *in vivo*. Recently, cannabinoids with little or non-psychotropic action have been shown to exert beneficial effects in colon carcinogenesis. Specifically, i) the atypical cannabinoid O-1602 was shown to reduced tumour area and tumour incidence in colitis-associated colon cancer (Kargl *et al.*, 2013); ii) LYR-8, a hexahydrocannabinol analog, exerted anti-tumor effects in human colorectal xenografted tumours (Thapa *et al.*, 2012).

2.0 AIM

The aim of the present work has been to evaluate the effect and the mode of action of a number of *Cannabis*-derived non-psychotropic cannabinoids in experimental models of intestinal inflammation and colon cancer. These compounds include CBD, CBG, CBC and THCV. Additionally, a standardized *Cannabis* extract with high content of CBD (derived from a *Cannabis* chemotype rich in CBD) has been investigated. In order to unravel the potential anti-inflammatory and antitumoural actions of pCBs in the gut, the DNBS model of colitis, the AOM model of colon cancer and the experimental tumours generated by xenograft injection of colorectal cancer cells have been used. The possible mode of action of the pCBs has been evaluated in isolated peritoneal macrophages (to investigate the anti-inflammatory effect) and in colorectal cancer cells (to assess possible antiproliferative, apoptotic and genoprotective actions).

3.0 MATERIALS AND METHODS

3.1 Drugs and reagents

Cannabichromene (CBC), [purity by high-performance liquid chromatography (HPLC): 96.3%]; cannabidiol (CBD) [purity by HPLC: 99.76%]; *Cannabis* sativa extract with a 65.6% w/w of CBD content [here named CBD botanical drug substance (CBD BDS), (see HPLC chromatogram in Figure 5 and composition in Table 1) was prepared as described below (see subheading "plant Material and extraction"); cannabidivarin (CBDV), (purity by HPLC; 95.0 %); cannabigerol (CBG) [purity by HPLC: 99.0 %]; tetrahydrocannabivarin (THCV) [purity by HPLC: 95.0%] were kindly supplied by GW Pharmaceuticals (Porton Down, Wiltshire, UK). The concentrations (or doses) of CBD BDS reported in the present thesis indicated the amount of CBD contained in the extract (*e.g.*, 1 µmol of CBD BDS contained 1 µmol of CBD). Rimonabant and SR144528 were supplied by SANOFI Recherche, (Montpellier, France).

ACEA, AMTB, AM251, AM630, capsazepine and JWH133 were purchased from Tocris (Bristol, UK).

Azoxymethane (AOM), cadmium, 2,3-iaminonaphtalene (DAN), 2′,7′-dichlorofluorescin diacetate (DCFH-DA), dinitrobenzene sulphonic acid (DNBS), fluorescein isothiocyanate (FITC)-conjugated dextran (molecular mass 3-5 kDa), hydrogen peroxide (H_2O_2), lipopolysaccharide (LPS, from Escherichia coli serotype O111:B4), myeloperoxidase (MPO) from human leucocytes, 3-(4,5-dimethylthiazol- 2-yl)-2,5-diphenyltetrazolium bromide (MTT), neutral red solution, ruthenium red, spermine, thioglycollate medium were purchase from Sigma (Milan, Italy).

Matrigel™ was obtained from BD Biosciences (Buccinasco, Milan, Italy).

All reagents for cell culture and western blot analysis were obtained from Sigma Aldrich S.r.l. (Milan, Italy), Amersham Biosciences Inc. (UK), Bio-Rad Laboratories (USA) and Microtech S.r.l. (Naples, Italy). Methyl-[^{3}H]-thymidine was purchased from PerkinElmer (Monza, Italy). For radioligand binding experiments, [^{35}S]GTPγS (1250 Ci/mmol) and [^{3}H]CP55940 (160 Ci/mmol) were obtained from PerkinElmer Life Sciences (Boston, MA), GTPγS from Roche Diagnostic (Indianapolis, IN), GDP from Sigma-Aldrich (UK).

The vehicle used for drugs dissolving for *in vivo* experiments was constituted by 10% (v/v) ethanol, 10% (v/v) Tween-20, 80% (v/v) saline, [2 ml/kg, intraperitoneally (*ip*); DNBS was dissolved in 50% ethanol (0.15 ml/mouse, intrarectally).

All the drugs used for *in vitro* experiments were dissolved in DMSO (0.01% DMSO v/v in cell media) and in the radioligand binding assays with hCB_1/hCB_2 CHO cells (0.1% DMSO v/v) had no effect on measured response.

Only CBC was dissolved in ethanol (for *in vitro* experiments), in DMSO (for radioligand assays) and its vehicles (0.01% ethanol *in vitro*; 0.1% DMSO for radioligand assays) had no significant effects on the responses under study.

Plant material and extraction

A *Cannabis sativa* chemotype cloned to have a controlled high amount of CBD was used (de Meijer *et al.*, 2003). *Cannabis sativa* was grown in highly secure computer-controlled glasshouses. All aspects of the growing climate, including temperature, air change and photoperiod, were computer-controlled and the plants were grown without the use of pesticides (see details at http://www.gwpharma.com). *Cannabis* dry flowers and leaves were extracted at room temperature with CO_2 to give an extract which, evaporated to dryness, was a brownish solid. A portion of the extract was dissolved in methanol for HPLC analysis (Agilent 1100)

using a C18 column (150 x 4.6 mm, 1 ml/min flow rate). HPLC chromatogram and composition of the main cannabinoids are reported in Figure 5 and Table 1, respectively.

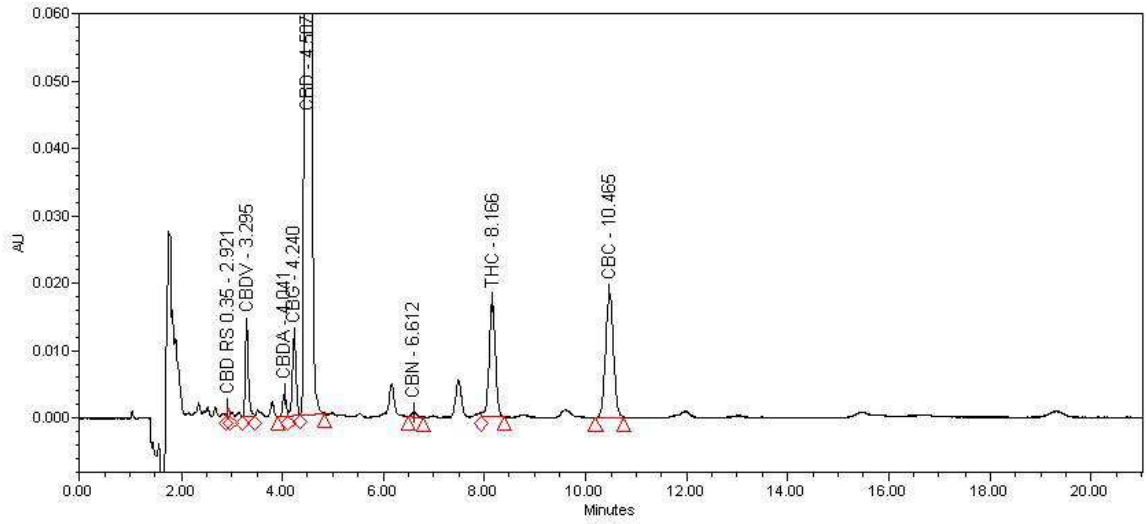

Figure 5. HPLC chromatogram of *Cannabis sativa* CO_2 extract. Retention time for cannabidiol (CBD) and the other phytocannabinoids [cannabidivarin (CBDV), cannabidiolic acid (CBDA), cannabinol (CBN), Δ^9-tetrahydrocannabinol (THC) and cannabichromene (CBC)] are indicated.

Table 1. Content of the main phytocannabinoids contained in *Cannabis*-extract with high content in cannabidiol (CBD BDS).

PHYTOCANNABINOID	CONTENT (% w/w)
Cannabidiol (CBD)	**65.9**
Δ^9-tetrahydrocannabinol	**2.4%**
Cannabigerol	**1.0%**
Cannabidivarin	**0.9%**
Cannabidiolic acid	**0.3%**
Cannabinol	**0.1%**

3.2 *In vivo* studies

3.2.1 Animals

For colorectal cancer azoxymethane (AOM) model, for dinitrobenzene sulphonic acid (DNBS)-induced colitis model and thioglycollate-elicitation mouse peritoneal macrophages experiments, male ICR mice, weighing 28–32 g, were used after 1-week acclimation period (temperature 23±2°C and humidity 60%). Mice were fed *ad libitum* with standard food, except for the 24-h period immediately preceding the administration of DNBS.

For colorectal cancer xenograft model athymic female mice were used, fed *ad libitum* with sterile mouse food and maintained under pathogen-free conditions. All the animals used were purchased from Harlan Laboratories (S. Pietro al Natisone, Italy).

All animal procedures were in conformity with the principles of laboratory animal care (NIH publication no.86–23, revised 1985) and the Italian D.L. no.116 of January 27, 1992 and associated guidelines in the European Communities Council Directive of November 24, 1986 (86/609/ECC).

3.2.2 Colorectal cancer azoxymethane (AOM) model

AOM (40 mg/kg in total, *ip*) was administered, at the single dose of 10 mg/kg, at the beginning of the first, second, third and fourth week. The phytocannabinoids (CBD 1 and 5 mg/kg, CBD BDS 5 mg/kg and CBG 1 and 5 mg/kg) were given (*ip*) three times a week starting one week before the first administration of AOM. All animals were euthanized by asphyxiation with CO_2 three months after the first injection of AOM. Based on our laboratory experience, this time (at the dose of AOM used) was associated with the occurrence of a significant number of aberrant crypt foci (ACF, which are considered pre-neoplastic lesions), polyps and tumours (Izzo *et al.*, 2008).

For ACF, polyps and tumours determination, the colons were rapidly removed after sacrifice, washed with saline, opened longitudinally, laid flat on a polystyrene board and fixed with 10% buffered formaldehyde solution before staining with 0.2% methylene blue in saline. Colons were examined using a light microscope at 20X magnification (Leica Microsystems, Milan Italy). The detection and quantization of ACF, polyps and tumours on the colon were performed as previously reported (Izzo *et al.*, 2008). Briefly, in comparison to normal crypts, aberrant crypts have greater size, larger and often elongated openings, thicker lining of epithelial cells, compression of adjacent crypts, and are more darkly stained with methylene blue. Only *foci* containing four or more aberrant crypts (which are best correlated with the final tumour incidence) were evaluated. The criterion to distinguish polyps from tumours was established considering the main characteristic features of these two lesions (i.e. crypt distortion around a central focus and increased distance from luminal to basal surface of cells for polyps and high grade of dysplasia with complete loss of crypt morphology for tumours) (Izzo *et al.*, 2008). For polyp and tumour evaluations, the colons of all mice were discolored with 70% ethanol and embedded in paraffin; thereafter, 5 micron sections were de-paraffinized with xilene, stained with hematoxylin-eosin and observed in a DM 4000 B Leica microscope (Leica Microsystems, Milan, Italy).

3.2.3 Colorectal cancer xenograft model

Colorectal carcinoma HCT 116 cells ($2.5x10^6$) were injected subcutaneously into the right flank of each athymic mice for a total volume of 200 µl *per* injection (50% cell suspension in PBS, 50% Matrigel^{TM}). Approximately 10 days after inoculation, mice were received *ip* the pharmacological treatment [CBD (5 mg/kg), CBD BDS (5 mg/kg) and CBG (1-10 mg/kg) were given once a day]. Tumour size was measured every day by digital caliper measurements, and

tumour volume was calculated according to the modified formula for ellipsoid volume (volume = $\pi/6 \times \text{length} \times \text{width}^2$) (Guo *et al.*, 2006).

3.2.4 Experimental colitis

Colitis was induced by the intracolonic administration of DNBS (Borrelli *et al.*, 2009). Briefly, mice were anesthetized and DNBS (150 mg/kg) was inserted into the colon using a polyethylene catheter (1 mm in diameter) *via* the rectum (4.5 cm from the anus). Three days after DNBS administration, all animals were euthanized by asphyxiation with CO_2, the mice abdomen was opened by a midline incision and the colon removed, isolated from surrounding tissues, opened along the antimesenteric border, rinsed, weighed and length measured (in order to determine the colon weight/colon length *ratio*). For biochemical analyses, tissues were kept at −80°C until use, while for histological examination and immunohistochemistry tissues were fixed in 10% (v/v) formaldehyde. The dose of DNBS was selected on the basis of preliminary experiments showing a remarkable colonic damage associated to high reproducibility and low mortality for the 150 mg/kg dose. The time point of damage evaluation (i.e., 3 days after DNBS administration) was chosen because maximal DNBS-induced inflammation has been reported in mice after 3 days (Massa *et al.*, 2004). Furthermore, previous studies have shown that 3 days after intracolonic DNBS administration in mice, the inflammatory response may be modulated by administration of cannabinoid drugs (Massa *et al.*, 2004; Borrelli *et al.*, 2009).

In our experimental design, we have used the curative protocol in which the pCBs tested [*i.e.* CBG (1-30 mg/kg), CBC (0.1 and 1 mg/kg), and THCV (0.3-5 mg/kg)] were injected *ip* for two consecutive days starting 24-h after DNBS administration.

3.3 *Ex vivo* studies

3.3.1 Cytokines measurement

Interleukin-1β (IL-1β), interferon-γ (IFN-γ) and interleukin-10 (IL-10 levels) were detected both in cell medium and in colonic homogenate. Specifically, their levels were quantified using commercial enzyme-linked immunosorbent assay (ELISA) kits (Tema Ricerca Srl, Bologna) according to the manufacturer's instructions, in (i) cell medium of LPS-treated peritoneal macrophages after 18-h exposure to CBC and THCV (both at 1 μM concentration) and in (ii) homogenate obtained from full-thickness colonic tissues of DNBS-induced colitis mice, treated or not with CBG (30 mg/kg).

3.3.2 Histology and immunohistochemistry

Histological and immunochemistry evaluations have been performed on colonic tissues from DNBS-induced colitis mice [treated or not with CBG and CBC given *ip* (30 mg/kg and 1 mg/kg, respectively)]. It was performed 3 days after DNBS administration and assessed on a segment of 1 cm of colon located 4 cm above the anal canal. After fixation for 24 h in saline 10% formaldehyde, samples were dehydrated in graded ethanol and embedded in paraffin. Thereafter, 5-μm sections were deparaffinized with xylene, stained with hematoxylin–eosin, and observed in a DM 4000 B Leica microscope (Leica Microsystems, Milan, Italy). For microscopic scoring we used a modified version of the scoring system reported by D'Argenio and colleagues. Briefly, colon was scored considering (1) the submucosal infiltration (0, none; 1, mild; 2–3, moderate; 4–5 severe), (2) the crypt abscesses (0, none, 1–2 rare; 3–5, diffuse) and (3) the mucosal erosion (0, absent; 1, focus; 2-3, extended until the middle of the visible surface; 4-5, extended until the entire visible surface) (D'Argenio *et al.*, 2006).

For immunohistochemical detection of Ki-67, paraffin-embedded slides were immersed in a Tris/ethylenediaminetetraacetic acid buffer (pH 9.0), were heated in a decloaking chamber at 125°C for 3 min and were cooled at room temperature for 20 min. After adding 3% hydrogen peroxide, sections were incubated for 10 min. After washing the sections with Tris-buffered saline Tween-20 (pH 7.6), they were stained with rabbit monoclonal antibody to Ki-67 (Ventana Medical systems, Tucson, Arizona). Briefly, each tissue section was incubated with primary antibody to Ki-67 (1:100) for 30 min at room temperature. The slides were washed three times with Tris-buffered saline Tween-20 and were incubated with secondary antibody for 30 min. After, the slides were reacted with streptavidin for 20 min, the reaction was visualized by 3,3'-diaminobenzidine tetrahydrochloride for 5 min. Finally, the slides were counterstained with Mayer's hematoxylin. The intensity and localization of immunoreactivities against the primary antibody used were examined on all sections with a microscope (Leica Microsystems, Milan, Italy).

3.3.3 Intestinal permeability

Intestinal permeability was examined in the serum collected from the blood of healthy mice and DNBS-treated mice [in the presence or absence of CBG (30 mg/kg) or CBC (1 mg/kg) *ip*] using a fluorescein isothiocyanate (FITC)-labeled-dextran method, as described by Osanai *et al.*, 2007. Briefly, two days after DNBS administration, mice were gavaged with 600 mg/kg body weight of fluorescein isothiocyanate (FITC)-conjugated dextran (molecular mass 3-5 kDa). One day later, blood was collected by cardiac puncture, and the serum was immediately analyzed for FITC-derived fluorescence using a fluorescent microplate reader with an excitation–emission wavelengths of 485–520 nm (LS55Luminescence Spectrometer, PerkinElmer Instruments). Serial-diluted FICT-dextran was used to generate a standard curve. Intestinal permeability was expressed as FITC nM found in the serum.

3.3.4 Myeloperoxidase (MPO) activity

Myeloperoxidase (MPO) activity was determined in the colon homogenized from control mice and in DNBS-treated mice [receiving or not CBG (30 mg/kg) or CBC (1 mg/kg), *ip*] as described by Goldblum *et al.*, 1985. Full-thickness colons were homogenized in an appropriate lysis buffer [0.5% hexadecyl-trimethylammonium bromide (HTAB) in 3-(N-morpholino)propanesulfonic acid (MOPS) 10 mM) in *ratio* 50 mg tissue /1 ml MOPS . The samples were then centrifuged for 20 minutes at 15,000 x g at 4° C. An aliquot of the supernatant was then incubated with sodium phosphate buffer (NaPP buffer pH 5.5) e tetra-methyl-benzidine 16 mM. After 5 minutes, H_2O_2 (9.8 M) in NaPP was added and the reaction stopped adding acetic acid. The rate of exchange in absorbance was measured by a spectrophotometer at 650 nm. Different dilutions of human MPO enzyme of known concentration were used to obtain a standard curve. MPO activity was expressed as units (U)/ml.

3.3.5 Superoxide dismutase (SOD) activity

A modified version of the Kuthan *et al.*, 1986 method was used to detect SOD activity. Full-thickness colons from control and DNBS-treated mice (treated or not with CBG 30 mg/kg *ip*) were homogenized in PBS 1X. Homogenates were centrifuged at 25.000 *g* for 15 min at 4°C. Extraction of Cu-Zn SOD was obtained treating the cytosolic lysates with ethanol (1:1) and chloroform (1:0.6) at 25°C for 15 min. After centrifugation (15.000 *g*, 15 min, 4°C), 125 µl of the surnatant was incubated (for 20 min) with 613 µl of a reaction mixture containing 0.12 mM xanthine, 48 mM Na_2CO_3, 0.094 mM EDTA, 60 mg/l bovine serum albumin (BSA), 0.03 mM nitro blue tetrazolium (NBT), 0.006 U/ml xanthine oxidase. Finally, $CuCl_2$ (0.8 mM) was added to stop the reaction. Absorbance readings at 560 nm were recorded using a Beckman

DU62 spectrophotometer. Superoxide radical scavenging capacity was expressed as ng SOD/mg tissues contained in the lysates.

3.3.6 Western blot analysis

Preparation of cytosolic lysates from intestinal tissues

Full-thickness colons from control, AOM- and DNBS-treated mice (treated or not with phytocannabinoids given *ip*) were homogenized in lysis buffer (1:2, w/v) containing 0.5 M β-glycerophosphate, 20 mM $MgCl_2$, 10 mM ethylene glycol tetraacetic acid (EGTA) and supplemented with 100 mM dithiothreitol (DTT) and protease/phosphatase inhibitors (100 mM dimethylsulfonyl fluoride, 2 mg/ml apronitin, 2 mM leupeptin, and 10 mM Na_3VO_4). Homogenates were centrifuged at 600 *g* for 5 min at 4°C; the supernatants were collected and centrifuged at 16,200 *g* for 10 min at 4°C. Proteins (50 μg) were determined with the Bradford method.

Preparation of cytosolic lysates from peritoneal macrophages

Macrophages were collected using the following lysis buffer: 20 mM (4-(2-hydroxyethyl)-1-piperazineethanesulfonic acid) HEPES, 1.5 mM $MgCl_2$, 400 mM NaCl, 1 mM ethylenediaminetetraacetic acid (EDTA) and EGTA, 1% NP-40, 20% glycerol, 1 mM DTT, 0.5 mM phenylmethanesulfonyl fluoride (PMSF), 15 μg/ml aprotinin, 3 μg/ml pepstatin A, 2 μg/ml leupeptin), and centrifuged at 11,200 *g* for 15 min at 4°C. Macrophages lysates (50 μg of proteins) were determined using the Bradford method.

Preparation of cytosolic lysates from Caco-2 cells

Caco-2 cells were collected using the buffer composed by: 50 mM Tris–HCl, pH 7.4, 0.25% sodium deoxycholate, 150 mM NaCl, 1 mM EGTA, 1 mM NaF, 1% NP-40, 1 mM PMSF, 1

mM Na_3VO_4 plus and enriched of a complete protease inhibitor cocktail (Roche Diagnostics, Mannheim, Germany). Caco-2 lysates (50-70 μg of proteins) was determined on supernatant (following centrifugation at 16,200 *g* for 15 min) using the Bradford method.

Measurement of protein expression

The cytosolic lysates obtained were subjected to electrophoresis on a sodium dodecyl sulphate (SDS) 10% polyacrylamide gel and electrophoretically transferred onto a nitrocellulose transfer membrane (Protran, Schleicher & Schuell, Germany). Proteins were visualized on the filters by reversible staining with Ponceau-S solution (Sigma) and de-stained in PBS containing 0,1 % Tween 20. All the membranes obtained were blocked at 4 °C in milk buffer (5% non-fat dry milk in PBS/Tween 0.1 %) and then incubated overnight at 4° C with several monoclonal primary antibodies, as detailed below:

i) the homogenates of colonic tissues obtained from control and AOM-treated mice (alone or treated with CBD 1 mg/kg *ip*) were used to investigate the expression of inducible nitric oxide synthase (iNOS), cycloxygenase (COX-2), phospho-Akt and caspase-3. The membranes were incubated with anti-iNOS, anti-COX-2 (BD Biosciences from Becton Dickinson, Buccinasco, Italy), anti-β-actin (Sigma, Milan, Italy), antiphosho- Akt or anti-Akt and anti-cleaved-caspase-3 (fragment p17) or anti-uncleaved caspase-3 (fragment p30) (Cell Signaling from Euroclone, Milan, Italy) to normalize the results, which have been expressed as a *ratio* of densitometric analysis of COX-2/β-actin, iNOS/β-actin, phospho-AKT/AKT and cleaved caspases 3 (p17)/uncleaved caspase 3 (p30) bands.

ii) the homogenates of colonic tissues obtained from control and DNBS-treated mice (alone or treated with CBG 30 mg/kg 1 mg/kg *ip*) and the cytosolic fractions from macrophages lysates [treated or not with LPS, 1 μg/ml for 18 h and exposed to CBG, CBC and THCV (all at 1 μM

concentration)] were used to investigate the involvement of inducible nitric oxide synthase (iNOS) and cycloxygenase (COX-2). The immunoblots were incubated with mouse anti-COX-2 (BD Bioscience, Belgium) and anti-iNOS (Cayman Chemical, USA) and subsequently with mouse anti-peroxidase-conjugated goat IgG (Jackson ImmunoResearch from LiStarFish, Milan, Italy). The membranes were probed with an anti β-actin antibody to normalize the results, which were expressed as a *ratio* of densitometric analysis of COX-2/β-actin and iNOS/β-actin bands. All the antibodies were used according to the dilution instructions reported on the their data sheets. All the signals obtained were visualized by enhanced chemiluminescence using ImageQuant 400 equipped with software ImageQuant Capture (GE Healthcare, Milan, Italy) and analysed using Quantity One Software version 4.6.3.

3.4 *In vitro* studies

3.4.1 Cell culture

Adenocarcinoma cell lines

For *in vitro* experiments, three human colon adenocarcinoma cell lines (i.e. Caco-2, DLD-1 and HCT116 cells, ATCC from LGC Standards, Milan, Italy), with a different genetic profile (*APC* gene mutated in Caco-2 cells, *K-RAS* mutated in HCT 116 cells, *p53* gene mutated in DLD-1 cells) (Rodrigues *et al.*, 1990; Fukuyama *et al.*, 2008; Dunn *et al.*, 2011) have been used. These cell lines were cultured in Dulbecco's modified Eagle's medium (DMEM) containing 10% foetal bovine serum (FBS), 100 U/ml penicillin and 100 μg/ml streptomycin, 1% non-essential amino acids, 2 mM L-glutamine and 1 M HEPES, in conformity with the manufacturer's protocols. Cell viability was evaluated by trypan blue exclusion.

Healthy colonic epithelial cells (HCEC)

The immortalized epithelial cells derived from human colon biopsies, the healthy human colonic epithelial cells (HCEC) have been used as a comparison with tumoural cells. HCEC, from Fondazione Callerio Onlus (Trieste, Italy), were cultured in Dulbecco's modified Eagle's medium (DMEM) supplemented with 10% FBS, 100 Units/ml penicillin, 100 µg/ml streptomycin, 200 mM L-Glutamine, 100 mM Na-pyruvate and 1 M HEPES. Cell viability was evaluated by trypan blue exclusion.

Human CB_1/CB_2 chinese hamster ovarian (CHO) cells

For radioligand binding assays, chinese hamster ovarian (CHO) cells, stably transfected with complementary DNA encoding human cannabinoid CB_1 receptors and human cannabinoid CB_2 receptors, were cultured in Eagle's medium nutrient mixture F-12 Ham supplemented with 1 mM L-glutamine, 10% v/v FBS and 0.6% penicillin-streptomycin together with geneticin (600 mg/mL). These CHO-hCB_1/hCB_2 cells were passaged twice a week using a non-enzymatic cell dissociation solution.

Mouse peritoneal macrophages

The peritoneal cavity is a membrane-bound and fluid-filled abdominal cavity of mammals that harbors a number of immune cells including macrophages, B cells and T cells. The presence of a high number of naïve macrophages in the peritoneal cavity makes it a preferred site for the collection of naïve tissue resident macrophages (Zhang et *al.*, 2008). Briefly, to evoke the production of peritoneal exudates rich in macrophages, mice were injected *ip* with 1 ml of 10% (w/v) sterile thioglycollate medium (Sigma, Milan, Italy). After 4 days, mice were killed and the peritoneal macrophages were collected and seeded in appropriate plates for performing *in vitro* experiments (Aviello *et al.*, 2011).

Peritoneal macrophages were cultured in Dulbecco's Modified Eagle Medium (DMEM) supplemented with 10% FBS, 100 Units/ml penicillin, 100 µg/ml streptomycin, 200 mM L-Glutamine, 100 mM Na-pyruvate and 1 M HEPES. Cell viability was evaluated by trypan blue staining. The inflammatory response in peritoneal macrophages was induced by lipopolysaccharides (LPS) from *Escherichia coli* serotype O111:B4 (1 µg/ml). The acute inflammatory response in macrophages required an LPS incubation time of 18 h (Aviello *et al.*, 2011).

For all the cell lines described the medium was changed every 48 h in conformity with the manufacturer's protocols.

3.4.2 Cytotoxicity assays

Cytotoxicity assays were performed using MTT assay and the neutral red assays:

MTT assay:

Cell respiration was assessed by the mitochondrial dependent reduction of 3-(4,5-dimethylthiazol- 2-yl)-2,5-diphenyltetrazolium bromide (MTT) to formazan (Mosmann, 1983). After incubation with the tested compounds for 24 hours cells, seeded in a 96-well plates with a cellular density depending on the cell type (see following), were incubated with MTT (250 µg/ml) for 1 h. After solubilisation in DMSO, the extent of reduction of MTT to formazan was quantitated by measuring the optical density at 490 nm (iMarkTM Microplate Assorbance Reader, BioRad). Treatments were compared with a reference cytotoxic drug (DMSO 20% v/v). Results are expressed as a percentage of the corresponding controls (without treatment), (n=3 experiments including 8-10 replicates for each experiment).

CBC (0.001-1 µM), the CB_1 receptor agonist ACEA (0.001-0.1 µM), the CB_2 receptor agonist JWH133 (0.001-0.1 µM), the CB_1 receptor antagonists rimonabant (0.1 µM) and AM251 (1

µM) and the CB_2 receptor antagonist SR 144528 (0.1 µM) were incubated for 24 hours for the evaluation of macrophage mitochondrial respiration.

CBG (1-30 µM) was incubated on Caco-2 and HCEC cells with medium containing 1% for 24 hours. The cytotoxic effect of CBG (10 µM) was evaluated in the presence of AM251 (1 µM, CB_1 receptor antagonist), AM630 (1 µM, CB_2 receptor antagonist) or ruthenium red (10 and 25µM, a non-selective TRP antagonist], all incubated 30 min before CBG.

CBD (1-30 µM), CBDV (1-30 µM), CBC (1-30 µM,), AMTB (5-50 µM, TRPM8 receptor antagonist) and WAY100635 (0.2 and 1 µM, 5HT1A receptor antagonist) were incubated (with 1% FBS medium for 24 hours) for the evaluation of Caco-2 cell viability.

Neutral Red (NR) assay:

The NR assay system, one of the most used and sensitive cytotoxicity test, is a mean of measuring living cells *via* the uptake of the vital dye neutral red. After incubation with the tested compounds for 24 h cells, seeded in a 96-well plate with a cellular density depending on the cell type (see following), were incubated with NR dye solution (50 µg/ml) for 3 h (Aviello *et al.*, 2011). Cells were lysed with 1% (v/v) acetic acid, and the absorbance was read at 532 nm (iMarkTM microplate absorbance reader, BioRad). Dimethyl sulphoxide (DMSO, 20%, v/v) was used as a positive control. The results are expressed as percentage of cell viability, (n=3 experiments including 8-10 replicates for each experiment).

CBD (at the concentration range of 0.01-10 µM) was incubated for 24 hours for the evaluation of Caco-2, HCT 116, DLD-1 and HCEC cells viability.

CBD BDS (1-5 µM) was incubated for 24 hours for the evaluation of HCT 116, DLD-1 and HCEC cells viability.

Cells were seeded in 96-well plates with the following cellular density *per* well and the adhesion time was 48 hours for all the cell lines used excepting for peritoneal macrophages, allowed to adhere for 3 hours:

HCT 116 and DLD-1 (tumoral cell lines): 2.5×10^3 cells *per* well; Caco-2 (tumoral cell line): 1.0×10^4 cells *per* well; HCEC (healthy colonic epithelial cells): 1.0×10^4 cells *per* well; peritoneal macrophages: 1×10^5 cells *per* well

3.4.3 DNA damage assay (comet assay)

Genotoxicity studies were performed by single cell electrophoresis assay (comet assay) (Aviello *et al.*, 2010). Following 24 hours exposure to CBD (10 μM), Caco-2 cells were incubated with 75 μM H_2O_2 (damaging *stimulus*) or phosphate-buffered saline PBS (undamaging *stimulus*) for 5 min. After centrifugation at 1,000 *g* for 5 min, pellets were mixed with 0.85% low melting point agarose and added to 1% normal melting point agarose gels. Gels were then suspended in 2.5 M NaCl, 100mM Na_2EDTA, 10 mM Tris and 1% Triton X-100, pH 10 at 4°C for 1 h and electrophoresed in alkaline buffer (300mM NaOH, 1 mM Na_2EDTA, pH 12) at 26 V, 300 mA for 20 min. After neutralisation in 0.4 M Tris–HCl (pH 7.5), gels were stained with 2 μg/ml ethidium bromide. Images were analysed using a Leica microscope equipped with a Casp software.

3.4.4 Identification and quantification of endocannabinoids and related molecules

Endocannabinoids, anandamide and 2-arachidonoylglycerol (2-AG), palmitoylethanolamide (PEA) and oleoylethanolamide (OEA) levels were measured in Caco-2 cells exposed to CBD (10 μM) for 24 h and in peritoneal macrophages (treated or not with LPS, 1 μg/ml for 18 h) and exposed to CBC (1 μM), added 30 min before LPS challenge. Cells were harvested in 70% methanol before cell processing, subsequently extracted, purified and analysed by isotope

dilution liquid chromatography-atmospheric pressure-chemical ionisation mass spectrometry (Izzo *et al.*, 2008).

3.4.5 Intracellular reactive oxygen species (ROS) measurement assay

Generation of intracellular reactive oxygen species (ROS) was estimated by the fluorescent probe, 2′,7′-Dichlorofluorescin diacetate (DCFH-DA) which diffuses readily through the cell membrane. In the cells, DCFH-DA is before enzymatically hydrolyzed by intracellular esterases to form non-fluorescent DCFH and then rapidly oxidized to form highly fluorescent dichlorofluorescein (DCF) in the presence of ROS. The DCF fluorescence intensity is paralleled to the amount of ROS formed intracellularly. Caco-2 cells and HCEC were plated in 96-well black plates at the density of 1×10^4 cells/well (Aviello *et al.*, 2011). After 48 h, the cells were incubated with a medium containing 1% FBS in presence or absence of CBG (10 μM, for 24-hours). After washing, cells were incubated for 1 hour with 200 μl of 100 μM H_2DCF-DA in HBSS containing 1% FBS. The Fenton's reagent (H_2O_2/Fe^{2+} 2 mM, 3 hours), was used as a positive control.

The DCF fluorescence intensity was detected using a fluorescent microplate reader (Perkin-Elmer Instruments), with the excitation wavelength of 485 nm and the emission wavelength of 538 nm. The intracellular ROS levels were expressed as fluorescence intensity (picogreen).

3.4.6 Measurement of caspases 3/7 activity

Apoptosis was evaluated by means of the Caspase-Glo®3/7 Chemiluminescence Assay Kit (Promega Corporation, Madison, WI, USA) following the manufacturer's protocol. Caco-2 cells were seeded in 12-well plates at a density of $5x10^4$ cells/well. After 48 hours, the cells were incubated with medium containing 1% FBS in presence or absence of CBG (10 μM, for 24 hours). After incubation, cells were trypsinized, washed with PBS and processed. The assay

was performed in 96-well white walled plates, adding to each well 100 µL of Caspase-Glo® 3/7 reagent to 100 µL of culture medium containing 5-40 µl of cells suspension (about 1000 cells/µl) in culture medium. The cell suspension concentration was evaluated by a cell counter (Bioad TC10TM) and confirmed by a DNA assay (Quant-it DNA assay kit, Invitrogen) considering 4 pg DNA/cell. After 1 h incubation in the dark at room temperature, chemiluminescence was measured by a VersaDoc MP System (Bio-Rad) equipped by the Quantity One® version 4.6 software. All samples were assayed in triplicate. Chemiluminescence mean values were plotted versus the cell number in the assay and the linear regression curve fit was calculated by the software (Excell-Windows). The increase of caspase 3/7 enzymatic activity was calculated by the *ratio* of the curve slopes.

3.4.7 Morphological assessment of apoptotic and necrotic cells

Cells were seeded on glass disk (1.3 cm in diameter) placed into wells of a 24-well plate, at a density of $5xl0^4$ cell/disk, for 48 hours and thereafter treated with a medium containing 1% FBS in presence or absence of CBG (10 µM, for 24-h). After incubation, the culture medium was removed, the glass disks were collected and pasted on slide. Subsequently, cells on slides were fixed and stained by the standard hematoxylin-eosin method. The slides were analyzed and the histological images were captured with the aid of a light microscope (at 200 X magnification). The number of apoptotic and necrotic cells was quantified using at least 100 cells per slide (n=3 independent experiments).

3.4.8 Nitrites measurement

Nitrites, stable metabolites of NO, were measured in macrophages medium as previously described (Aviello *et al.*, 2011). Mouse peritoneal macrophages (5×10^5 cells *pe*r well seeded in a 24-well plate) were incubated with the drugs tested (see following) for 30 min and

subsequently with LPS (1 μg/ml) for 18 h. After reduction of nitrates to nitrites by cadmium, cell supernatants were incubated with 2,3-diaminonaphtalene (DAN) (50 μg/ml) for 7 min. After stopping the reaction with 2.8 N NaOH, nitrite levels were measured using a fluorescent microplate reader (LS55 Luminescence Spectrometer, PerkinElmer Instruments, excitation–emission wavelengths of 365–450 nm).

For the evaluation of nitrite levels, mouse peritoneal macrophages were incubated with CBG, CBC and THCV (0.001–1 μM) in presence or not of LPS (1 μg/ml) for 18 hours. In a subsequent set of experiments, rimonabant (0.1 μM, CB_1 receptor antagonist) and SR144528 (0.1 μM, CB_2 receptor antagonist) were incubated 30 min before CBG, CBC and/or THCV (1 μM) + LPS (1 μg/ml) for 18 hours.

In some experiments, cells were also treated with ACEA (0.001-0.1 μM, CB_1 agonists) and JWH133 (0.001-0.1 μM, CB_2 receptor agonist) incubated 30 min before LPS stimulation.

3.4.9 Proliferation assays:

Proliferation assays were performed using MTT assay and the ^{3}H-thymidine incorporation:

^{3}H-thymidine incorporation

Cell proliferation was evaluated in colorectal carcinoma cell line Caco-2 using the ^{3}H-thymidine incorporation as previously described (Aviello *et al.*, 2010). Briefly, Caco-2 cells were seeded in 24-well plates at a density of $1.0x10^{4}$ in DMEM supplemented with 10% FBS and grown for 24 hours. The resulting monolayers were washed three times with phosphate buffered saline (PBS) and then 1 ml of serum-free DMEM was added to each well. After 24 hours of serum starvation, the cells were washed three times with PBS and incubated with DMEM supplemented with 10% FBS containing CBD (0.01–10 μM) in the presence of [methyl-3H]-thymidine (1 μCi/well) for 24 hours, scraped in 1 M NaOH and collected in

plastic miniature vials (PerkinElmer) filled up with liquid for scintillation counting (UltimaGold® PerkinElmer). Treatments were compared with 300 μM spermine. Cell proliferation was expressed as count *per* minute on μg of protein (CPM/μg protein) of incorporating ^{3}H-thymidine cells using a β-counting (PerkinElmer, Milan, Italy). The treatments were carried out in triplicate and three independent experiments were performed. The protein content was quantified using the Bradford method.

MTT assay

The MTT assay, beyond its use as a cytotoxicity assay, can also be used for the evaluation of cell proliferation. For this purpose, it is necessary to synchronize cells at the same cellular cycle phase (G_1/G_o) by serum deprivation (*i.e.* starvation). Caco-2 (at a density of $1.0x10^4$), HCT116, DLD-1 (both at a density of $2.5x10^3$) and HCEC (at a density of $1.0x10^4$) cells were seeded, allowed to adhere for 48 hours and starved by serum deprivation for 24 h. Briefly, for the MTT assay, cells were treated with CBD (0.01–10 μM in Caco-2 HCT116, DLD-1 and HCEC), CBD BDS, (0.3-5 μM in HCT116, DLD-1 and HCEC cells) for 24 h and incubated with MTT (250 μg/ml) for 1 h at 37°C. The mitochondrial reduction of MTT to formazan was then quantitated at 490 nm (iMarkTM microplate reader, BioRad, Italy). Using this assay, the antiproliferative effect of CBD and CBD BDS was evaluated in Caco-2 and DLD-1 cells in the presence of several selective receptor antagonists all incubated 30 min before the addition of CBD or CBD BDS.

3.4.10 Radioligand [^{35}S] GTPγS binding assay

Binding assays with [^{35}S] guanosine 5"-(gamma-thio)triphosphate (GTPγS) were performed with CB_1-CHO cell membranes. The cells were removed from flasks by scraping and then frozen as pellets at -20ºC until required. Before use in a radioligand binding assay, cells were

defrosted, diluted in Tris-buffer (50 mM Tris-HCl, 50 mM Tris-Base) and homogenized. Protein assays were performed using a Bio-Rad Dc kit (Hercules, CA).

Measurement of agonist-stimulated [^{35}S]GTPγS binding to cannabinoid CB_1 receptors was described previously (Brown *et al.*, 2010). The assays were carried out with GTPγS binding buffer (50 mM Tris-HCl, 50 mM Tris-Base, 5 mM $MgCl_2$, 1 mM EDTA, 100 mM NaCl, 1 mM DTT and 0.1% bovine serum albumin) in the presence of [^{35}S]GTPγS and guanosine diphosphate (GDP), in a final volume of 500 µl. Binding was initiated by the addition of [^{35}S]GTPγS to the wells. Non-specific binding was measured in the presence of 30 µM GTPγS. The cannabinoid receptor antagonist rimonabant (0.1µM) was incubated 30 min before CBC (1µM), at 30ºC. Total incubation time was 60 min. The reaction was terminated by a rapid vacuum filtration method using Tris-binding buffer, as described previously, and the radioactivity was quantified by liquid scintillation spectrometry. In all the [^{35}S]GTPγS binding assays, we used 0.1 nM [^{35}S]GTPγS, 30 µM GDP and 33 µg *per* well of proteins.

3.4.11 Radioligand displacement assay

Displacement assay was performed with membranes from CHO cells transfected with human CB_1 or CB_2 receptors (Ross *et al.*, 2000). The CHO cells were removed from flasks by scraping and then frozen as a pellet at -20°C until required. Before use in a radioligand binding assay, cells were defrosted, diluted in 50 mM Tris buffer and homogenized with a 1 ml hand-held homogenizer. Protein assays were performed using a Bio-Rad Dc kit (Bio-Rad, Hercules, CA, USA). The assay was carried out, as previously described by Ross *et al.*, 2000, with [^{3}H]CP55940, 50mM Tris HCl, 50 mM Tris Base and 1 mg/ml BSA (assay buffer), total assay volume 500 µl. CBD, CBD BDS (0.0001-10 µM) and [^{3}H]CP55940 were each added in a volume of 50 µl following their dilution in assay buffer. Binding was initiated by the addition of hCB_1- or hCB_2-CHO cell membranes (25 µg protein *per* tube) and all assays were performed

at 37°C for 60 min before termination by the addition of ice-cold wash buffer (50 mM Tris buffer, 1 mg/ ml BSA) and vacuum filtration using a 24-well sampling manifold (Brandel Cell Harvester) and Whatman GF/B glass-fibre filters that have been soaked in wash buffer at 4°C for 24h. Each reaction tube was washed three times with a 4 ml aliquot of buffer. The filters were oven-dried for 60 min and then placed in 5 ml of scintillation fluid (Ultima Gold XR, Packard). Radioactivity was quantified by liquid scintillation spectrometry. Specific binding was defined as the difference between the binding that occurs in the presence and absence of 1 µM unlabeled CP55940. The concentration of [^{3}H]CP55940 used in the displacement assays was 0.7 nM.

3.4.12 Quantitative (real-time) RT-PCR analysis

Total RNA was extracted according to the manufacturer's recommendations and further purified and DNA digested by the Micro RNA purification system (Invitrogen). Total RNA eluted from spin cartridge was UV-quantified by a Bio-Photometer® (Eppendorf, Santa Clara, CA, USA), and purity of RNA samples was evaluated by the RNA-6000-Nano® microchip assay using a 2100 Bioanalyzer® equipped with a 2100 Expert Software® (Agilent, Santa Clara, CA, USA) following the manufacturer's instructions. For all samples tested, the RNA integrity number was greater than 8 relative to a 0–10 scale. One microgram of total RNA, as evaluated by the 2100 Bioanalyzer, was reverse transcribed in cDNA by the SuperScript III SuperMix (Invitrogen). The reaction mixture was incubated in a termocycler iCycler-iQ5® (Bio-Rad, Hercules, CA, USA) for a 5 min at 60°C step, followed by a rapid chilling for 2 min at 4°C. The protocol was stopped at this step and the reverse transcriptase was added to the samples, except the negative controls (–RT). The incubation was resumed with two thermal steps: 10 min at 25°C followed by 40 min at 50°C. Finally, the reaction was terminated by heating at 95°C for 10 min. Quantitative real time PCR was performed by an iCycler-iQ5® in a 20mL

reaction mixture containing 1 X SYBR green supermix (Bio-Rad), 10 ng of cDNA (calculated on the basis of the retro-transcribed RNA) and 330 nM for each primer. Primer sequences and optimum annealing temperature (TaOpt) were designed by the AlleleID software (PremierBiosoft). The amplification profile consisted of an initial denaturation of 2 min at 94°C and 40 cycles of 30 s at 94°C, annealing for 30 s at TaOpt and elongation for 45 s at 68°C. Fluorescence data were collected during the elongation step. A final melt-curve data analysis was also included in the thermal protocol. Assays were performed in quadruplicate (maximum Ct of replicate samples <0.5), and a standard curve from consecutive fivefold dilutions (100 to 0.16 ng) of a cDNA pool representative of all samples was included for PCR efficiency determination. Relative normalized expression was evaluated as previously described (Di Marzo *et al.*, 2008). For the targets evaluated in the colorectal cancer cells and human healthy colonic epithelial cell line a qualitative arbitrary scale to define the level of mRNA expression was considered as follows: high expression (HE) from 20 to 25 Cq; middle expression (ME) from 25 to 30 Cq; low expression (LE) from 30 to 33Cq, very low expression (VLE) over 33Cq. Furthermore two quality parameters have been utilized in evaluating expression data: i) the maximum acceptable standard deviation for replicate samples was put ≤ 0.500 (note that at high Cq the standard deviation normally draws to increase); ii) the expression data is significant if Δ (Cq_{mean}-Cq_{bkg}) ≥ 5. Assays were performed in quadruplicate in two independent experiments, by using 20 ng of cDNA (as evaluated from the input RNA used for reverse-transcription).

The targets investigated were:

i) CB_1, CB_2, TRPA1, TRPV1, TRPV2, TRPM8 and 5HT1A mRNA expression in colorectal carcinoma cell line (Caco-2) and human healthy colonic epithelial cell line (HCEC)

ii) CB_1, CB_2, iNOS and COX-2 mRNA expression in peritoneal macrophages (treated or not with CBC and/or CBG 1 µM, 30 min before LPS)

All the cell lines used were collected and homogenized in 1.0 mL of Trizol® (Invitrogen).

3.5 Statistical analysis

Statistical analysis has been carried out using GraphPad Prism 5.0 (GraphPad Software, San Diego, CA, USA). Data are expressed as the mean ± standard error (SEM) or standard deviation (SD) of n experiments. To determine statistical significance, Student's t test was used for comparing a single treatment mean with a control mean, and an one-way analysis of variance followed by a Tukey-Kramer multiple comparisons test was used for analysis of multiple treatment means. ANOVA was used to compare different concentration-effect curves with $P<0.05$ considered significant. The IC_{50} (concentration that produced 50% inhibition of cell viability) value was calculated by nonlinear regression analysis using the equation for a sigmoid concentration–response curve (GraphPad Prism). P values < 0.05 were considered significant.

Values obtained from the radioligand assays have been expressed as means and variability as SEM or as 95% confidence limits. Net agonist stimulated [^{35}S]GTPγS binding values were calculated by subtracting basal binding values (obtained in the absence of agonist) from agonist-stimulated values (obtained in the presence of agonist) as detailed elsewhere (Brizzi *et al.*, 2005). Values for EC_{50}, maximal effect (E_{max}) and SEM or 95% confidence limits of these values have been calculated by nonlinear regression analysis using the equation for a sigmoid concentration-response curve (GraphPad Prism). The concentration of a drug that produces a 50% displacement of [^{3}H]CP55940 from specific binding sites (IC_{50}) is calculated using GraphPad Prism 5. Its dissociation constant (K_i value) is calculated using the equation of Cheng

and Prusoff (1973). The parameters for [^{3}H]CP55940 binding to hCB_1 and hCB_2 CHO cell membranes have been determined by fitting data from saturation binding experiments to a one-site saturation plot using GraphPad Prism 5. They are 57.00 pmol/mg and 215 pmol/mg (B_{max}), and 1.1 nM and 4.3 nM (K_d) in hCB_1 and hCB_2 CHO cell membranes, respectively.

4.0 RESULTS

4.1 INFLAMMATORY BOWEL DISEASE (IBD)

4.1.1 CANNABIGEROL (CBG)

4.1.1.1 Effect of CBG on colon weight/colon length *ratio*

DNBS administration caused a significant increase in colon weight/colon length *ratio*, a simple and reliable marker of intestinal inflammation/damage (Gálvez *et al.*, 2000). CBG (1-30 mg/kg) given after the inflammatory insult, significantly reduced the effects of DNBS on colon weight/colon length *ratio*. Significant protection was achieved starting from the 5 mg/kg (Figure 6).

4.1.1.2 Effect of CBG on histological damage and inflammation

Histological evaluations of colonic mucosa of healthy control animals showed normal appearance with intact epithelium (Figure 7A). In the DNBS group, colons showed tissue injury which was mainly characterized by necrosis involving the full thickness of the mucosa, infiltrations of granulocytes into the mucosa/*sub*-mucosa and *oedema* of *sub*-mucosa (Figure 7B). CBG (30 mg/kg, given after the inflammatory insult) reduced the signs of colon injury (microscopic score: control, 0.50±0.22; DNBS, 9.0±0.45$^{\#}$; CBG 30 mg/kg, 6.0±0.45*, n=4, $^{\#}p<0.001$ *vs* control and $*p<0.01$ *vs* DNBS alone). In the colon of CBG (30 mg/kg)-treated animals, the glands were regenerating, the *oedema* in *sub*-mucosa was reduced, and the erosion area was superficial (Figure 7C).

4.1.1.3 Effect of CBG on immunohistochemical detection of Ki-67

The curative action of CBG was further confirmed by immunohistochemistry. In normal colonic mucosa, the predominant area of cell proliferation is localized to the lower of the crypts

as revealed by Ki-67 distribution (Figure 8A). In the colon from DNBS-treated mice, total necrosis with Ki-67 immunoreactivity on inflammatory cells and in a few remaining surface elements was observed (Figure 8B). CBG (30 mg/kg, given after the inflammatory insult) partially counteracted the effect of DNBS on cell proliferation, its mitotic activity being restricted to the lower half of the mucosa (*i.e.* the mature superficial cells were not in a proliferative state) (Figure 8C).

4.1.1.4 Effect of CBG on intestinal barrier function

FITC-conjugated dextran presence (index of membrane integrity) was not detected in the serum of healthy control animals. The administration of DNBS induced FITC-conjugated dextran appearance in the serum. CBG treatment (30 mg/kg) completely abolished DNBS-induced increased intestinal permeability (Figure 9A).

4.1.1.5 Effect of CBG on neutrophil infiltration in inflamed colon

MPO activity is considered to be an index of neutrophil infiltration (because MPO is predominantly found in these cells) and it is largely used to quantify intestinal inflammation (Krawisz *et al.*, 1984). DNBS-induced colitis was associated with significantly increased neutrophil infiltration, as evaluated by MPO (Figure 9B). CBG, given after the inflammatory insult at the dose of 30 mg/kg, counteracted DNBS-induced increase in MPO activity (Figure 9B).

4.1.1.6 Effect of CBG on SOD activity in inflamed colon

DNBS produced a significant decrease in SOD activity. CBG, at the dose of 30 mg/kg, counteracted DNBS-induced reduction in SOD activity (Figure 9C).

4.1.1.7 Effect of CBG on iNOS and COX-2 protein expression in inflamed colon

Densitometric analysis indicated a significant increase in the expression of both iNOS and COX-2 in the inflamed colons (Figure 10 A-B). CBG (30 mg/kg) reduced iNOS (Figure 10A), but not COX-2 (Figure 10B) over-expression induced by DNBS.

4.1.1.8 Effect of CBG on IL-1β, IL-10 and interferon-γ in the inflamed colon

The levels of IL-1β and interferon-γ (IFN- γ) were significantly increased by DNBS (Figure 11 A and B). By contrast, IL-10 production significantly decreased in the colon from DNBS-treated mice (Figure 11C). Treatment with CBG (30 mg/kg) counteracted the changes in IL-1β, IL-10 and IFN-γ levels observed in the inflamed colons (Figure 11A-C).

4.1.1.9 Cytotoxicity assay on murine peritoneal macrophages

Cytotoxicity was evaluated performing the MTT assay and CBG, at the concentrations ranging from 0.001 to 1 µM, did not affect mitochondrial respiration (expressed as percentage of viability ± SEM) after 24-h exposure: [control 99.93 ± 3.69; CBG 0.001 µM 95.58 ± 4.21; CBG 0.01 µM 95.58 ± 1.21; CBG 0.1 µM 102.3 ± 4.12; CBG 1 µM 105.60 ± 3.73; CBG 10 µM 38.23 ± 2.96$^{\#}$; $^{\#}p<0.001$ *vs* control (n=3 experiments)]. Similarly, the CB_1 receptor antagonist rimonabant (0.1 µM) and the CB_2 receptor antagonist SR144528 (0.1 µM) did not exert cytotoxic effects (data not shown).

4.1.1.10 Effect of CBG on nitrite production in macrophages alone and in presence of CB_1/CB_2 receptor antagonists

LPS (1 µg/ml for 18 h) administration caused a significant increase in nitrite production (Figure 12A). A pre-treatment with CBG (0.001-1 µM, 30 min before LPS) caused a significant reduction in nitrite production. Since CBG can inhibit endocannabinoid metabolism and hence

indirectly activate cannabinoid receptors (De Petrocellis *et al.*, 2011), in the second set of experiments we verified if CBG effect on nitrite production was sensitive to selective CB_1 and CB_2 receptor antagonists. We found that rimonabant (0.1 µM, CB_1 receptor antagonist) did not modify the inhibitory effect of CBG (1 µM) (Figure 12B). By contrast, SR144528 (0.1 µM, CB_2 receptor antagonist) enhanced the inhibitory effect of CBG (1 µM) on nitrite production (Figure 12C). Rimonabant and SR144528, at the concentrations used, did not modify *per se* nitrite levels induced by LPS stimulation (Figure 12B and C).

4.1.1.11 Effect of CBG on iNOS and COX-2 (mRNA and protein) expression in LPS-treated murine peritoneal macrophages

The inhibitory effect of CBG (1 µM) on nitrite production in LPS-treated macrophages was accompanied by decrease of iNOS protein with no significant changes in its transcriptional levels (*i.e.* of iNOS mRNA) (Figure 13A and C). COX-2 is a key enzyme involved in the macrophages function. Similarly to iNOS, LPS administration caused up-regulation of COX-2 mRNA and protein expression. CBG (1 µM) incubated 30 min before LPS stimulation, did not modify LPS-induced COX-2 up-regulation (Figure 13B and D).

4.1.1.12 Effect of CBG on CB_1/CB_2 mRNA expression in macrophages

A challenge with LPS (1 µg/ml for 18 h) caused up-regulation of CB_1 receptors and down-regulation of CB_2 receptors (Figure 14A and B). CBG (1 µM) did not modify cannabinoid CB_1 and CB_2 receptor mRNA expression both in control and in LPS-treated macrophages (Figure 14A and B).

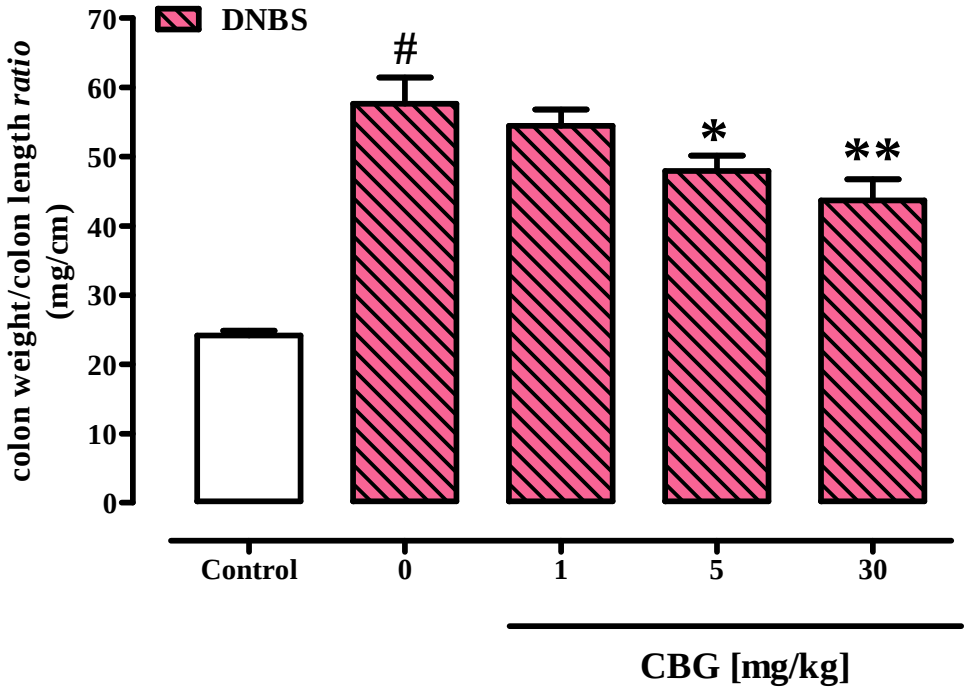

Figure 6. Dinitrobenzene sulfonic acid (DNBS)-induced colitis in mice. Colon weight/length *ratio* of colons from untreated and DNBS-treated mice in the presence or absence of cannabigerol (CBG). Tissues were analyzed 3 days after vehicle or DNBS (150 mg/kg, intracolonically) administration. CBG (1-30 mg/kg) was administered (*ip*) once a day for two consecutive days starting 24-h after the inflammatory insult. Bars are mean ± SEM of 12-15 mice for each experimental group. $^{\#}p<0.001$ *vs* control, $^{*}p<0.05$ and $^{**}p<0.01$ *vs* DNBS alone.

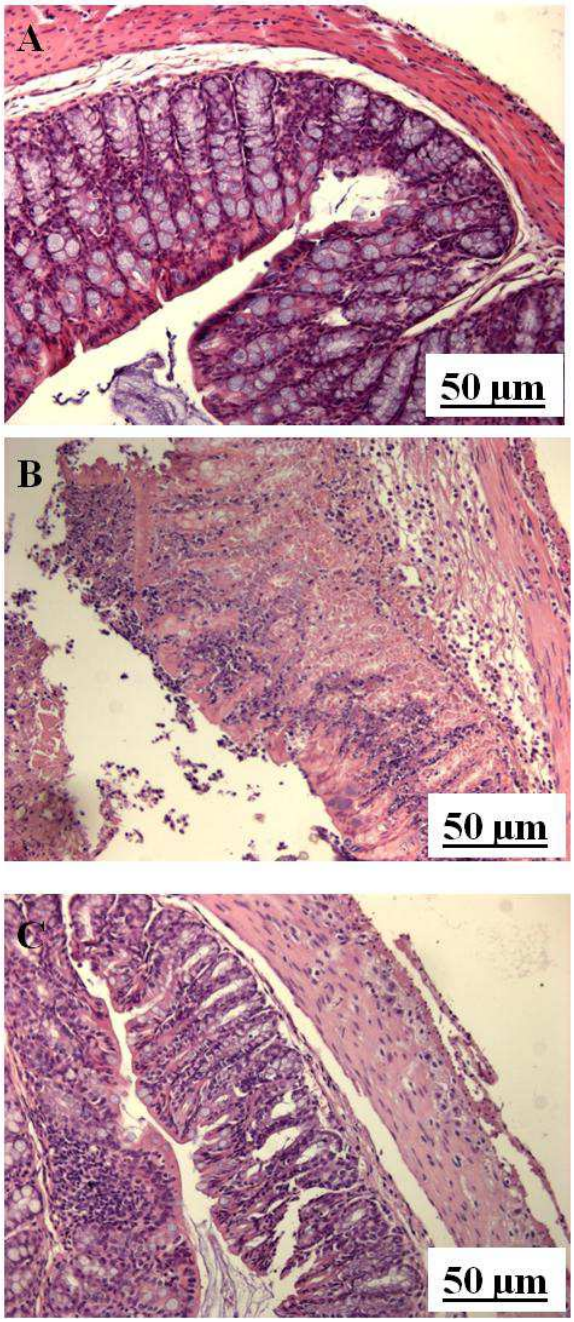

Figure 7. Histological evaluations of inflamed and non-inflamed colons: effect of cannabigerol (CBG). No histological modification was observed in the mucosa and *sub*-mucosa of control mice (A); mucosal injury induced by dinitrobenzene sulfonic acid (DNBS) administration (B); treatment with CBG reduced colon injury by stimulating regeneration of the glands (C). Histological analysis was performed 3 days after DNBS administration. CBG (30 mg/kg) was administered (*ip*) for two consecutive days starting 24-h after the inflammatory insult (curative protocol). Original magnification x200 . The figure is representative of 4 experiments.

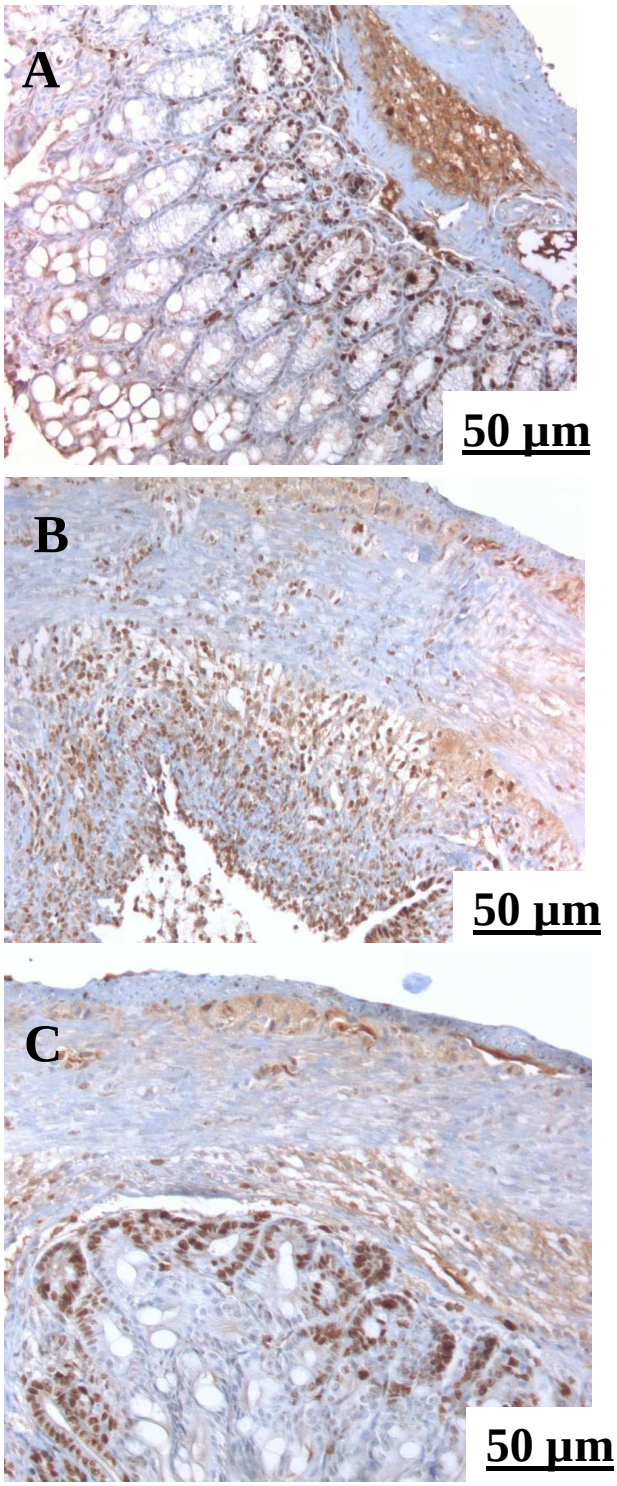

Figure 8. Different patterns of Ki-67 immunoreactivity in the colonic mucosa of control mice (A), dinitrobenzene sulfonic acid (DNBS)-treated mice (B) and mice treated with DNBS plus cannabigerol(CBG) (C). (A) Ki-67 immunopositive cells were localised to the lower part of the crypts. (B) Ki-67 immunopositive cells were observed on inflammatory cells. (C) Ki-67 immunopositive cells were observed only in the expanded basal zone. CBG (30 mg/kg) was administered (*ip*) for two consecutive days starting 24-h after the inflammatory insult. The figure is representative of 4 experiments.

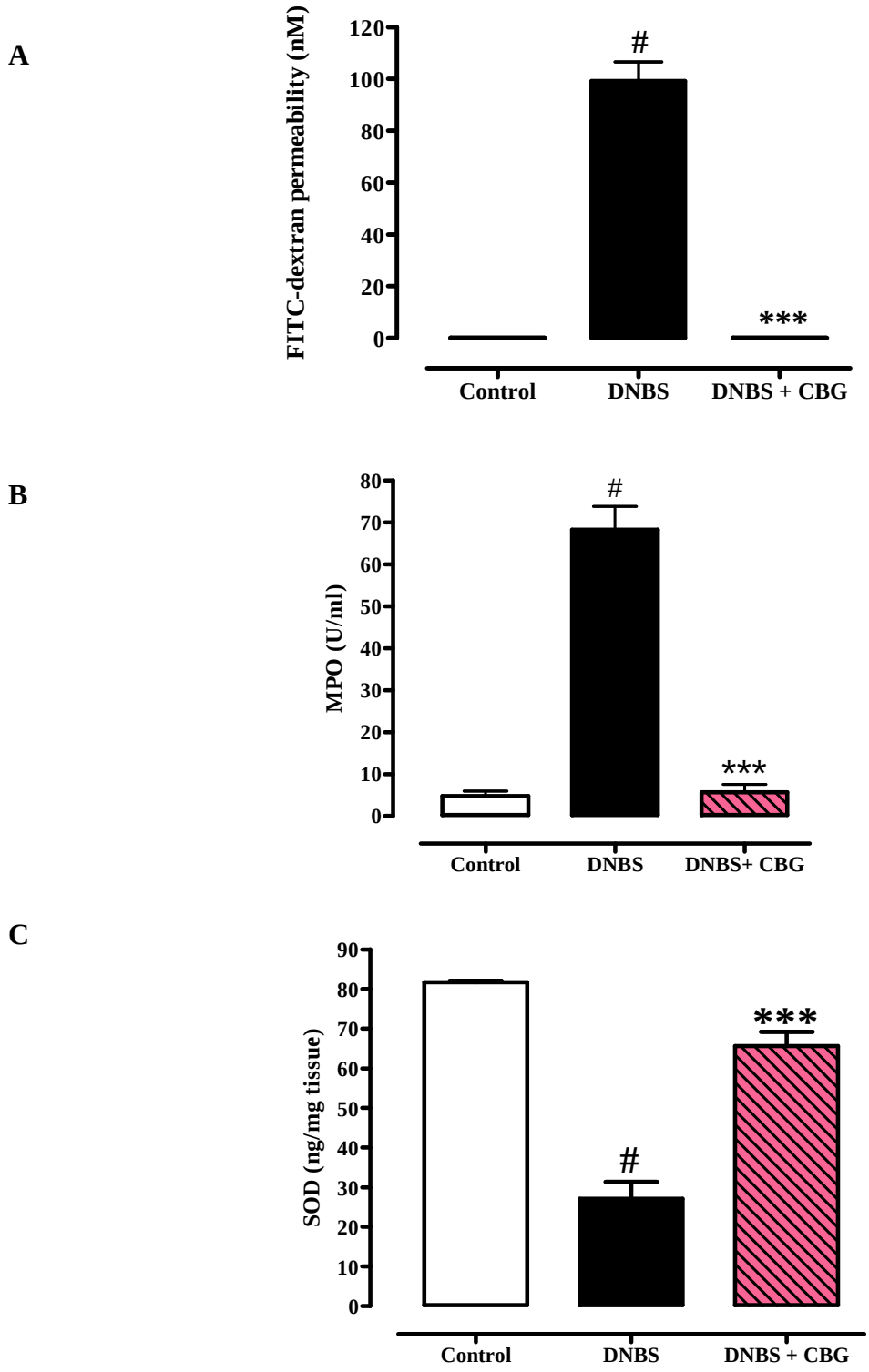

Figure 9. Effect of cannabigerol (CBG) on intestinal permeability (evaluated as FITC-dextran permeability) (A) , myeloperoxidase (MPO) activity (B) and superoxide dismutase (SOD) activity (C) in dinitrobenzene sulfonic acid (DNBS)-induced colitis in mice. Colons (for MPO and SOD activities) and blood (for intestinal permeability) were analysed 3 days after vehicle or DNBS (150 mg/kg, intracolonically) administration. CBG (30 mg/kg) was administered (*ip*) for two consecutive days starting 24-h after the inflammatory insult (curative protocol). Bars are mean±SEM of 5 mice for each experimental group. $^{\#}p< 0.001$ vs control and $^{***}p< 0.001$ *vs* DNBS alone.

A

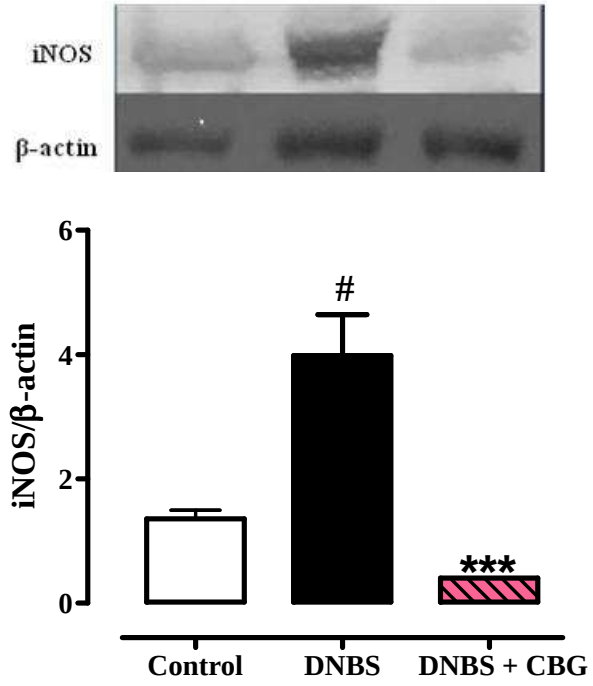

B

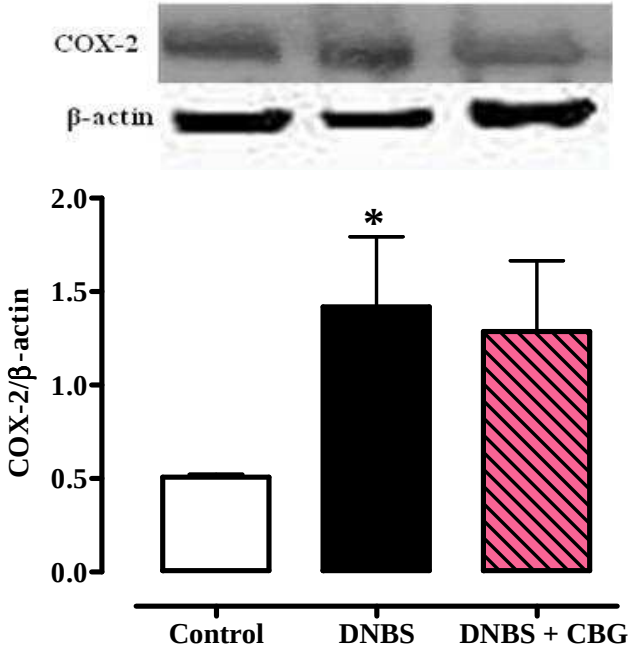

Figure 10. Inducible nitric oxide synthase (iNOS) (A) and cyclooxygenase-2 (COX-2) (B) expression in colonic tissues of animals treated or not with dinitrobenzene sulfonic acid (DNBS): effect of cannabigerol (CBG). Measurements were performed 3 days after DNBS (150 mg/kg, intracolonically) administration. CBG (30 mg/kg) was administered (*ip*) for two consecutive days starting 24-h after the inflammatory insult. Results are mean±SEM of 3–4 experiments. $^{*}p<0.05$ and $^{\#}p< 0.001$ *vs* control; $^{***}p< 0.001$ *vs* DNBS alone.

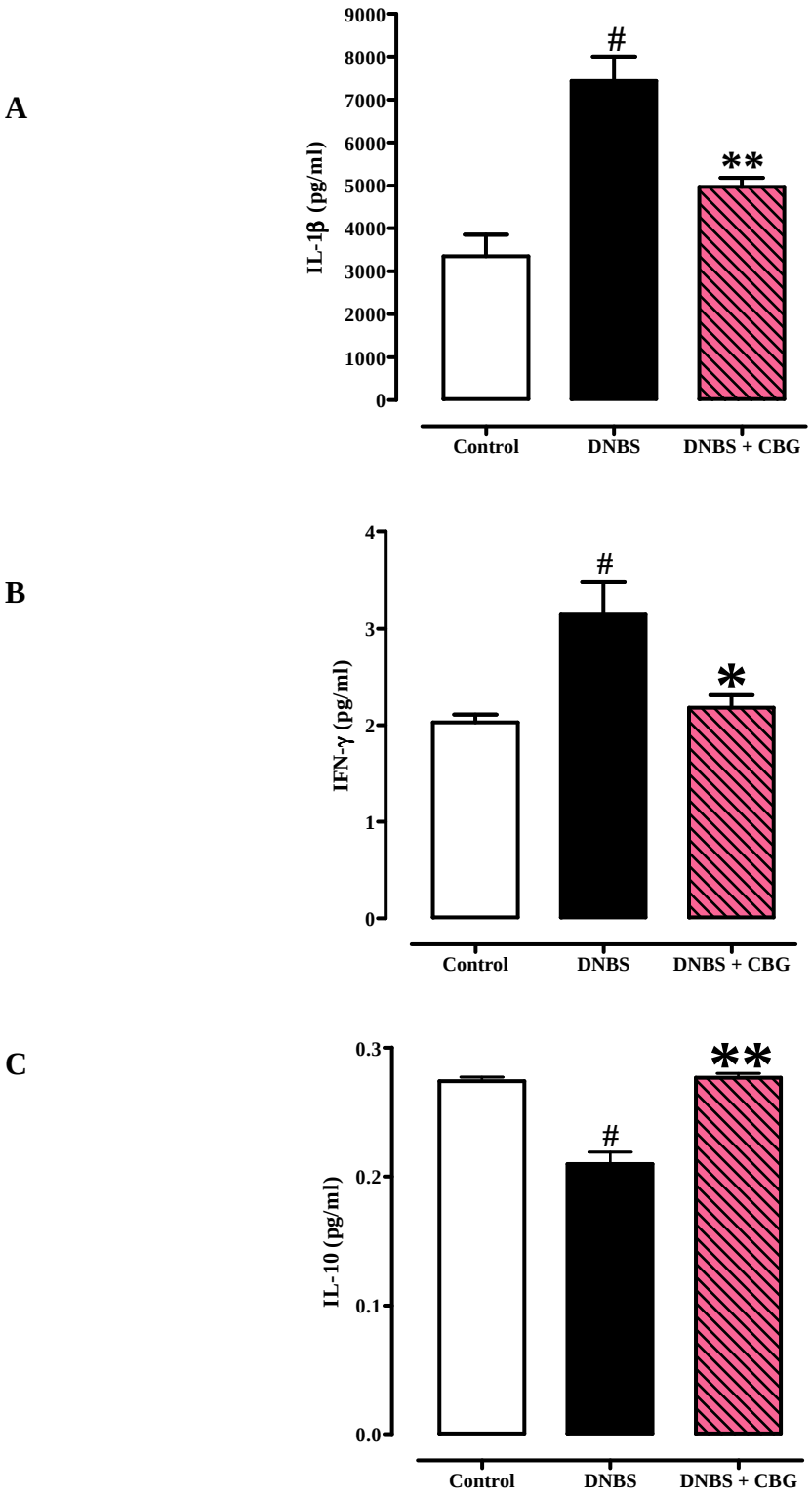

Figure 11. Effect of cannabigerol (CBG) on interleukin-1β (IL-1β) (A), interferon γ (IFN-γ) (B) and interleukin-10 (IL-10) (C) levels in mouse colons treated with dinitrobenzene sulfonic acid (DNBS). Measurements were performed 3 days after DNBS (150 mg/kg, intracolonically) administration. CBG (30 mg/kg) was administered (*ip*) for two consecutive days starting 24-h after the inflammatory insult. Results (expressed as picograms per ml of proteic extract) are mean± SEM of 3–4 experiments. $^{\#}p$<0.01–0.001 *vs* control, $^{*}p$< 0.05 and $^{**}p$< 0.01 *vs* DNBS alone.

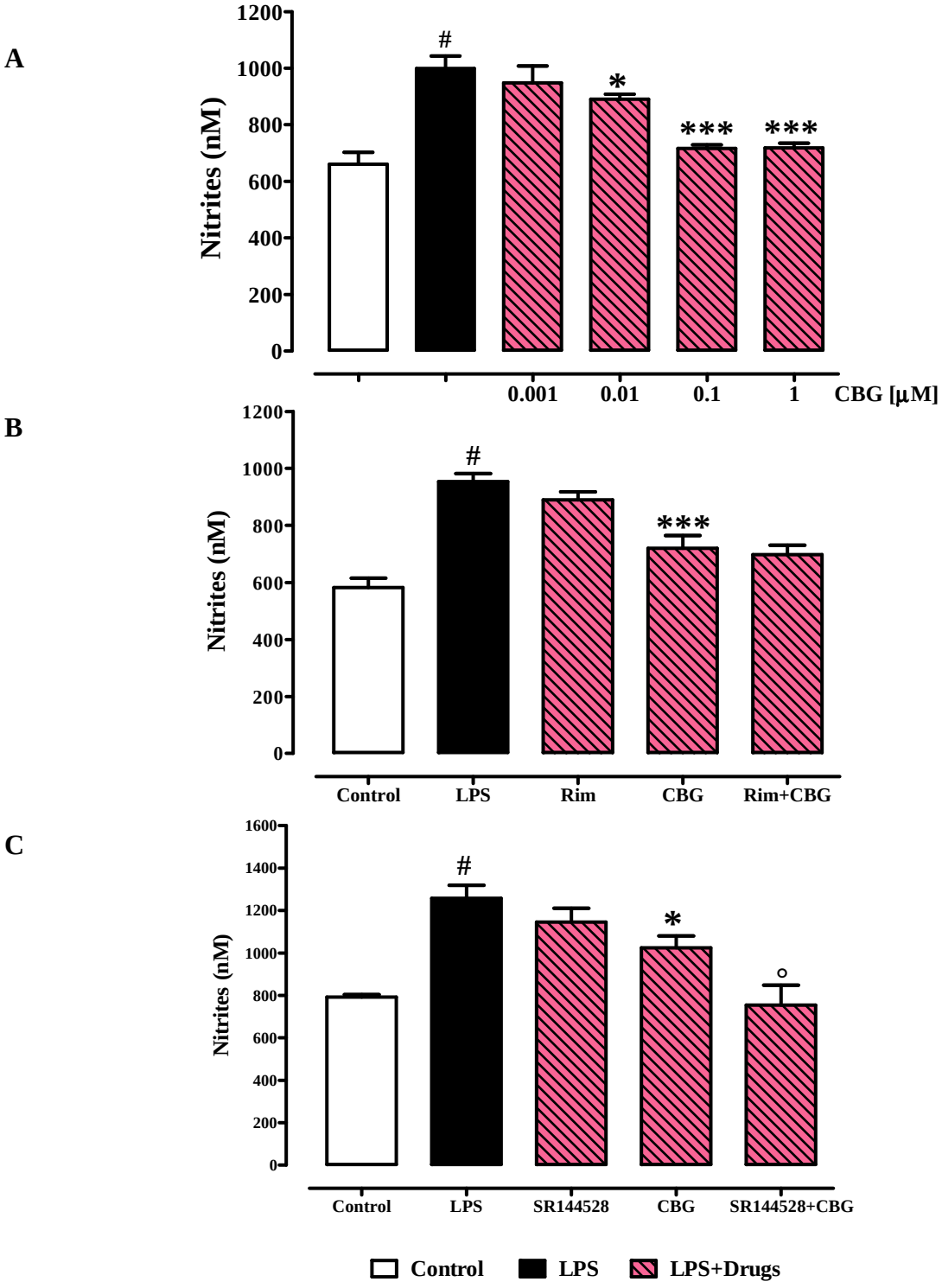

Figure 12. Effect of cannabigerol (CBG) on nitrite levels (A) in the cell medium of murine peritoneal macrophages incubated with lipopolysaccharide (LPS, 1 mg/ml) for 18 h. CBG (0.001–1 µM) was added to the cell media 30 min before LPS challenge. B and C show the effect of CBG, (1 µM) alone or in presence of the cannabinoid CB_1 receptor antagonist rimonabant (Rim, 0.1 µM) (B) or the cannabinoid CB_2 receptor antagonist SR144528 (0.1 µM) (C) on nitrite levels in the cell medium of murine peritoneal macrophages incubated with LPS (1 µg/ml) for 18 h. The antagonists were added to the cell media 30 min before CBG exposure. LPS was incubated 30 min after CBG. Results are means±SEM of three experiments (in triplicates). $^{\#}p<0.001$ *vs* control; $^{*}p< 0.05$ and $^{***}p< 0.001$ *vs* LPS alone; $^{\circ}p< 0.001$ *vs* LPS + CBG.

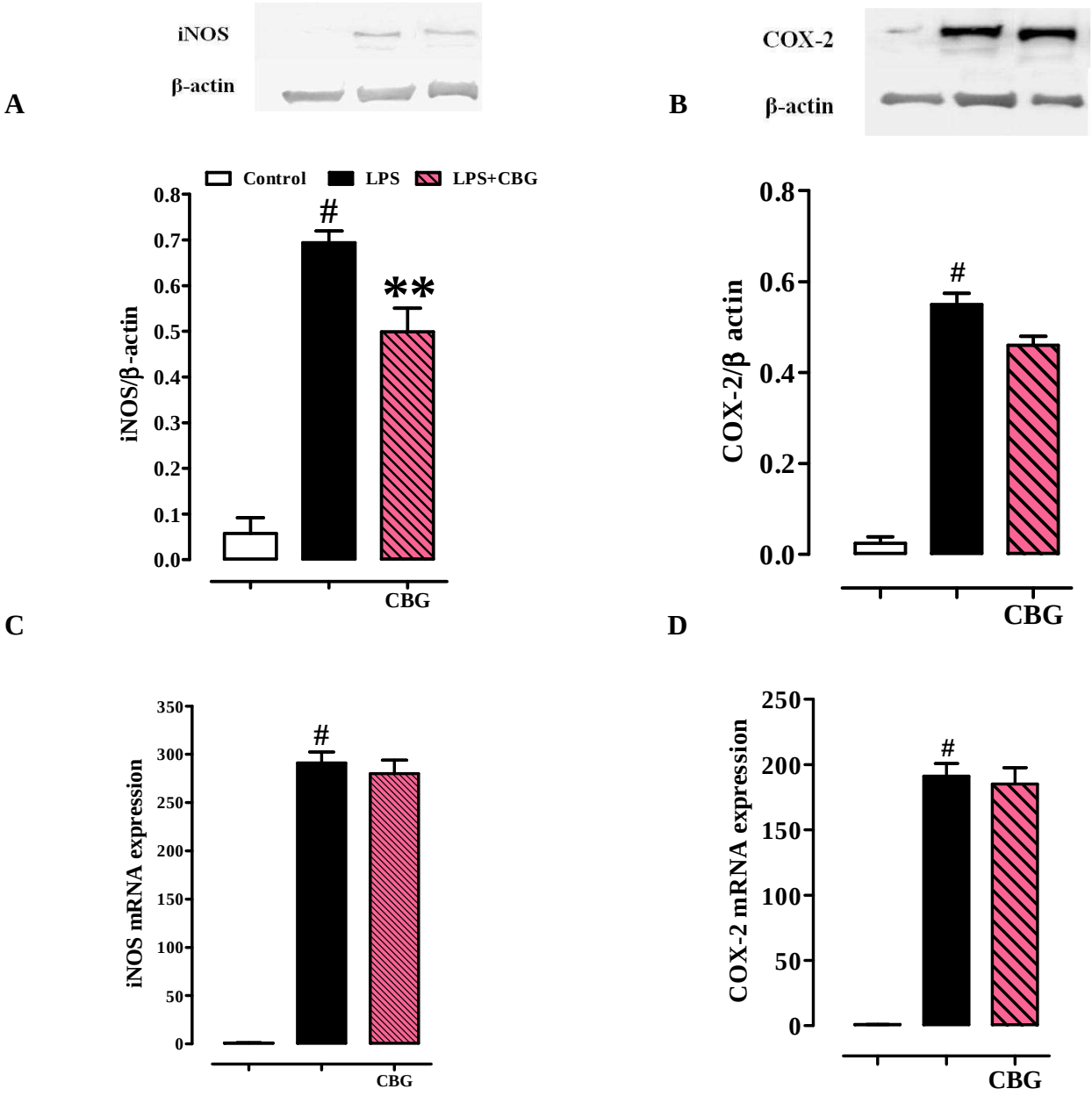

Figure 13. Inducible nitric oxide synthase (iNOS) (A, C) and cyclooxygenase-2 (COX-2) (B, D) protein and mRNA levels in cell lysates from macrophages incubated or not with lipopolysaccharide (LPS, 1 mg/mL) for 18 h. mRNA expression was evaluated by RT-PCR. The expression levels, normalized with respect to the reference genes, were scaled to the expression value of the control, considered as 1. Protein expression was evaluated by Western blot analysis. Cannabigerol (CBG, 1 µM) was added to the cell media 30 min before LPS challenge. $^{\#}p< 0.001$ versus control; $^{**}p<0.01$ *vs* LPS (n = 4–5 experiments).

A

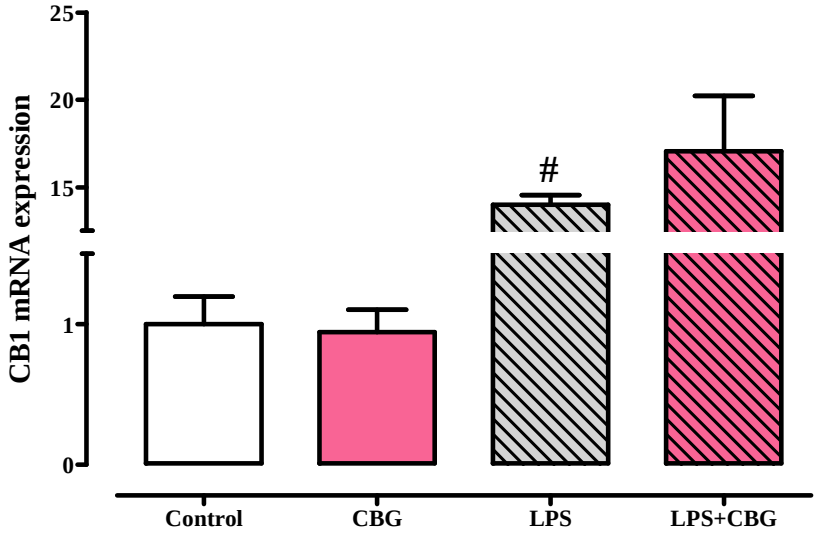

B

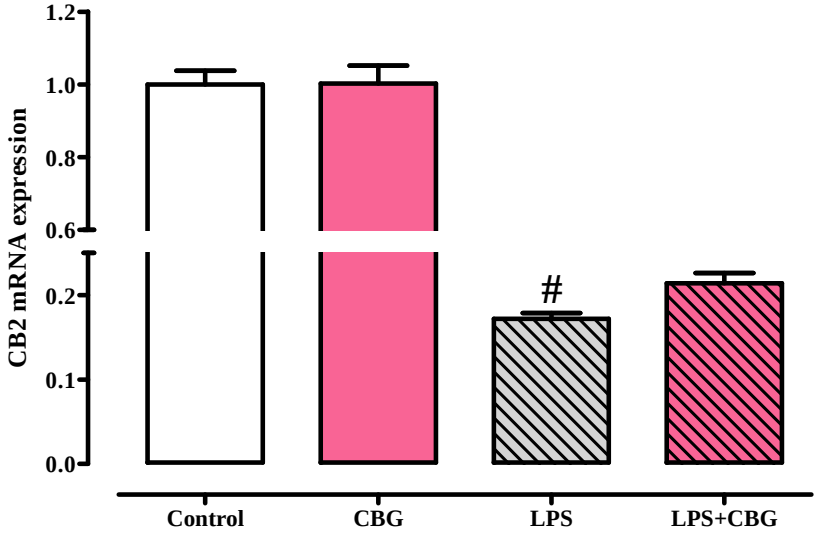

Figure 14. Relative mRNA expression of cannabinoid CB_1 receptor (A), cannabinoid CB_2 receptor (B) in cell lysates from macrophages incubated or not with lipopolysaccharide (LPS, 1 µg/ml) for 18h. Cannabigerol (CBG, 1 µM) was added alone to the cell media or 30 min before LPS challenge. Data were analysed by GENEX software for group wise comparisons and statistical analysis. Results are means±SEM of four experiments. $^{\#}p< 0.001$ *vs* control.

4.1.2 CANNABICHROMENE (CBC)

4.1.2.1 Effect of CBC on DNBS-induced colitis (colon weight/colon length *ratio*, intestinal permeability and myeloperoxidase activity)

DNBS administration caused a significant increase in colon weight/colon length *ratio* (Figure 15). CBC, at the doses of 0.1 and 1 mg/kg, (*ip*) after the inflammatory insult, significantly reduced the effects of DNBS on colon weight/colon length *ratio*. The effect was significant for the dose of 1 mg/kg. At the 1 mg/kg dose, CBC significantly reduced DNBS-induced increase in intestinal permeability (Figure 16A) and MPO activity (Figure 16B).

4.1.2.2 Effect of CBC on histological damage and on immunohistochemical detection of Ki-67

Histological analysis showed, in control mice, a normal appearance, with intact epithelium of the colonic mucosa (Figure 17A). In DNBS-treated mice, subtotal erosions of the mucosa, and diffuse lymphocyte infiltration involving the *muscularis mucosae* and the *sub*-mucosa were observed (Figure 17B). CBC treatment (1 mg/kg, given intraperitoneally after DNBS) resulted in a regenerative area surrounding the residual focal erosions (Figure 17C).

Immunohistochemical analyses confirmed the beneficial effect of CBC on inflamed colonic mucosa. In control tissues, Ki-67 immunoreactivity revealed proliferative activity on the *fundus* of the foveole glands (Figure 18A). In the colon from DNBS-treated mice, total necrosis with Ki-67 immunoreactivity on inflammatory cells was observed (Figure 18B). CBC (1 mg/kg, given intraperitoneally after DNBS) reduced the effect of DNBS on cell proliferation, the mitotic activity being restricted to one half of the mucosa (Figure 18C).

4.1.2.3 Cytotoxicity assay on murine peritoneal macrophages

Cytotoxicity was evaluated performing the MTT assay and CBC, at the concentrations ranging from 0.001 to 1 µM, did not affect mitochondrial respiration (expressed as percentage of viability ± SEM) after 24-h exposure: [control 99.93 ± 4.70; CBC 0.001 µM 103.7 ± 8.0; CBC 0.01 µM 101.3 ± 4.40; CBC 0.1 µM 96.29 ± 2.9; CBC 1 µM 103.8 ± 3.60; DMSO 20% v/v (used as positive control) 24.50 ± 1.78$^{\#}$; $^{\#}p<0.001$ *vs* control (n=3 experiments)]. Similarly the CB_1 agonist ACEA (0.001-0.1 µM), the CB_2 receptor agonist JWH133 (0.001-0.1 µM), the CB_1 receptor antagonists rimonabant (0.1 µM) and AM251 (1 µM), the CB_2 receptor antagonist SR144528 (0.1 µM) did not exert cytotoxic effects (data not shown)

4.1.2.4 Nitrites measurements in murine peritoneal macrophages

In cells not treated with LPS, CBC (0.001-1 µM) did not modify basal nitrite levels [nitrite levels (nM) ±SEM: control 614.4 ±31.5, CBC 0.001 µM 620.5±32.1, CBC 0.01 µM 618.4±24.6, CBC 0.1µM 612.7±29.6, CBC 1µM 626.9±36.2; n=12]. LPS (1 µg/ml for 18 h) administration caused a significant increase in nitrite production (Figure 19). A pre-treatment with CBC (0.001-1 µM), 30 min before LPS, significantly reduced LPS-increased nitrite levels (Figure 19). CBC was also effective when given 15 hours after LPS challenge (*i.e.* three hours before nitrite assay) (see insert to Figure 19). No significant differences were found in CBC effect when the compound was given 30 min before LPS or 15 h after LPS (*i.e.* three hours before the nitrite assay, see overlapping curves in the insert to Figure 19). Like CBC, the CB_1 agonist ACEA (0.001-0.1 µM) and the CB_2 receptor agonist JWH133 (0.001-0.1 µM) reduced the production of nitrites stimulated by LPS when given 30 min before LPS [nitrite levels (nM) ±SEM: control 642.2±51.6, LPS 1µg/ml 911.3±42.4$^{\#}$, ACEA 0.001µM 782.3±12.0*, ACEA 0.01 µM 730.9±20.4**, ACEA 0.1 µM 699.8±18.1***; n=6, $^{\#}p<0.01$ *vs* control, $^{*}p<0.05$, $^{**}p<0.01$ and $^{***}p<0.001$ *vs* LPS alone. Control 842.0±18.4, LPS 1µg/ml 1200±55.3$^{\#}$, JWH133

0.001µM 942.5±70.7[*], JWH133 0.01 µM 965.8±58.7[*], JWH133 0.1 µM 707.0±83.6[***]; n=6, [#]p<0.001 *vs* control, [*]p<0.05 and [***]p<0.001 *vs* LPS alone].

4.1.2.5 Effect of CBC on iNOS and COX-2 (mRNA and protein) expression in LPS-treated murine peritoneal macrophages

In order to verify if the effect of CBC on the increased nitrite production was associated to changes in iNOS expression, we measured the mRNA and protein levels of this enzyme both by RT-PCR and by western blot. LPS administration up-regulated iNOS mRNA and protein expression (Figure 20A-C). CBC (1 µM) incubated 30 min before LPS stimulation, did not modify LPS-induced changes in iNOS expression (Figure 20A-C**)**. Similarly to iNOS, LPS administration caused up-regulation of COX-2 mRNA and protein expression (Figure 20B-D). CBC (1 µM) incubated 30 min before LPS stimulation, did not modify LPS-induced COX-2 up-regulation (Figure 20B-D).

4.1.2.6 Effect of CBC on IL-1β, IL-10 and IFN-γ levels in LPS-treated murine peritoneal macrophages

Interleukins and interferon-*γ* are important cytokines involved in LPS-evoked responses in macrophages. The levels of IL-1β, IFN-γ and IL-10 in macrophages medium were significantly increased after 18-h exposure to LPS (Figure 21A-C). A pre-treatment with CBC (1 µM), incubated 30 min before LPS stimulation, significantly reduced IL-10 and interferon-*γ* (but not IL-1β) levels in macrophages (Figure 21A-C).

4.1.2.7 Effect of CBC in presence of selective CB_1/CB_2 receptor antagonists

Because CBC can inhibit endocannabinoids inactivation (De Petrocellis *et al.*, 2011), in this set of experiments we verified if CBC effect on nitrite production was reduced or counteracted by selective CB_1 and CB_2 receptor antagonists. We found that rimonabant (0.1 µM) (CB_1 receptor

antagonist) not only did not counteract but, instead, significantly enhanced the inhibitory effect of CBC (1 µM) on nitrite production (Figure 22A). By contrast, the CB_2 receptor antagonist SR 144528, at a concentration (0.1 µM) able to block the effect of the selective CB_2 receptor agonist JWH133 (0.1 µM) on nitrite production (data not shown) did not modify CBC (1 µM)-induced changes in nitrite production (Figure 22B). Rimonabant and SR 144528, at the concentrations used, did not modify, *per se,* nitrite levels induced by LPS ([nitrite levels (nM) ±SEM: control 611.9±27.4, LPS 1µg/ml 899.1±25.2$^{\#}$, rimonabant 0.1 µM 863.1±24.8, SR144528 0.1 µM 917.1±27.2; n=6, $^{\#}p<0.001$ *vs* control].

Next, using [^{35}S]GTPγS binding assays, we found that when tested at concentrations from 1 nM up to 1 µM, CBC did not display any significant ability to stimulate or inhibit [^{35}S]GTPγS binding to hCB_1-CHO cell membranes (data not shown). In contrast, using the same experimental conditions, we found that, when incubated by itself, 0.1 µM rimonabant induced, as expected, a marked inhibition of [^{35}S]GTPγS binding in this bioassay. When 1 µM CBC was added 30 min after 0.1 µM rimonabant, no significant change in E_{max} of this inverse agonist/antagonist was observed (Figure 23).

4.1.2.8 Effect of CBC on CB_1, CB_2 mRNA expression in murine peritoneal macrophages

Results of the experiments measuring mRNA expression are shown in Figure 24 A-B. LPS (1 µg/ml for 18 h) challenge caused up-regulation of CB_1 receptors and down-regulation of CB_2 receptors. CBC did not modify CB_1 and CB_2 mRNA expression in LPS-treated macrophages (Figure 24 A-B).

4.1.2.9 Effect of CBC on endocannabinoids and related molecules in murine peritoneal macrophages

Table 2 reports the levels of endocannabinoids, PEA and OEA in murine peritoneal macrophages treated with LPS. The exposure to LPS (1μg/ml) for 18 h induced a significant increase in anandamide (but not 2-AG, PEA or OEA) levels. CBC (1 μM) did not change the levels of the endocannabinoids and PEA in control macrophages (*i.e.* not treated with LPS), nor in macrophages challenged with LPS (Table 2). By contrast, CBC significantly increased OEA levels in LPS-treated macrophages (Table 2).

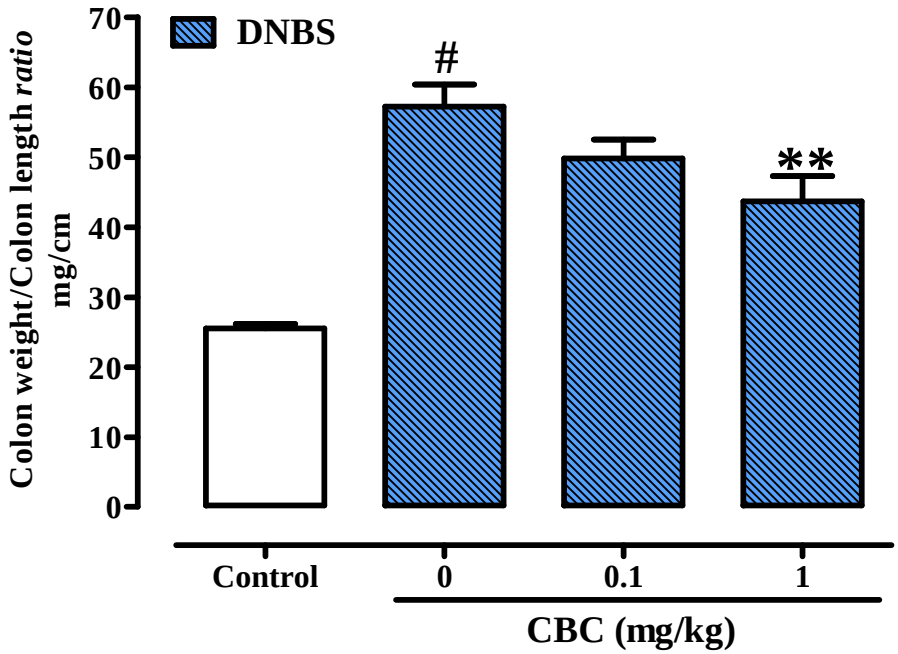

Figure 15. Dinitrobenzene sulfonic acid (DNBS)-induced colitis in mice. Colon weight/colon length *ratio* of colons from untreated and DNBS-treated mice in the presence or absence of cannabichromene (CBC). Tissues were analyzed 3 days after vehicle or DNBS (150 mg/kg, intracolonically) administration. CBC (0.1 and 1 mg/kg) was administered (*ip*) once a day for two consecutive days starting 24-h after the inflammatory insult. Bars are mean ± SEM of 12-15 mice for each experimental group. $^{\#}p<0.001$ *vs* control; $^{**}p<0.01$ *vs* DNBS alone.

A

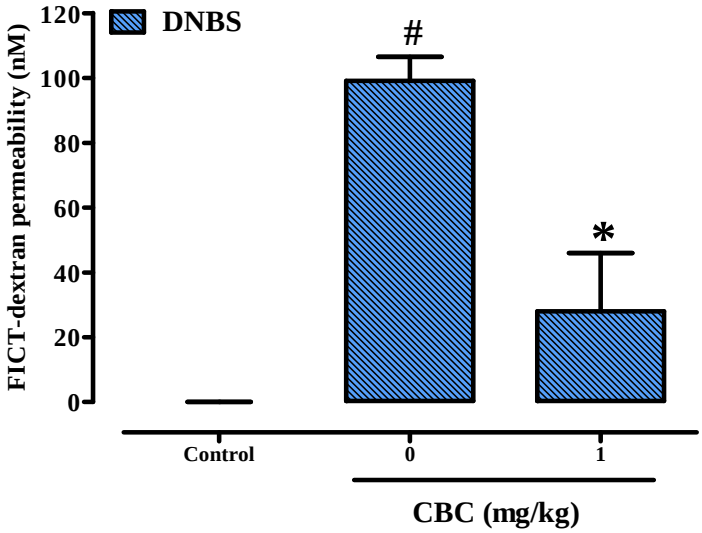

B

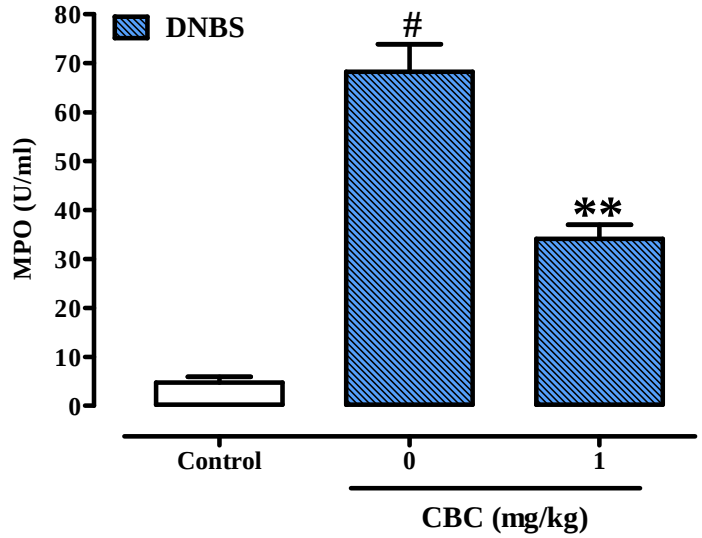

Figure 16. Inhibitory effect cannabichromene (CBC) on serum FICT-dextran concentration (a measure of intestinal barrier function) (A) and myeloperoxidase (MPO, a marker of intestinal inflammation) activity (B) in dinitrobenzene (DNBS)-induced colitis in mice. Permeability and MPO activity were measured on colonic tissues 3 days after vehicle or DNBS (150 mg/kg, intracolonically). CBC (1 mg/kg) was administered (*ip*) for two consecutive days starting 24-h after the inflammatory insult. Bars are mean ± SEM of 5 mice for each experimental group. $^{\#}p<0.001$ *vs*control; $^{*}p<0.05$ and $^{**}p<0.01$ *vs* DNBS alone.

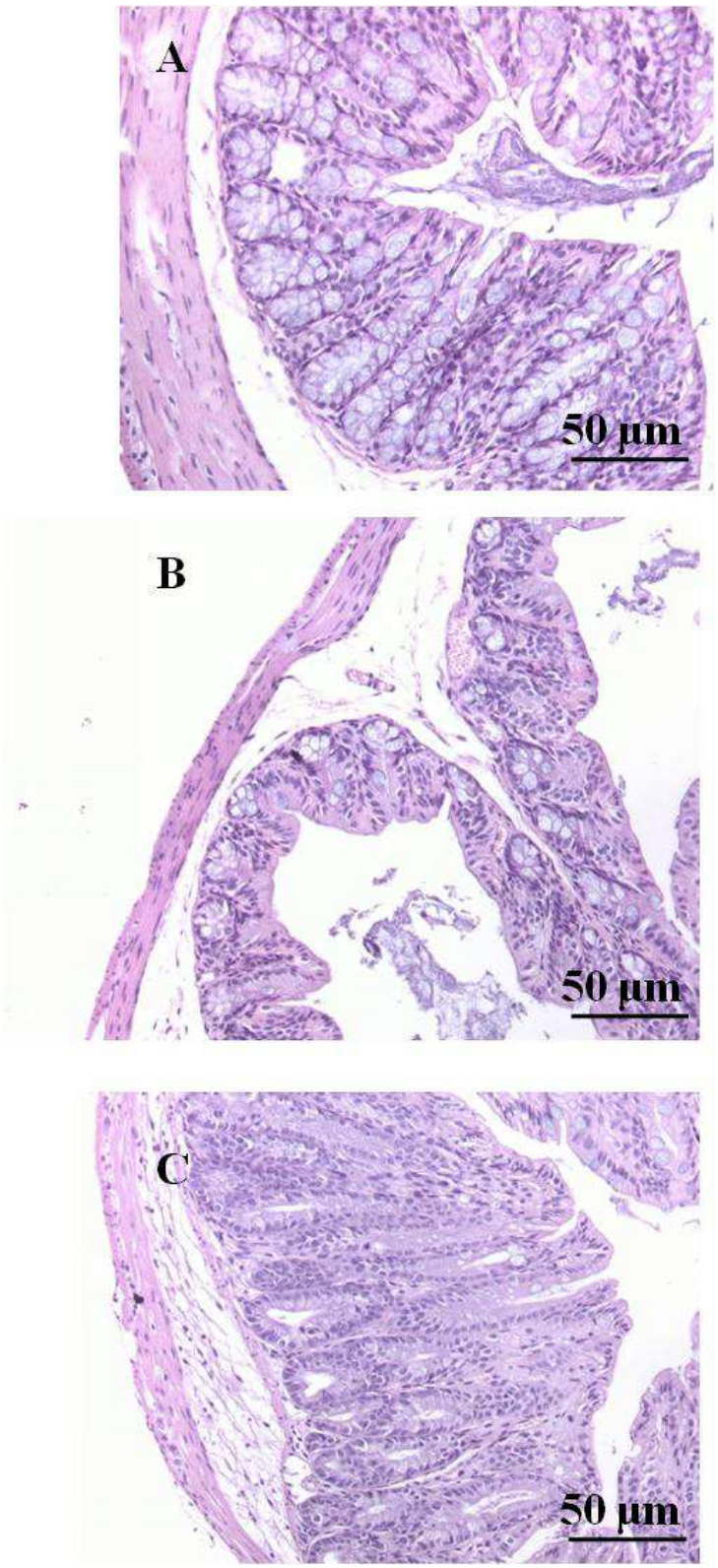

Figure 17. Histological evaluations of inflamed and non-inflamed colons: effect of cannabichromene (CBC). No histological modification was observed in the mucosa and *sub*-mucosa of control mice (A); mucosal injury induced by dinitrobenzene sulfonic acid (DNBS) administration (B); treatment with CBC reduced colon injury stimulating a regeneration of the glands (c). CBC (1 mg/kg) was administered (*ip*) for two consecutive days starting 24-h after the inflammatory insult. Histological analysis was performed 3 days after DNBS (150 mg/kg, intracolonically). Original magnification x200. The figure is representative of 3 experiments

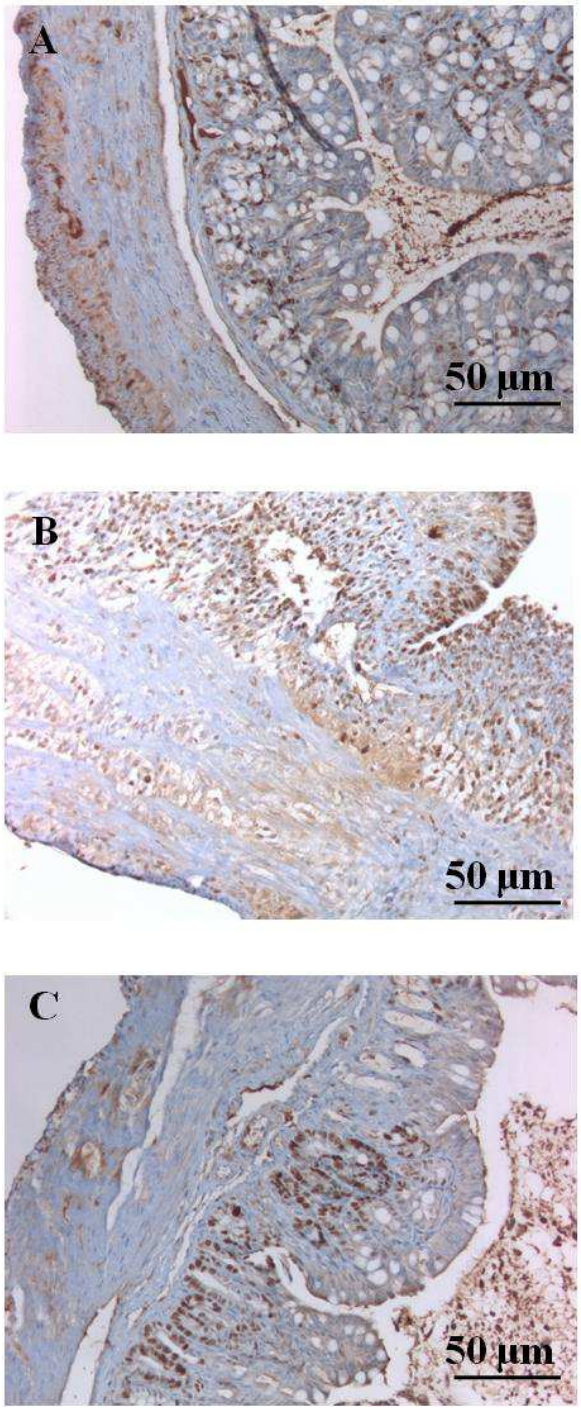

Figure 18. Different patterns of Ki-67 immunoreactivity in the colonic mucosa of control mice (A), dinitrobenzene sulfonic acid (DNBS)-treated mice (B) and mice treated with DNBS plus cannabichromene (CBC) (C). (A) Ki-67 immunopositive cells localised to the lower of the crypts. (B) Ki-67 immunoreactivity was observed on inflammatory cells. (C) Ki-67 immunopositive cells observed only in the expanded basal zone. CBC (1 mg/kg) was administered (*ip*) for two consecutive days starting 24-h after the inflammatory insult. The figure is representative of 3 experiments.

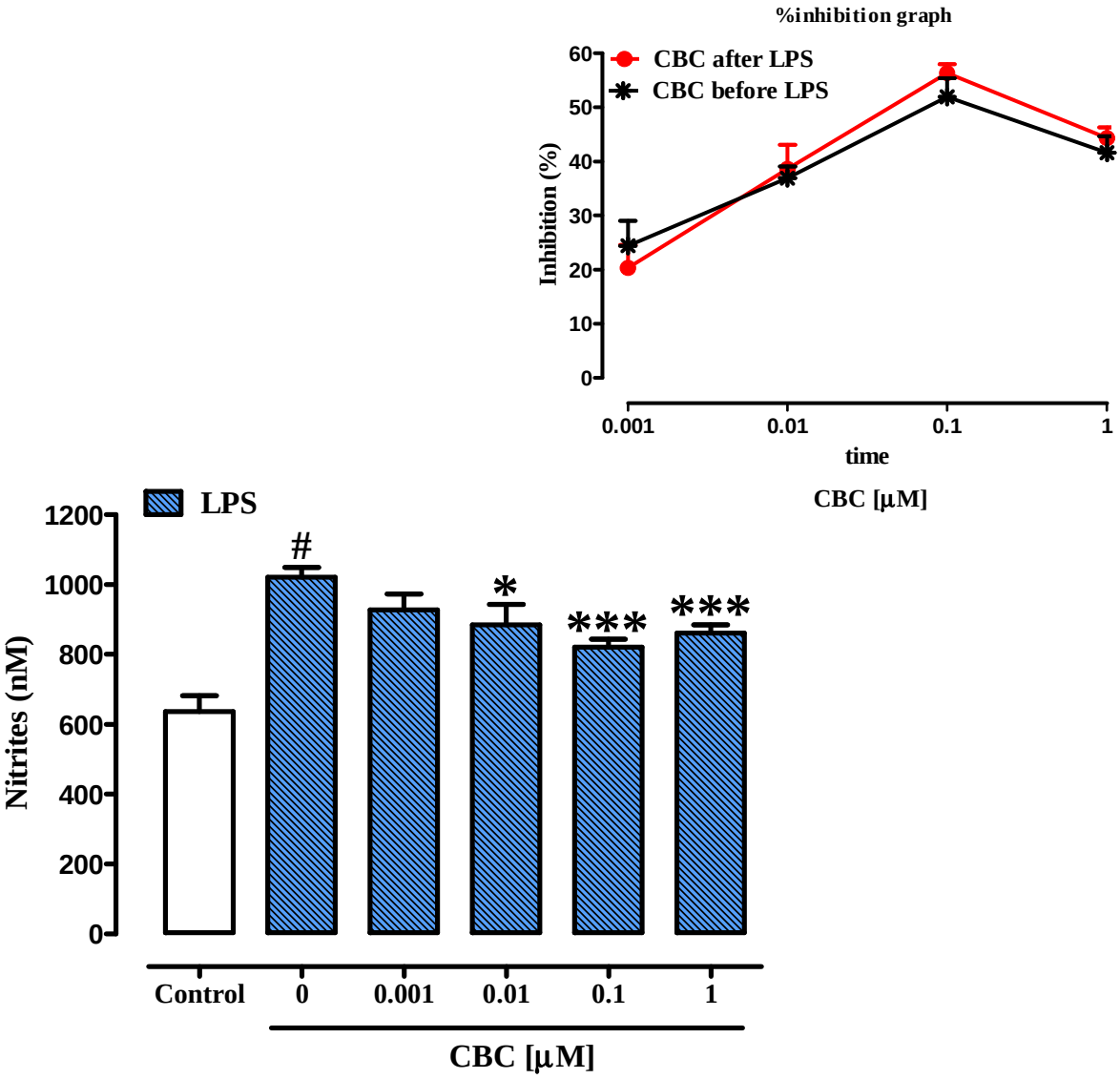

Figure 19. Inhibitory effect of cannabichromene on nitrite levels in the cell medium of murine peritoneal macrophages incubated with lipopolysaccharide (LPS, 1 µg/ml) for 18h. Cannabichromene (CBC, 0.001–1 µM) was added to the cell media 30 min before LPS challenge (*i.e.* 18.5 hours before nitrites assay). Results are mean±SEM of six experiments (in triplicates). $^{\#}p<0.001$ *vs* control; $^{*}p<0.05$ and $^{***}p<0.001$ *vs* LPS alone. The insert (on top of the figure) shows the effect of CBC (expressed as percentage of inhibition of the corresponding control values, with the difference between LPS and control considered as 100%) when given 30 min before LPS (CBC before LPS) or 15 hours after LPS (CBC after LPS). No statistically significant difference was observed between the two concentration–response curves reported in the insert.

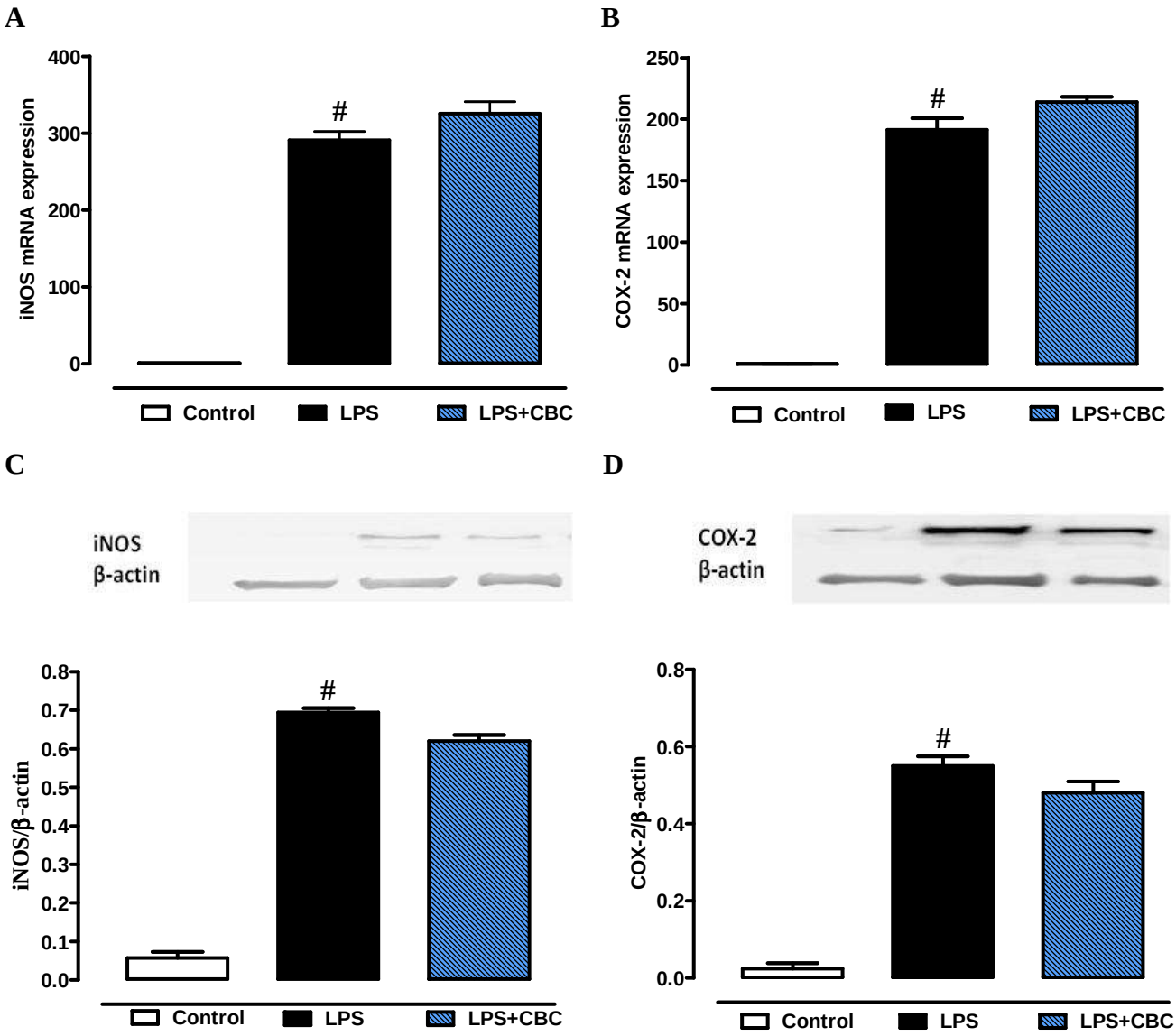

Figure 20. Inducible nitric oxide synthase (iNOS) (A, B) and cyclooxygenase-2 (COX-2) (C, D) mRNA and protein levels in cell lysates from macrophages incubated or not with lipopolysaccharide (LPS, 1 mg/mL) for 18 h. mRNA expression was evaluated by RT-PCR. The expression levels, normalized with respect to the reference genes, were scaled to the expression value of the control, considered as 1. The means of the quantitative-cycles (Cq) for the control were: 26.00 and 25.58 for iNOS and COX-2 respectively. Protein expression was evaluated by Western blot analysis. Cannabichromene (CBC, 1 μM) was added to the cell media 30 min before LPS challenge. $^{\#}p< 0.001$ versus control (n = 4–5 experiments).

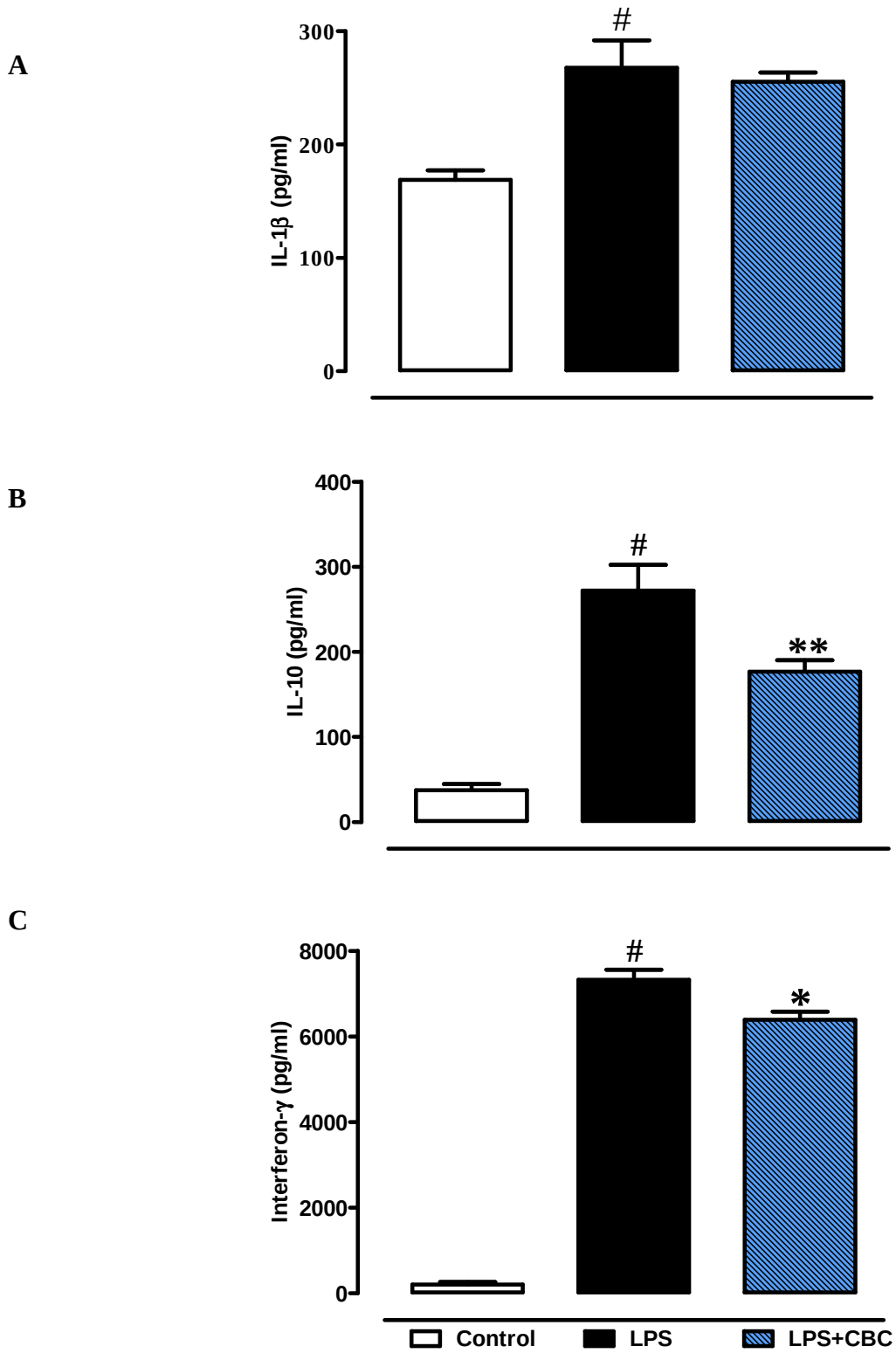

Figure 21. Effect of cannabichromene (CBC) on interleukin-1β (IL-1β) (A), interleukin-10 (IL-10) (B) and interferon-γ (C) levels detected in the cell media of macrophages incubated with lipopolysaccharide (LPS, 1 μg/ml) for 18h. CBC (1 μM) was added to the media 30 min before LPS challenge. Results are means±SEM of four experiments (in quadruplicates). $^{\#}p<0.001$ *vs* control, $^{*}p<0.05$ and $^{**}p<0.01$ *vs* LPS.

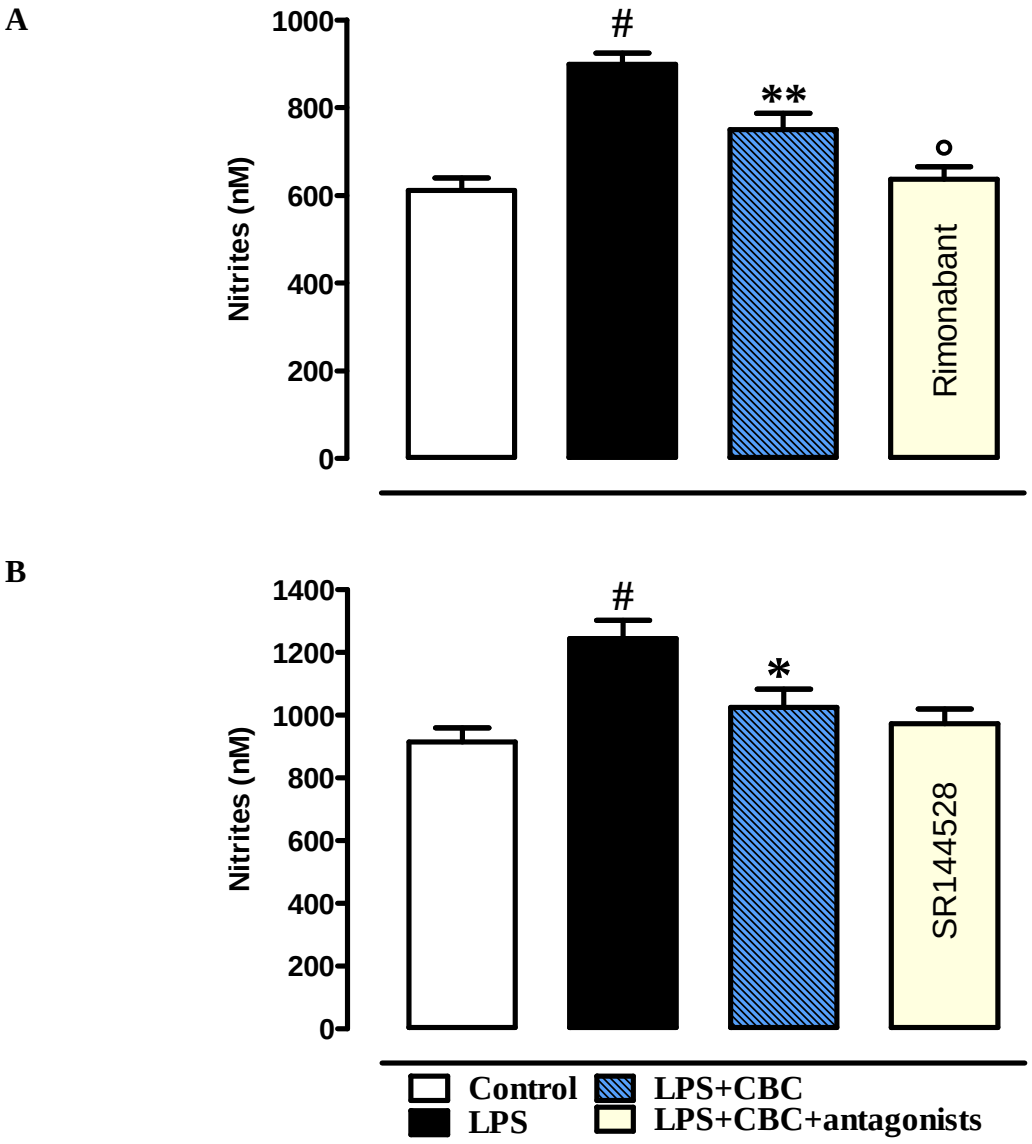

Figure 22. Effect of cannabichromene (CBC, 1 μM) alone or in presence of the cannabinoid CB_1 receptor antagonist rimonabant (0.1 μM) (A) as well as in the presence of the cannabinoid CB_2 receptor antagonist SR144528 (0.1 μM) (B) on nitrite levels in the cell medium of murine peritoneal macrophages incubated with lipopolysaccharide (LPS, 1 μg/ml) for 18 h. The antagonists were added to the cell media 30 min before CBC exposure. LPS (1 μg/ml for 18 h) was incubated 30 min after CBC. Results are means±SEM of three experiments (in triplicates). $^{\#}p<0.001$ *vs* control; $^{*}p<0.05$ and $^{**}p<0.01$ *vs* LPS; $^{\circ}p<0.05$ *vs* LPS+CBC.

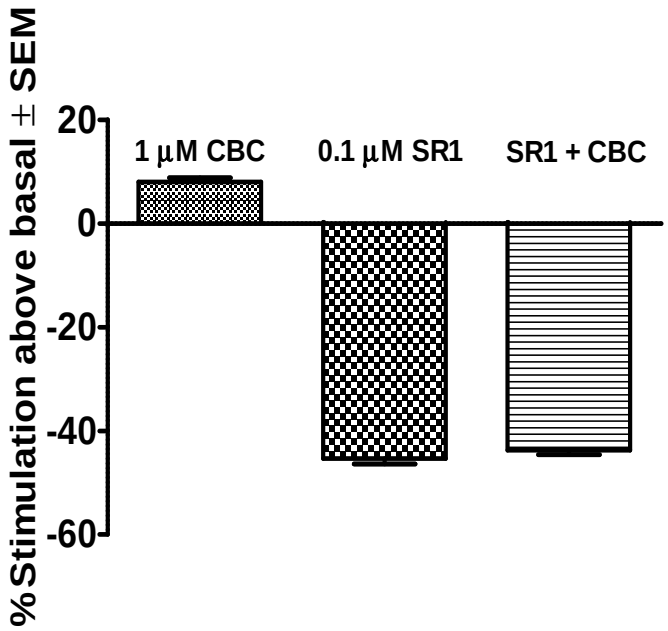

Figure 23. Effects of 1 µM cannabichromene alone (CBC), SR141716A alone (SR1, 0.1 µM; CB_1 receptor antagonist), and 1 µM CBC which was added 30 min after 0.1 µM SR141716A on [^{35}S]GTPγS binding to hCB_1- CHO cell membranes (n-12-16) (B). Symbols represent mean values ± SEM.

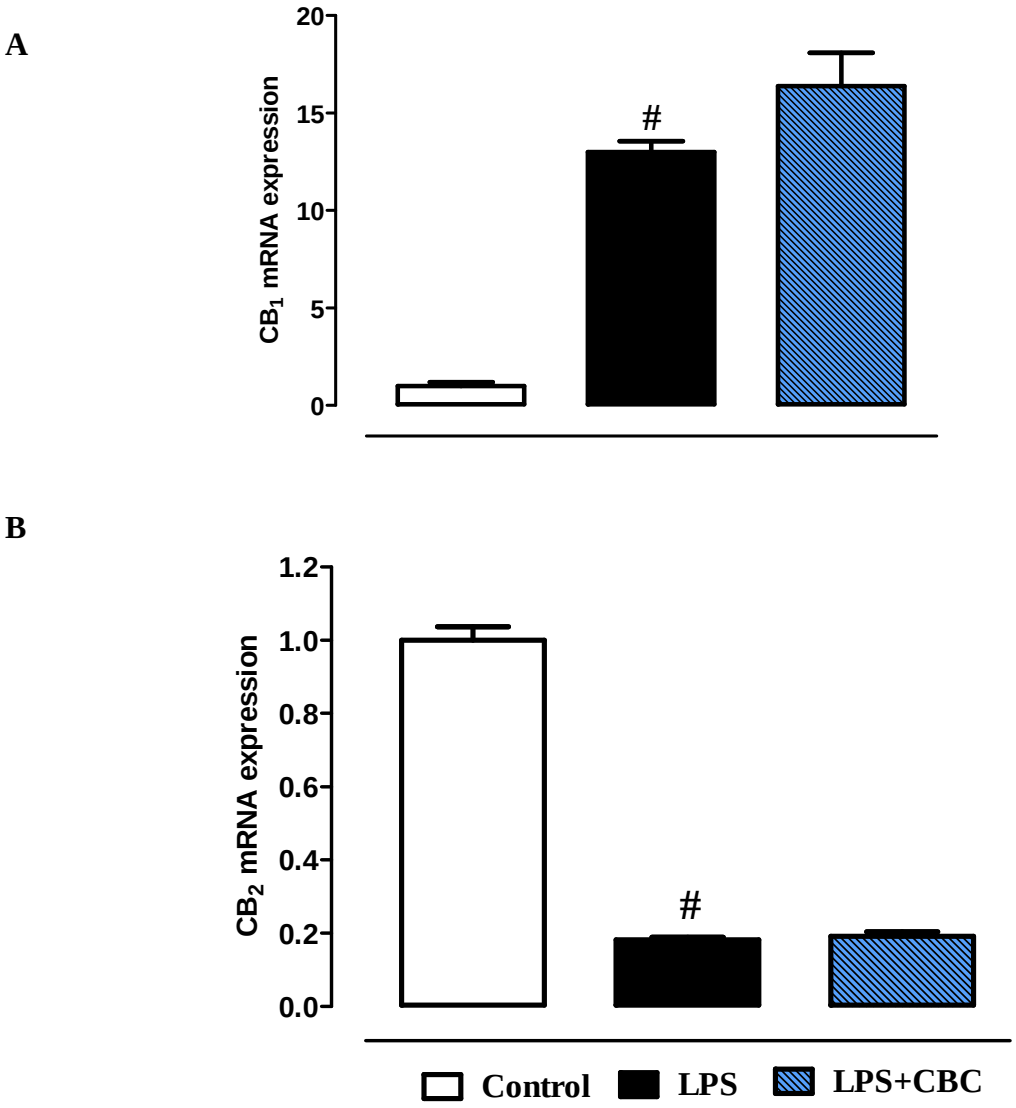

Figure 24. Relative mRNA expression of cannabinoid CB_1 receptor (A) and cannabinoid CB_2 receptor (B) in cell lysates from macrophages incubated or not with lipopolysaccharide (LPS, 1 µg/mL) for 18h: effect of cannabichromene (CBC, 1 µM, added to the cell media or 30 min before LPS challenge). The expression levels of mRNA, evaluated by RT-PCR and normalized with respect to the reference genes, was scaled for all conditions to the expression value of the control, considered as 1. The means of the quantitative-cycles (Cq) for the control values were: 31.2 (CB_1 receptor)and 24.48 (CB_2 receptor). The reaction background was 37.30 Cq and 36.60 Cq for CB_1 receptor and CB_2 receptor, respectively, at 40 reaction cycles. $^{\#}p < 0.001$ *vs* control ($n = 4$).

Table 2. Anandamide (AEA), 2-arachydonylglycerol (2-AG), palmitoylethanolamide (PEA) and oleoylethanolamide (OEA) levels in cell lysates from macrophages incubated or not with lipopolysaccharide (LPS, 1 μg/ml) for 18 h: effect of cannabichromene (CBC, 1 μM, added alone to the cell media or 30 min before LPS challenge).

Drugs	AEA	2-AG	PEA	OEA
Vehicle	0.58 ± 0.13	102.1 ± 15.9	18.4 ± 2.9	9.52 ± 1.4
CBC	0.65 ± 0.22	121.8 ± 38.9	18.3 ± 5.5	7.7 ± 2.4
LPS	1.85 ± 0.55#	122.7 ± 25.9	25.6 ± 6.0	9.73 ± 2.4
LPS + CBC	1.5 ± 0.72	173.9 ± 23.0	33.9 ± 4.2	20.4 ± 2.9*

Results (pmol/mg lipid) are mean±SEM of 3-6 experiments. $^{\#}p<0.01$ *vs* control; $^{*}p<0.05$ *vs* LPS

4.1.3 Δ^9-TETRAHYDROCANNABIVARIN (THCV)

4.1.3.1 Effect of THCV on DNBS-induced colitis (colon weight/colon length *ratio*)

DNBS administration caused a significant increase in colon weight/colon length *ratio* (Figure 25). THCV (0.3-5 mg/kg, intraperitoneally), at the dose of 1 mg/kg (given after the inflammatory insult), significantly reduced the effects of DNBS on colon weight/colon length *ratio* (Figure 25).

4.1.3.2 Effect of THCV on murine peritoneal macrophages viability

Cytotoxicity was evaluated performing the MTT assay and THCV, at the concentrations ranging from 0.001 to 1 µM, did not affect mitochondrial respiration (expressed as percentage of viability ± SEM) after 24-h exposure: [control 99.98 ± 4.58; THCV 0.001 µM 111.30 ± 3.87; THCV 0.01 µM 104.7 ± 6.45; THCV 0.1 µM 105.6 ± 6.18; THCV 1 µM 112.60 ± 6.88; THCV 10 µM 17.16 ± 1.62$^{\#}$; $^{\#}p<0.001$ *vs* control (n=3 experiments)]. Similarly, the CB_1 receptor antagonists rimonabant (0.1 µM) and the CB_2 receptor antagonist SR 144528 (0.1 µM) did not exert cytotoxic effects (data not shown).

4.1.3.3 Effect of THCV on nitrite levels in murine peritoneal macrophages

In cells not treated with LPS, THCV (1 µM) did not modify *per se* basal nitrite levels [nitrite levels (nM)±SEM: control 653.2±38.79, THCV 1µM 669.6±47.53; n=18]. LPS (1 µg/ml for 18 h) administration caused a significant increase in nitrite production (Figure 26). A pre-treatment with THCV (0.001-1 µM, both), 30 minutes before LPS, significantly reduced LPS-increased nitrite levels (Figure 26).

4.1.3.4 Effect of THCV on nitrite production in murine peritoneal macrophages in presence of selective cannabinoid receptors antagonists

Since some phytocannabinoids may exert pharmacological action via direct or indirect activation of cannabinoid receptors (Izzo *et al.*, 2009), in this set of experiments we verified if THCV effects on nitrite production was reduced or counteracted by selective CB_1 and CB_2 receptor antagonists. We observed that rimonabant (0.1 μM, CB_1 receptor antagonist) did not modify THCV (1 μM)-induced changes in nitrite production (Figure 27A). On the other hand, selective cannabinoid CB_2 receptor antagonists (SR 144528 0.1 μM) counteracted the effect of THCV on nitrite levels in LPS-stimulated macrophages (Figure 27B). The cannabinoid receptor antagonists employed in this set of experiments, at the concentrations used, did not affect, *per se*, nitrite levels induced by LPS (data not shown).

4.1.3.5 Effect of THCV on iNOS and COX-2 protein expression in LPS-treated macrophages

In order to verify if the effect of THCV on nitrite production in LPS-treated peritoneal macrophages was associated to changes in iNOS expression, we measured, by western blot, the protein levels of this enzyme. LPS administration caused an up-regulation on iNOS and COX-2 protein expression (Figure 28A-B). THCV (1 μM concentration), incubated 30 min before LPS stimulation, significantly reduced the LPS-induced changes in iNOS and COX-2 expression (Figure 28A-B**)**.

4.1.3.6 Effect of THCV on IL-1β levels in LPS-treated murine peritoneal macrophages

Interleukins are important cytokines involved in LPS-evoked responses in macrophages and IL-1β represents one of the main pro-inflammatory cytokines able to induce COX-2 expression in macrophages. The level of IL-1β in macrophages medium was significantly increased after 18-

h exposure to LPS (Figure 29). A pre-treatment with THCV (1 µM), incubated 30 min before LPS stimulation, significantly reduced IL-1β level in LPS-stimulated macrophages (Figure 29).

4.1.3.7 Effect of THCV on cannabinoid receptors mRNA expression in LPS-treated macrophages

LPS up-regulated CB_1 receptors and down-regulated CB_2 receptor mRNA expression in macrophages (Figure 30A-B). THCV did not affect cannabinoid CB_1 and CB_2 mRNA expression in un-stimulated macrophages, but it was able to reduce significantly the up-regulation of CB_1 mRNA expression induced in macrophages by LPS (Figure 30A).

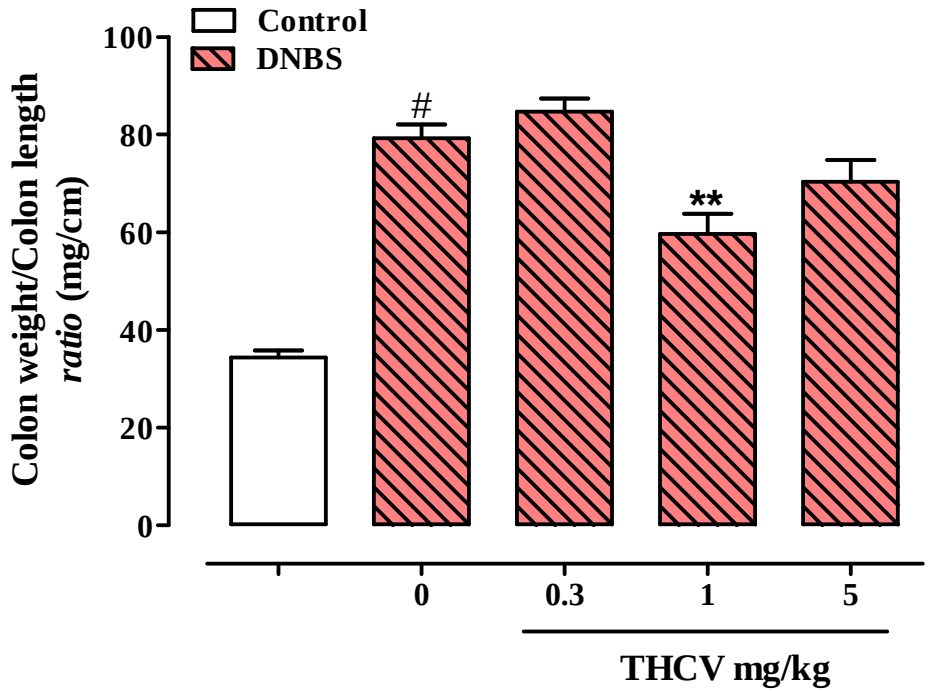

Figure 25. Dinitrobenzene sulfonic acid (DNBS)-induced colitis in mice. Colon weight/colon length *ratio* of colons from untreated and DNBS-treated mice in the presence or absence of Δ^9-tetrahydrocannabivarin (THCV). Tissues were analyzed 3 days after vehicle or DNBS (150 mg/kg, intracolonically) administration. THCV (0.3-5 mg/kg) was administered (*ip*) once a day for two consecutive days starting 24-h after the inflammatory insult. Bars are mean ± SEM of 12-15 mice for each experimental group. $^{\#}p<0.001$ *vs* control; $^{**}p<0.01$ *vs* DNBS alone.

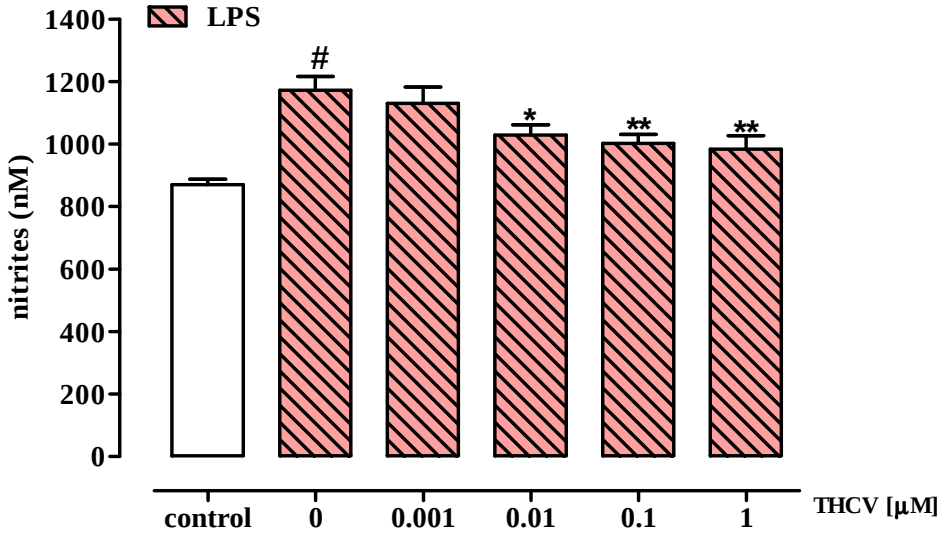

Figure 26. Inhibitory effect of Δ^9-tetrahydrocannabivarin (THCV) on nitrite levels in the cell medium of murine peritoneal macrophages incubated with lipopolysaccharide (LPS, 1 µg/ml) for 18 h. THCV (0.001-1 µM) was added to the cell media 30 min before LPS *stimulus* (*i.e.* 18.5 hours before nitrites assay). Results are mean±SEM of three experiments (in triplicates). $^{\#}p<0.001$ *vs* control; $^{*}p<0.05$ and $^{**}p<0.01$*vs* LPS alone.

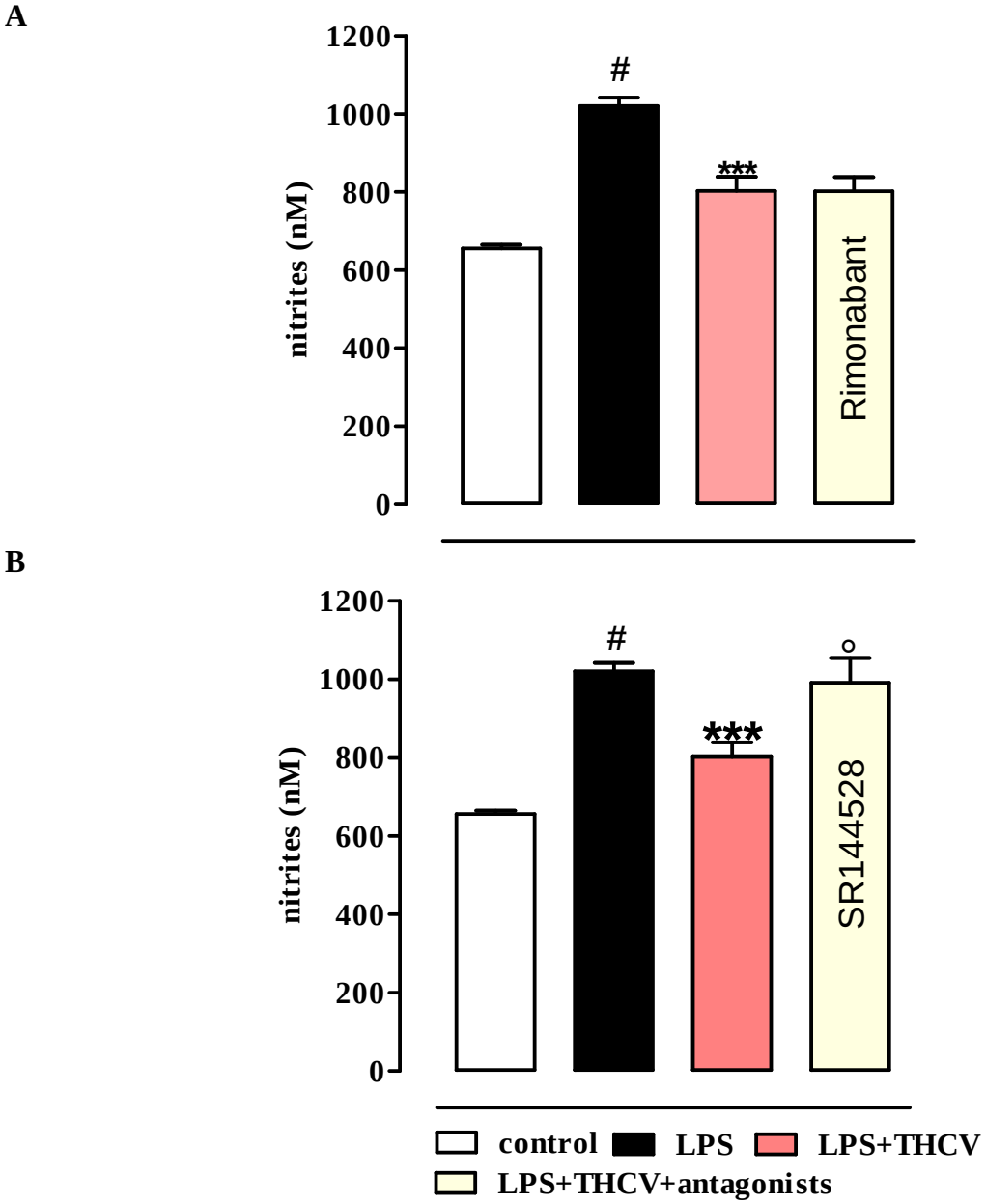

Figure 27. Effect of Δ^9-tetrahydrocannabivarin (THCV, 1 μM) alone or in presence of the cannabinoid CB_1 receptor antagonist rimonabant (0.1 μM) (A) and of the cannabinoid CB_2 receptor antagonist SR144528 (0.1 μM) (B) on nitrite levels in the cell medium of murine peritoneal macrophages incubated with lipopolysaccharide (LPS, 1 μg/ml) for 18 h. The antagonists were added to the cell media 30 min before THCV exposure. LPS (1 μg/ml for 18 h) was incubated 30 min after THCV. Results are means±SEM of three experiments (in triplicates). $^{\#}p<0.001$ *vs* control; $^{***}p<0.001$ *vs* LPS; $^{\circ}p<0.001$*vs* LPS+THCV.

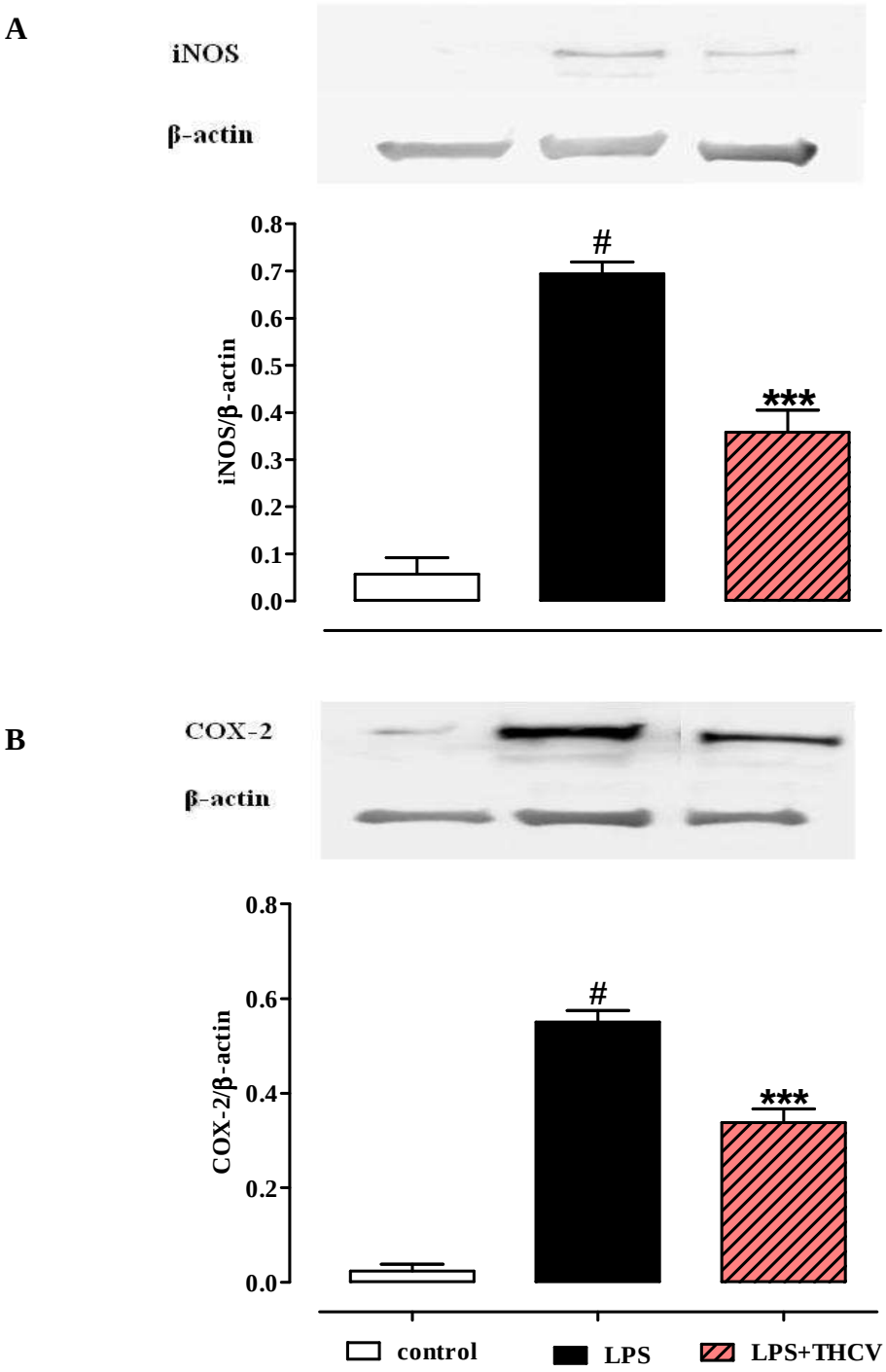

Figure 28. Inducible nitric oxide synthase (iNOS) (A) and cyclooxygenase-2 (COX-2) (B) protein levels in cell lysates from macrophages incubated or not with lipopolysaccharide (LPS, 1 µg/mL) for 18 h evaluated by Western blot analysis. Δ^9-tetrahydrocannabivarin (THCV, 1 µM) was added to the cell media 30 min before LPS challenge. $^{\#}p< 0.001$ *vs* control; $^{***}p< 0.001$ *vs* control (n = 4–5 experiments).

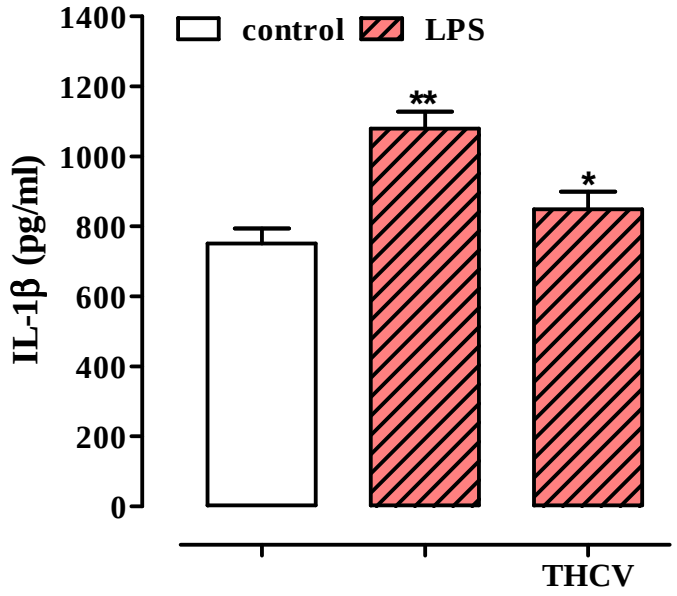

Figure 29. Effect of Δ^9-tetrahydrocannabivarin (THCV) on interleukin-1β (IL-1β) levels detected in the cell media of macrophages incubated with lipopolysaccharide (LPS, 1 μg/ml) for 18h. THCV (1 μM) was added to the media 30 min before LPS challenge. Results are means±SEM of three experiments $^{**}p<0.01$ *vs* control, $^{*}p<0.05$ *vs* LPS.

A

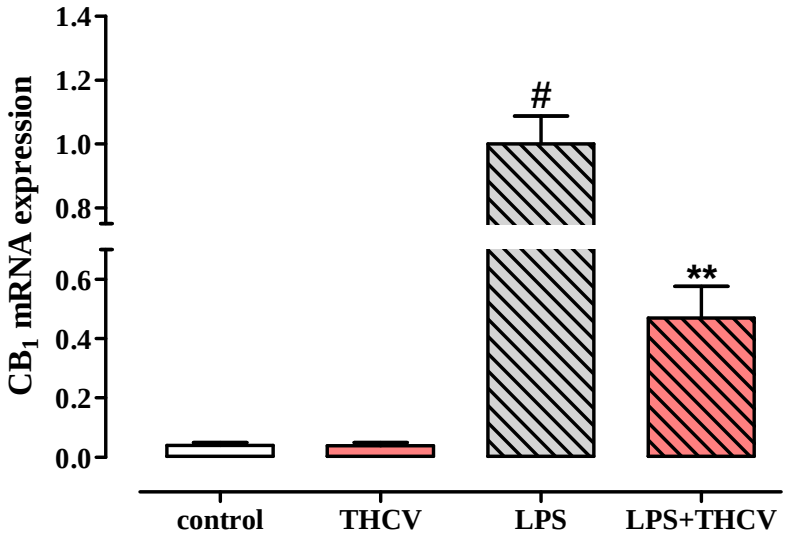

B

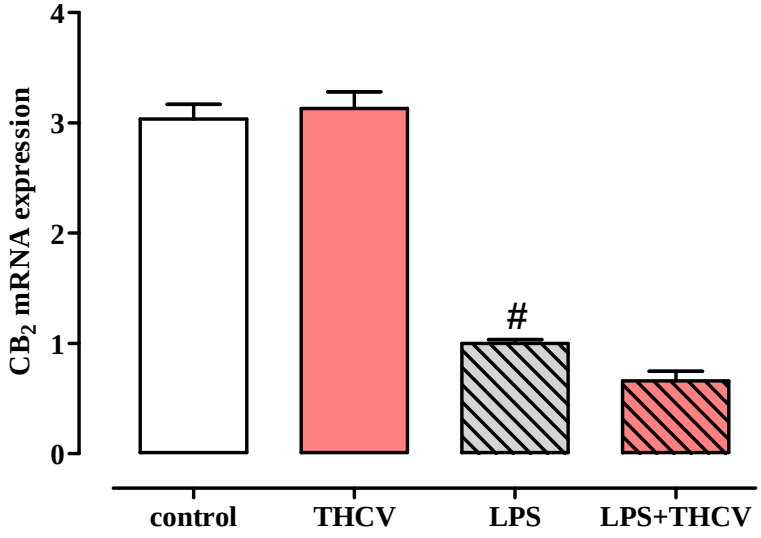

Figure 30. Relative mRNA expression of cannabinoid CB_1 receptor (A), cannabinoid CB_2receptor (B) in cell lysates from macrophages incubated or not with lipopolysaccharide (LPS, 1 µg/ml) for 18h. Δ^9-tetrahydrocannabivarin (THCV, 1 µM) was added alone to the cell media or 30 min before LPS challenge. Data were analysed by GENEX software for group comparisons and statistical analysis. Results are means±SEM of four experiments. $^{\#}p< 0.001$ *vs* control; $^{**}p< 0.01$ *vs* LPS.

4.2 COLON CANCER

4.2.1 CANNABIDIOL (CBD) AND *CANNABIS*-EXTRACT WITH HIGH CONTENT IN CANNABIDIOL (CBD BDS)

4.2.1.1 Effect of CBD and CBD BDS on the formation of aberrant crypt foci (ACF), polyps and tumors

The carcinogenic agent AOM given alone induced the expected appearance of ACF (Figure 31B), polyps (Figure 31C) and tumours (Figure 31D) after 3 months of treatment. CBD (1 mg/kg, *ip*) significantly reduced AOM-induced ACF (67% inhibition) (Figure 31B), polyps (57% inhibition) (Figure 31C) and tumours (66% inhibition) (Figure 31D). CBD (5 mg/kg, *ip*) significantly reduced only the formation of polyps (Figure 31C). The *Cannabis*-extract with high content in cannabidiol, here named CBD BDS, at the dose of 5 mg/kg (*ip*), significantly reduced AOM-induced ACF (86% inhibition) and polyps (79% inhibition). CBD BDS also reduced tumour formation by 40%, although a conventional statistical significance was not fully achieved (Figure 32B-D).

4.2.1.2 Effect of CBD and CBD BDS in xenograft colorectal tumours in mice

To assess the potential curative effect of CBD and CBD BDS on colorectal cancer, athymic nude mice bearing colorectal tumor xenografts were treated daily with CBD and CBD BDS (both at 5 mg/kg dose, *ip*). CBD was able to reduce tumour volume comparison to the control mice (mice not receiving any treatment) (Figure 31A). On the other hand, the average tumour volume in mice treated with CBD BDS was significantly lower compared with vehicle-treated control mice (Figure 32A). For example, 4 days after the commencement of CBD BDS challenge, the average tumor volume in control mice (mean±SEM: 1130±171.6mm^3) was approximately 1.5 fold higher as compared to mice treated with 5 mg/kg CBD BDS

(mean±SEM: 755±124 mm^3). However, no differences in tumour growth were observed after 7-days CBD BDS treatment.

4.2.1.3 Effect of CBD on COX-2, iNOS, phospho-Akt and caspase-3 protein expression in colonic tissues

Western blot analysis revealed protein expression of COX-2, iNOS, phospho-Akt and caspase-3 (Figure 33A-D) in colonic tissues of both healthy and AOM-treated animals. The densitometric analysis indicated a significant increase in the expression of COX-2 (Figure 33A), iNOS (Figure 33B) and phospho-Akt (Figure 33C) in the colons of AOM-treated mice. CBD (1 mg/kg) did not cause significant changes in the expression of COX-2 and iNOS in AOM-treated animals (Figure 33A-B) but significantly reduced AOM-induced Akt protein phosphorylation (Figure 33C). AOM treatment caused a significant down-regulation of cleaved caspase-3 expression, which was restored by cannabidiol (Figure 33D).

4.2.1.4 Effect of CBD and CBD BDS on cell viability

The effect of CBD and CBD BDS on cell viability was evaluated in human colorectal cancer cell lines such as Caco-2, HCT116 and DLD-1cells as well as in human healthy colonic epithelial cell line (HCEC) by using the neutral red assay. CBD, at the concentration ranging from 0.01 to 10 μM, and CBD BDS, at the concentration ranging from 1 to 5 μM, did not affect both colorectal cancer and healthy cells viability (expressed as percentage of viability ± SEM) after 24-h exposure: [Caco-2 cells: control 100.2 ± 6.1; CBD 0.01 μM: 98.0 ± 8.6; CBD 0.1 μM: 100.5 ± 2.0; CBD 1 μM: 97.0 ± 2.47; CBD 10 μM: 99.25 ± 4.5; HCT 116 cells: control 100.1 ± 2.5; CBD 0.01 μM: 105.3 ± 2.5; CBD 0.1 μM: 102.0 ± 5.5; CBD 1 μM: 101.7 ± 2.5; CBD 10 μM: 106.1 ± 1.7; control 100 ± 7.05; CBD 1 μM: 111.4 ± 6.56; CBD 3 μM: 116.3 ± 6.49; CBD 5 μM: 110.4 ± 4.30; CBD BDS 1 μM: 108.3 ± 5.11; CBD BDS 3 μM: 107 ± 4.75;

CBD BDS 5 µM: 105.5 ± 5.44; DLD-1 cells: control 100 ± 5.84; CBD BDS 1 µM: 106 ± 4; CBD BDS 3 µM: 103 ± 3.3; CBD BDS 5 µM: 99.6 ± 3.7; CBD 1 µM: 106.0 ± 5.4; CBD 3 µM: 102.8 ± 6.99; CBD 5 µM: 102.9 ± 5.18; HCEC cells: control 100 ± 7.05; CBD BDS 1 µM: 86.74 ± 4.8; CBD BDS 3 µM: 95.19 ± 5.93; CBD BDS 5 µM: 92.81 ± 4.08; CBD 1 µM: 101.6 ± 4.99; CBD 3 µM: 101.6 ± 4.99; CBD 5 µM: 97.03 ± 5.66) (n=3 experiments for each cell line). DMSO (20% v/v), used as positive control, significantly reduced both colorectal cancer and healthy cells viability (data not shown).

4.2.1.5 Effect of CBD and CBD BDS on healthy colonic epithelial cells (HCEC) proliferation

In order to verify if the effect of *Cannabis*-based products was specific for cancer cells, we investigated the effect of both CBD and CBD BDS on proliferation in HCEC. Both CBD and CBD BDS, up to 5 µM, did not affect significantly proliferation in HCEC (Figure 34A-B). Spermine (300 µM), used as a positive control, significantly reduce HCEC proliferation (Figure 34A-B).

4.2.1.6 Effect of CBD and CBD BDS on human colon adenocarcinoma cells proliferation

The effect of non-cytotoxic concentrations of CBD (0.01–10 µM) was evaluated on cell proliferation in Caco-2 (Figure 35A), HCT 116 (Figure 35 C and Figure 36 C) and DLD-1 (Figure 36 A) cells by MTT assay and ^{3}H-thymidine incorporation (only for Caco-2 cells and HCT 116) (Figure 35B and Figure 35D respectively). In the cell lines tested CBD, with both techniques, exerted a significant antiproliferative effect. The effect of non-cytotoxic concentrations of CBD BDS (0.3–5 µM) was evaluated on cell proliferation in both DLD-1 (Figure 36B) and HCT116 cells (Figure 36D) using the MTT assay in which it showed a

significant antiproliferative effect. No difference in potency and efficacy were observed between CBD and CBD BDS (see inserts on top of figure 36).

4.2.1.7 Effect of CBD and CBD BDS on colorectal cancer cell proliferation in presence of selective receptor antagonists

Using the MTT assay, we found that the effect of cannabidiol (CBD, 10 μM) on Caco-2 cell proliferation was counteracted by rimonabant (0.1 μM) and AM251 (1 μM) (two CB_1 receptor antagonists), capsazepine (1 μM, a TRPV1 receptor antagonist) and GW9662 (10 μM, a PPARγ receptor antagonist) (Figure 37A-B-E-F). By contrast, the effect of CBD was not significantly changed by SR144528 (10 μM) and AM630 (1 μM) (CB_2 receptor antagonists) (Figure 37C-D). In other set of experiments we investigated the effect of CBD and CBD BDS on DLD-1 cell proliferation in the presence of selective cannabinoid CB_1 and CB_2 receptor antagonists. We found that selective cannabinoid CB_1 receptor antagonists (*i.e.* rimonabant 0.1 μM and AM251 1μM) counteracted the effect of both CBD and CBD BDS (both at 3 μM concentration) on cell proliferation (Figure 38A-D). On the other hand, selective cannabinoid CB_2 receptor antagonists (*i.e.* SR144528 0.1 μM and AM630 1 μM) counteracted the effect of CBD BDS (3 μM), but not the effect of pure CBD (3 μM), on cell proliferation (Figure 39A-D). All receptor antagonists employed in this set of experiments were not cytotoxic and did not affect, *per se*, cell proliferation (data not shown).

4.2.1.8 CBD and CBD BDS: binding profiles on cannabinoid receptors

Because selective CB_1 and CB_2 receptor antagonists differently affected the response to CBD and CBD BDS in DLD-1 cell line, we performed displacement binding assays to compare the cannabinoid binding profiles of CBD to CBD BDS. CBD BDS showed greater affinity for cannabinoid receptors than pure CBD in both hCB_1-CHO and hCB_2-CHO cell membranes

(Figure 40A-B). The CBD BDS Ki values for CB_1 and CB_2 receptors were 0.18 μM and 0.14 μM, respectively; pure CBD only (and partially) displaced [^{3}H]CP55940 at the highest concentration tested (10 μM) (Figure 40A-B).

4.2.1.9 Effect of CBD on endocannabinoids, palmitoylethanolamide and oleoylethanolamide levels in Caco-2 cells

The exposure to CBD (0.1–10 μM) for 24 h induced an increase in 2-AG levels (Figure 41B) in *sub*-confluent Caco-2 cells. The effect was significant for the 0.1 μM concentration. No significant differences were observed in anandamide, palmitoylethanolamide and oleoylethanolamide levels following CBD (0.1–10 μM) incubation for 24 h (Figure 41A-C-D).

4.2.1.10 Effect of CBD on genotoxicity in Caco-2 cells

Compared to the control cells (A), CBD (10 μM) alone did not significantly affect DNA damage after 24-h exposure (C), suggesting the absence of a genotoxic effect (Figure 42). Exposure of Caco-2 cells to hydrogen peroxide H_2O_2 (75 μM) produced a significant increase in the percentage of DNA in comet tails (B), whereas a pre-treatment with CBD (10 μM) (D) for 24 h significantly reduced the H_2O_2-induced DNA damage (Figure 42).

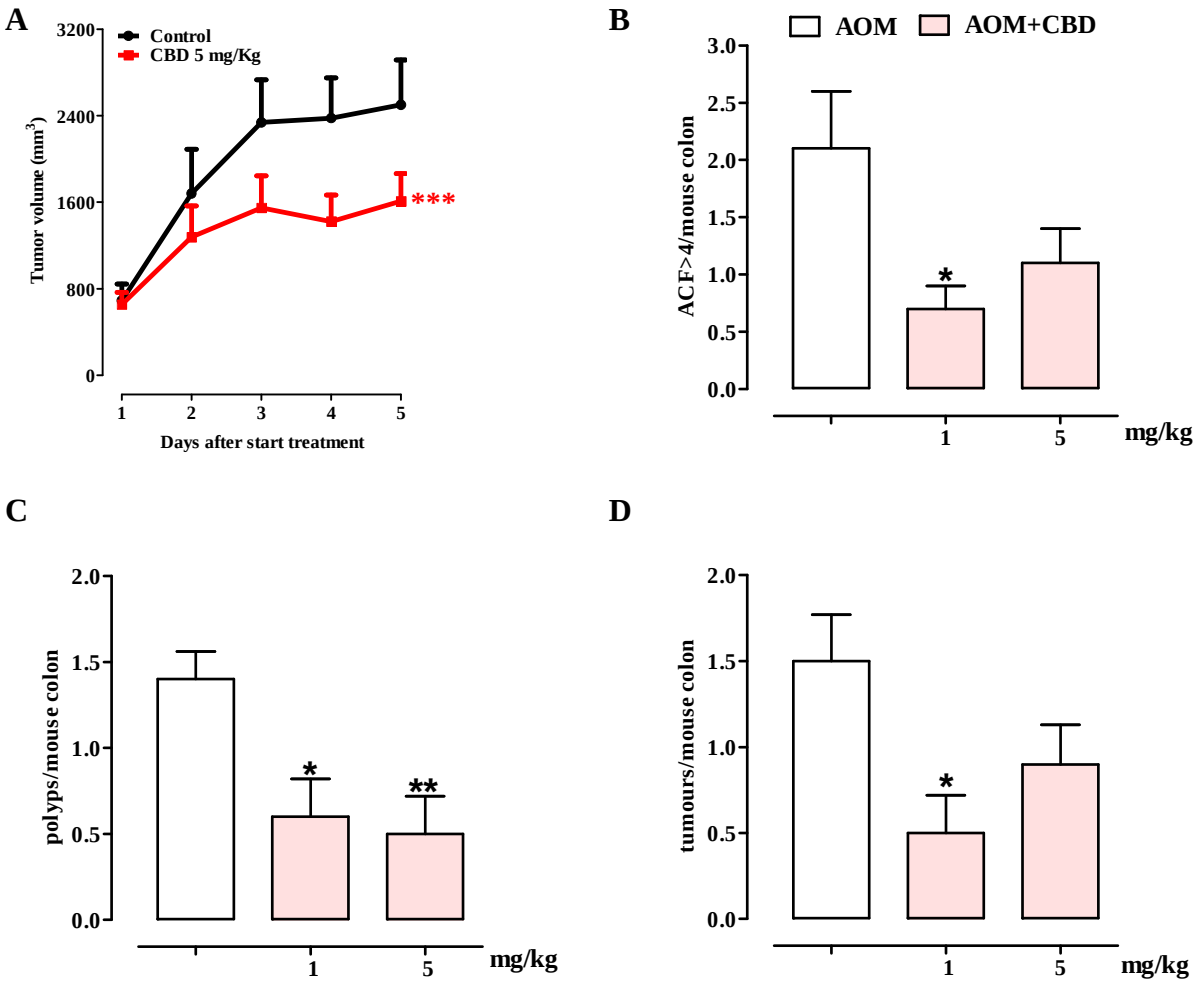

Figure 31. Cannabidiol (CBD, 1-5 mg/kg, *ip*) reduces colon carcinogenesis *in vivo*. Figure 31A reports the inhibitory effect of CBD (5 mg/kg, *ip*) on xenograft formation induced by subcutaneous injection of HCT 116 cells into the right flank of athymic female mice. Treatment started approximately after 10 days of cell inoculation. Tumour size was measured every day by digital caliper measurements, and tumour volume was calculated. CBD (5 mg/kg, *ip*) was given every day for the whole duration of the experiment. Figure 31B-D reports the inhibitory effect of CBD (1-5 mg/kg, *ip*) on aberrant crypt foci with four or more crypts (ACF≥4/mouse) (B), polyps (C) and tumours (D) induced in the mouse colon by azoxymethane (AOM). CBD was given *ip* three times a week for the whole duration of the experiment starting 1 week before the first administration of AOM. Measurements were performed 3 months after the first injection of AOM. Each point for xenograft curve represents the mean ± SEM of 8 animals for each experimental group. $^{***}p<0.001$; ANOVA CBD curve *vs* control curve. For AOM model, each bar represents bar represents the mean±SE mean of 9–11 mice. $^{*}p<0.05$ and $^{**}p<0.01$ *vs* vehicle

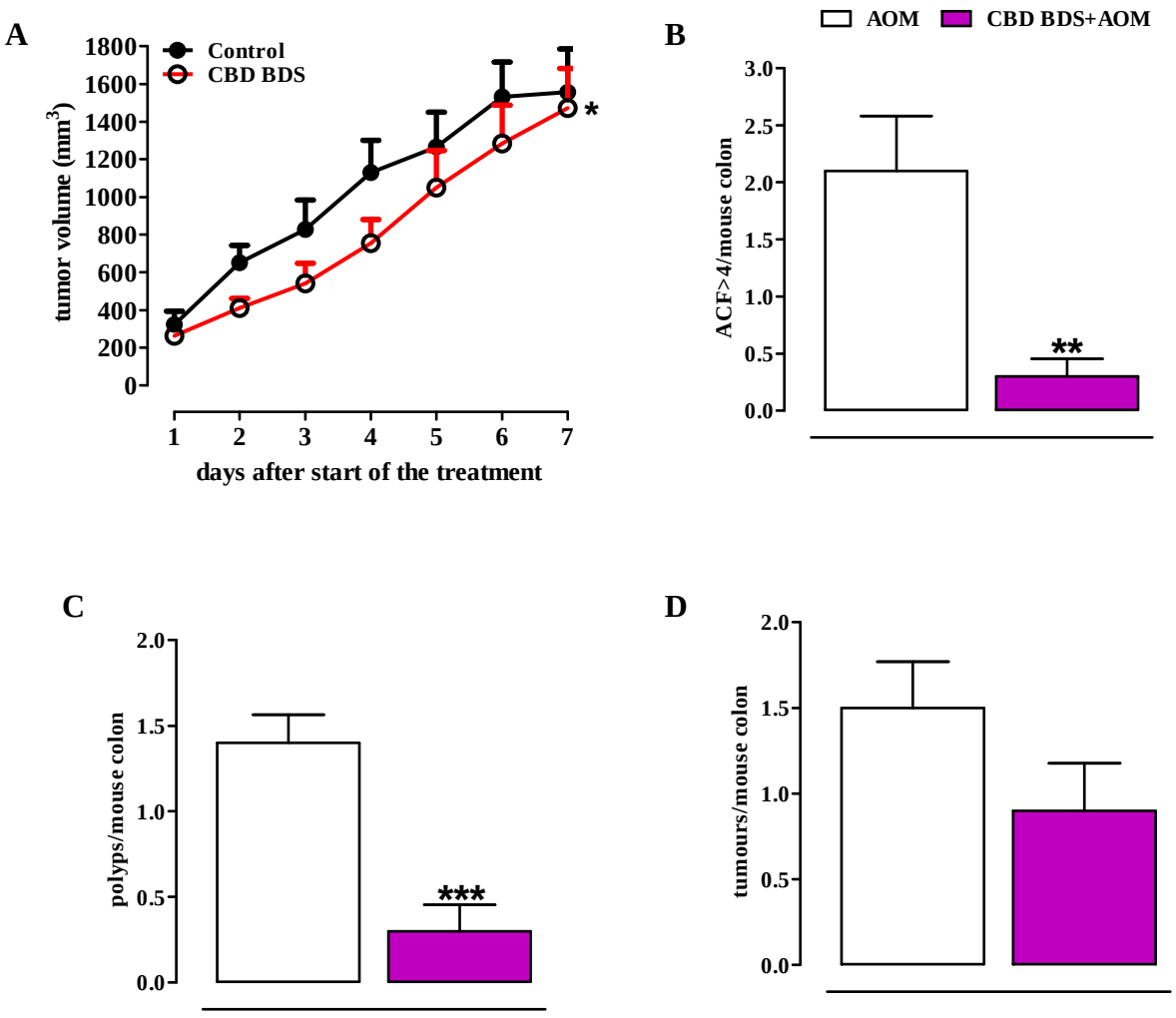

Figure 32. A *Cannabis sativa* extract with high content of CBD (CBD BDS, 5 mg/kg, *ip*) reduces colon carcinogenesis *in vivo*. Figure 32A reports the inhibitory effect of *Cannabis sativa* extract with high content of CBD (CBD BDS, 5 mg/kg, *ip*) on xenograft formation induced by subcutaneous injection of HCT 116 cells into the right flank of athymic female mice. Approximately treatment started after 10 days of cell inoculation. Tumour size was measured every day by digital caliper measurements, and tumour volume was calculated. CBD BDS (5 mg/kg, *ip*) was given every day for the whole duration of the experiment. Figure 32B-D report the inhibitory effect of CBD BDS (5 mg/kg, *ip*) on aberrant crypt foci with four or more crypts (ACF≥4/mouse) (B), polyps (C) and tumours (D) induced in the mouse colon by azoxymethane (AOM). CBD BDS was given *ip* three times a week for the whole duration of the experiment starting 1 week before the first administration of AOM. Measurements were performed 3 months after the first injection of AOM. Each point for xenograft curve represents the mean ± SEM of 8 animals for each experimental group. $^{*}p<0.05$; ANOVA CBD BDS curve *vs* control curve. For AOM model, each bar represents the mean±SEM of 9–11 mice. $^{**}p<0.01$ and $^{***}p<0.001$ *vs* AOM.

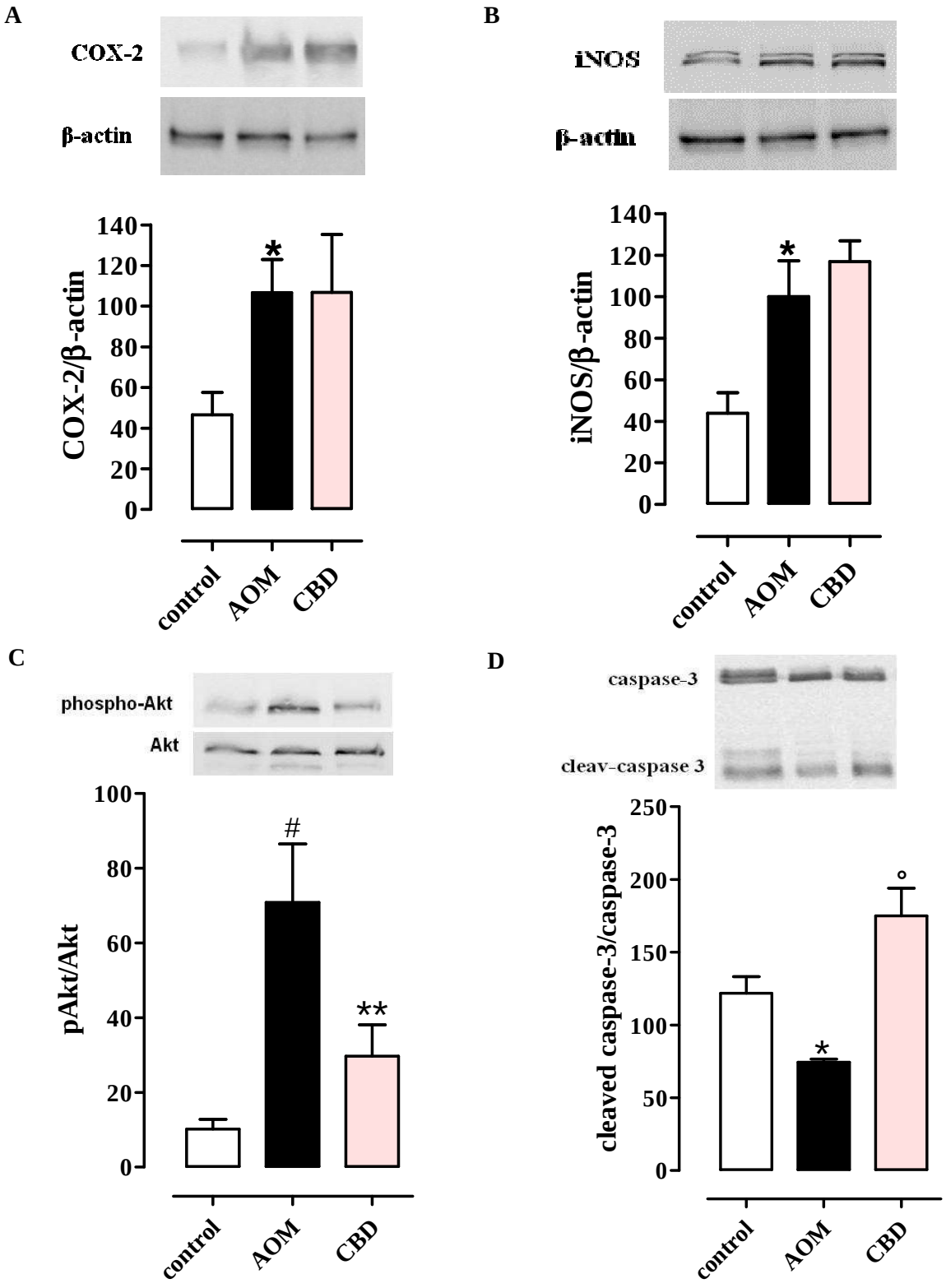

Figure 33. Cyclooxygenase-2 (COX-2) (A), inducible nitric oxide synthase(iNOS) (B), phospho-Akt (C) and cleaved caspase-3 (active fragmentp17) (D) expression in colonic tissues of mice treated or not with AOM:effect of cannabidiol (CBD, 1 mg/kg*ip*). Each bar represents themean±SE mean of four/five independent experiments. $^{*}p<0.05$ and $^{\#}p<0.001$*vs*control; **p<0.01 and $^{\circ}p<0.001$*vs* AOM.

A

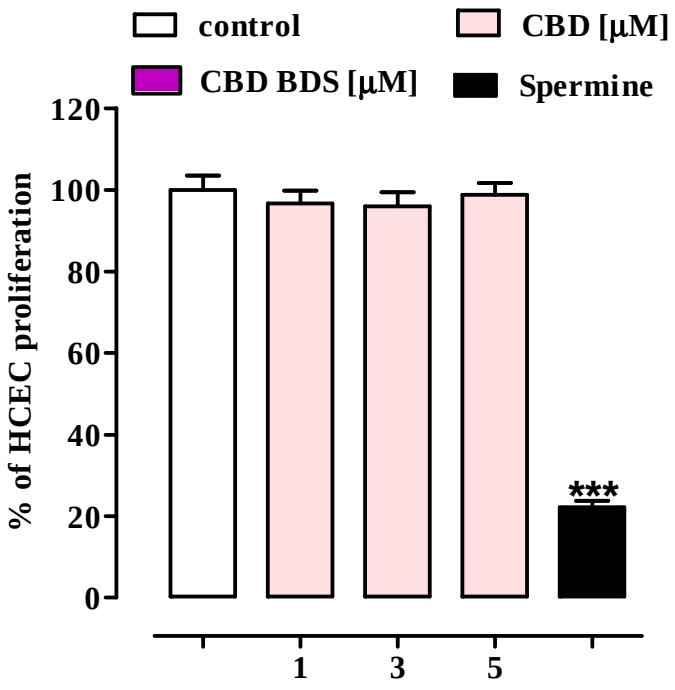

B

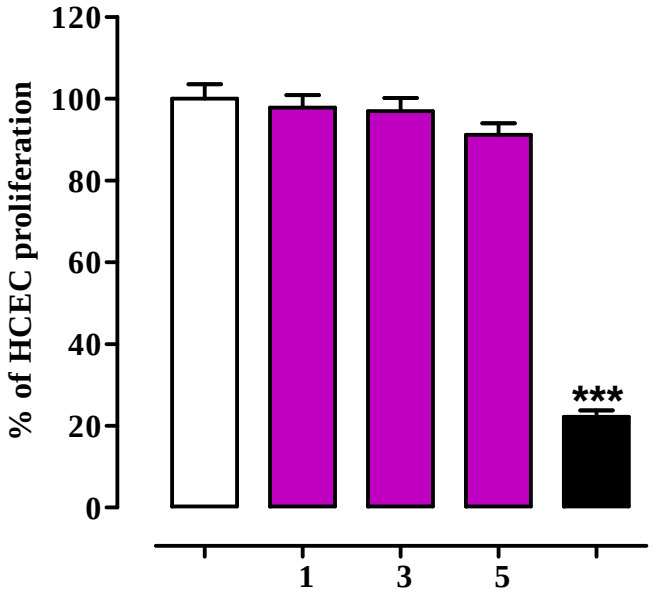

Figure 34. Effect of cannabidiol(CBD, 1–5 μM, 24-h exposure) and a *Cannabis sativa* extract with high content of CBD (CBD BDS, 1-5 μM) on cell proliferation in healthy human colonic epithelial cells (HCEC). Proliferation rate was studied using the MTT assay. Each bar represents the mean±SEM of two independent experiments. Spermine (300 μM) was used as a positive control. $^{***}p<0.001$ *vs* control.

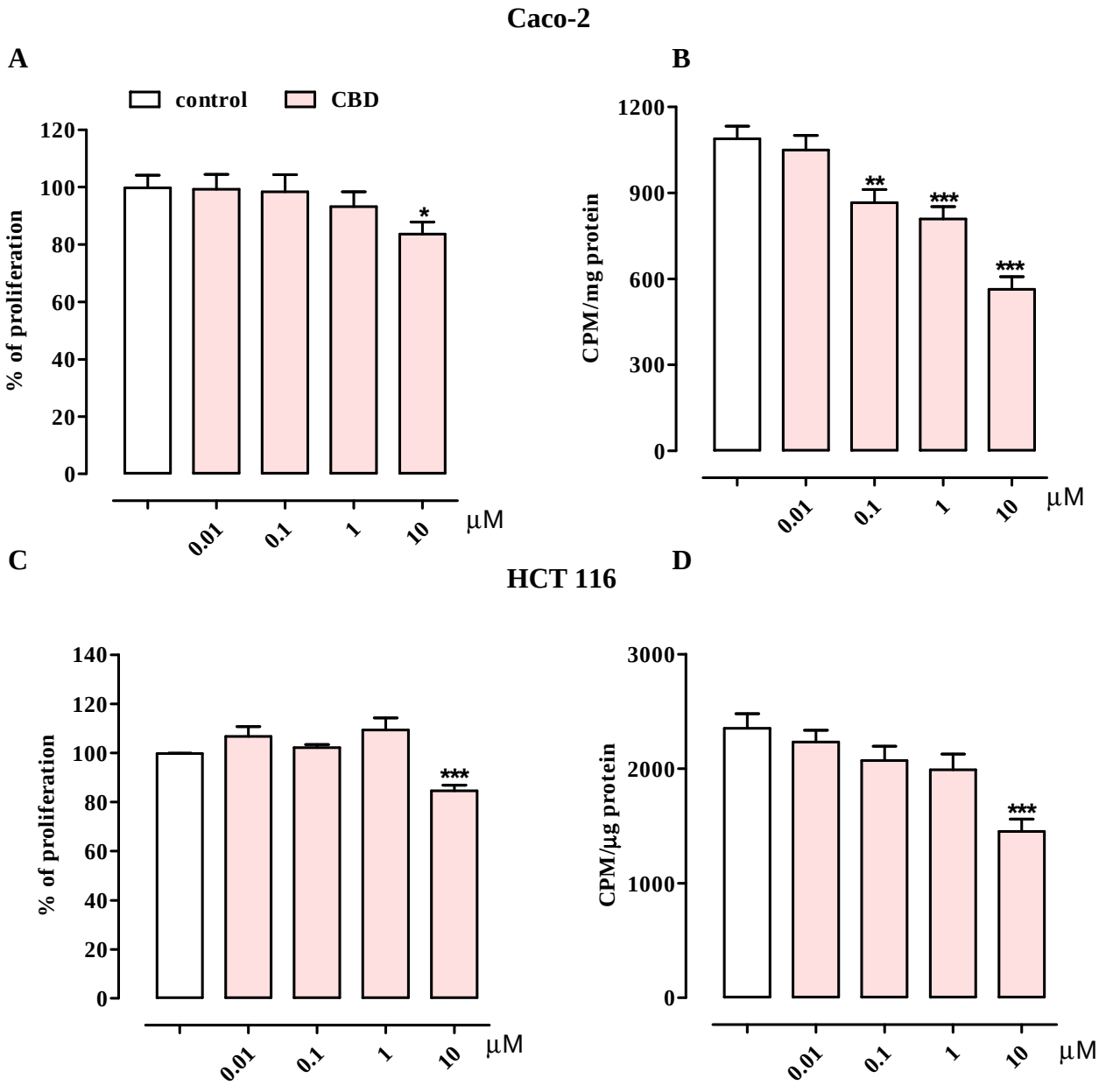

Figure 35. Antiproliferative effects of cannabidiol (CBD, 0.01–10 µM, 24h exposure) in Caco-2 (A, B) and HCT116 (C, D) cells. Proliferation rate was studied using two different techniques: the MTT assay (A, C) and the ^{3}H-thymidine incorporation (B, C). Each bar represents the mean±SE mean of three independent experiments. $^{*}p<0.05$, $^{**}p<0.01$ and $^{***}p<0.001$ *vs* control.

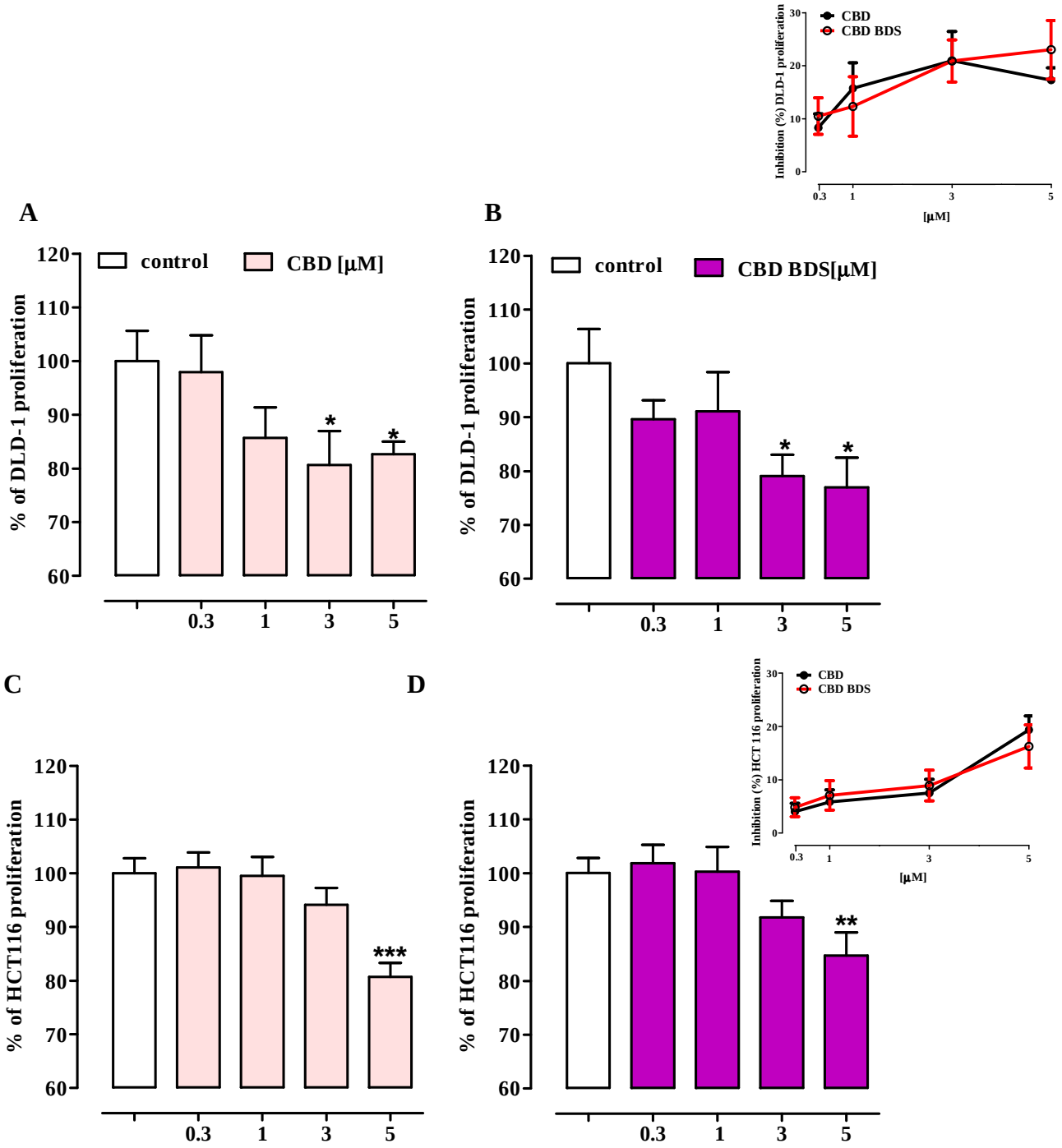

Figure 36. Antiproliferative effects of cannabidiol (CBD, 0.3–5 µM, 24-h exposure) and a *Cannabis sativa* extract with high content of CBD (CBD BDS, 0.3–5 µM, 24-h exposure) in DLD-1 (A-B) and HCT 116 cells (C-D). Proliferation (expressed as percentage of cell proliferation) rate was studied using the MTT assay. Each bar represents the mean±SEM of three independent experiments. $^{*}p<0.05$, $^{**}p<0.01$ and $^{***}p<0.001$ *vs* control. The inserts (on top of the figures) show the effect of CBD and CBD BDS (expressed as percentage of cell proliferation inhibition). No statistically significant difference was observed between the cannabinoids response curves reported in the inserts.

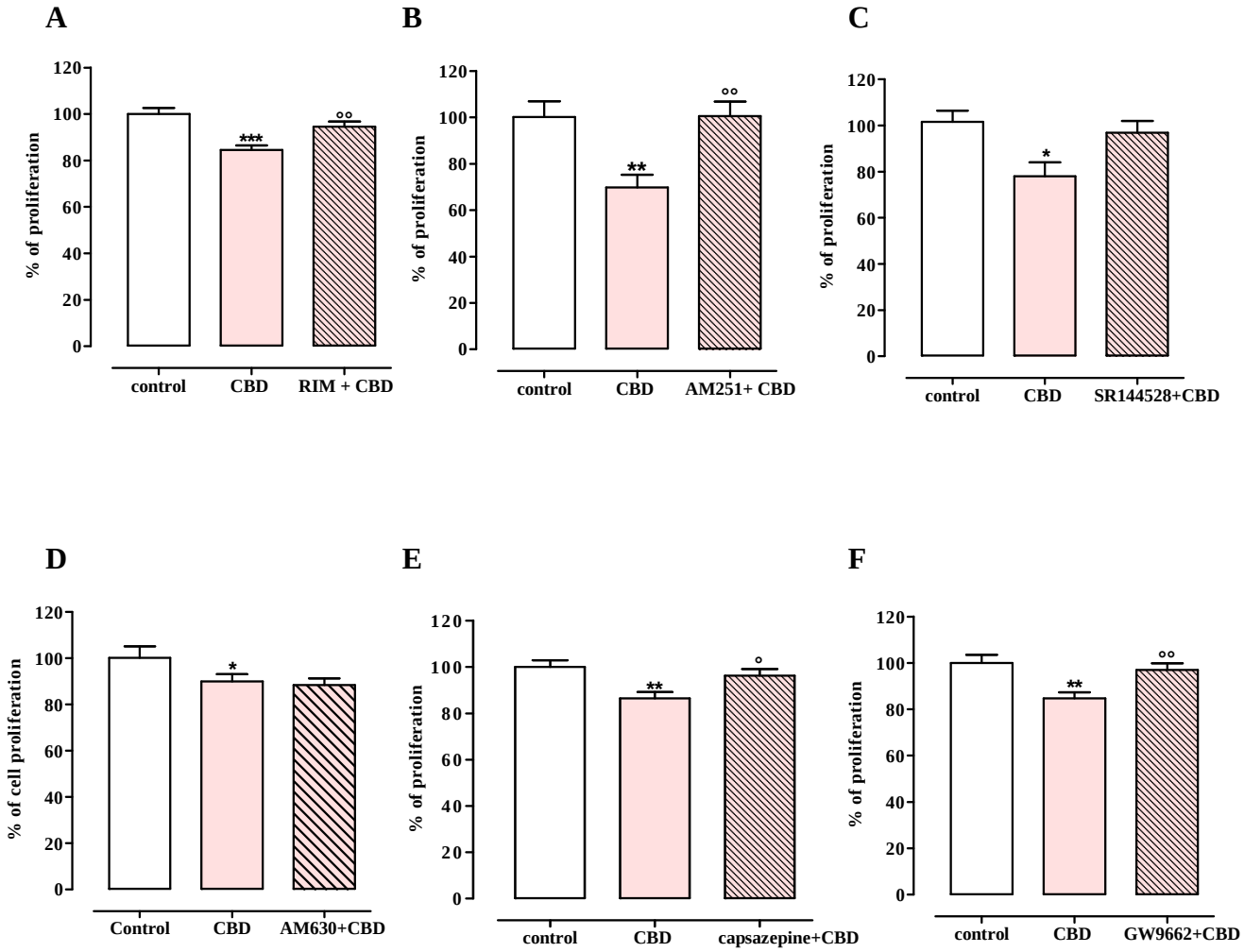

Figure 37. Antiproliferative effects, evaluated by MTT assay, of cannabidiol (CBD, 10μM, 24 h-exposure) alone or in the presence of rimonabant (RIM, 0.1 μM, A) and AM251 (1 μM, B) (two selective CB_1 receptor antagonists), SR144528 (10 μM, C) and AM630 (1 μM, D) (two selective CB_2 receptor antagonists), capsazepine (1 μM, E) (a TRPV1 antagonist) and GW9662 (10 μM) (a PPARγ antagonist, F). The antagonists were incubated 30 min before CBD. Each bar represents the mean±SE mean of three independent experiments. $^{*}p<0.05$, $^{**}p<0.01$ and $^{***}p<0.001$ *vs* control; $^{\circ}p<0.05$ and $^{\circ\circ}p<0.01$ *vs* CBD.

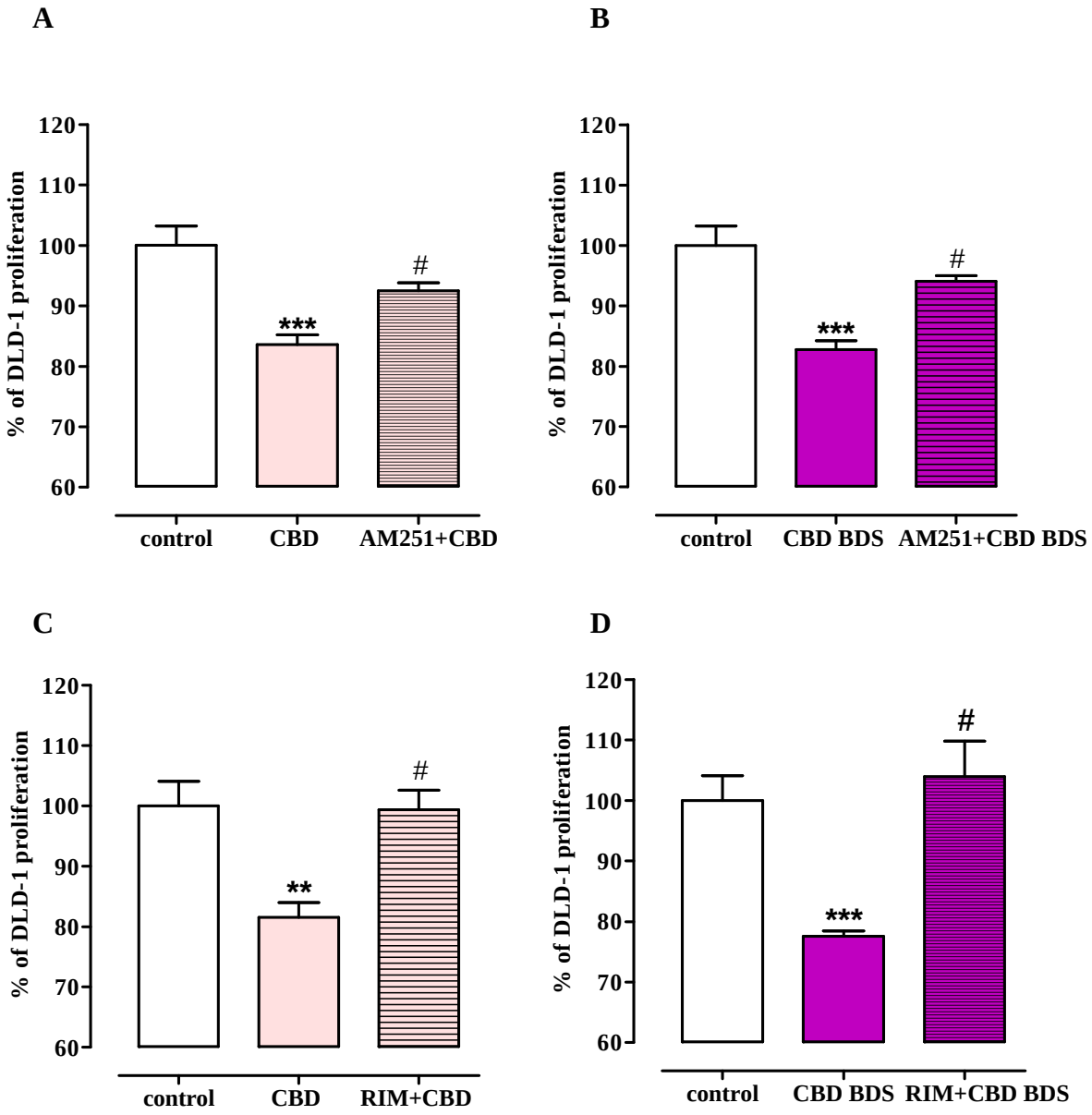

Figure 38. Antiproliferative effect, evaluated by MTT assay, of cannabidiol (CBD) and a *Cannabis sativa* extract with high content of CBD (CBD BDS, both at 3 μM, 24 h-exposure) alone or in the presence of one or other of two selective cannabinoid CB_1 receptor antagonists, *i.e.* rimonabant (RIM, 0.1 μM) and AM251 (1 μM). The antagonists were incubated 30 min before cannabinoid drugs. Each bar represents the mean±SEM of two independent experiments. $^{**}p<0.01$ and $^{***}p<0.001$ *vs* control; $^{\#}p<0.001$ *vs* CBD (or CBD BDS).

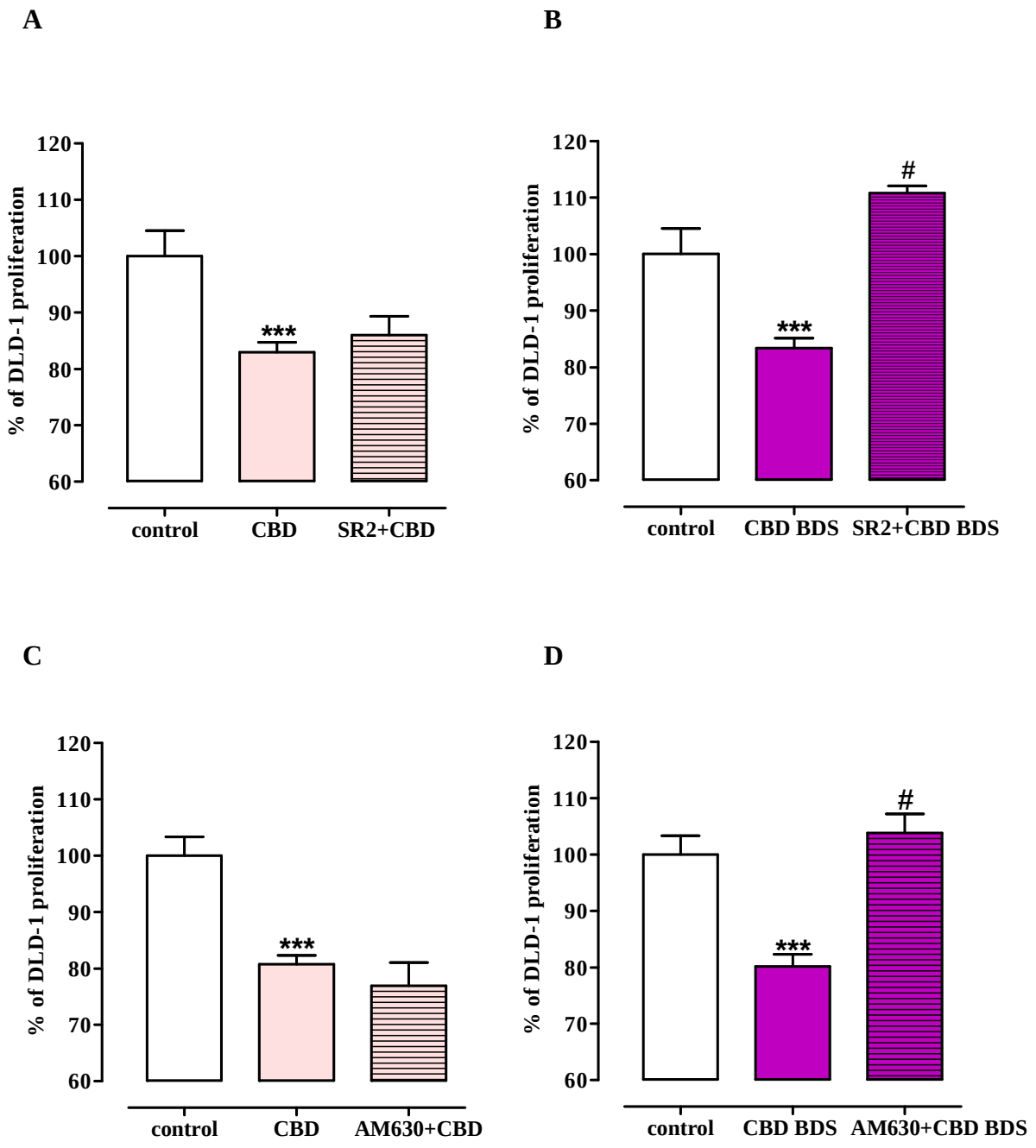

Figure 39. Antiproliferative effect, evaluated by MTT assay, of cannabidiol (CBD) and a *Cannabis sativa* extract with high content of CBD (CBD BDS, both at 3 µM, 24 h-exposure) alone or in presence of one or other of two selective cannabinoid CB_2 receptor antagonists, *i.e.* SR144528 (SR2, 0.1 µM) and AM630 (1 µM). The antagonists were incubated 30 min before cannabinoid drugs. Each bar represents the mean±SEM of two independent experiments. $^{***}p<0.001$ *vs* control; $^{\#}p<0.001$ *vs* CBD (or CBD BDS).

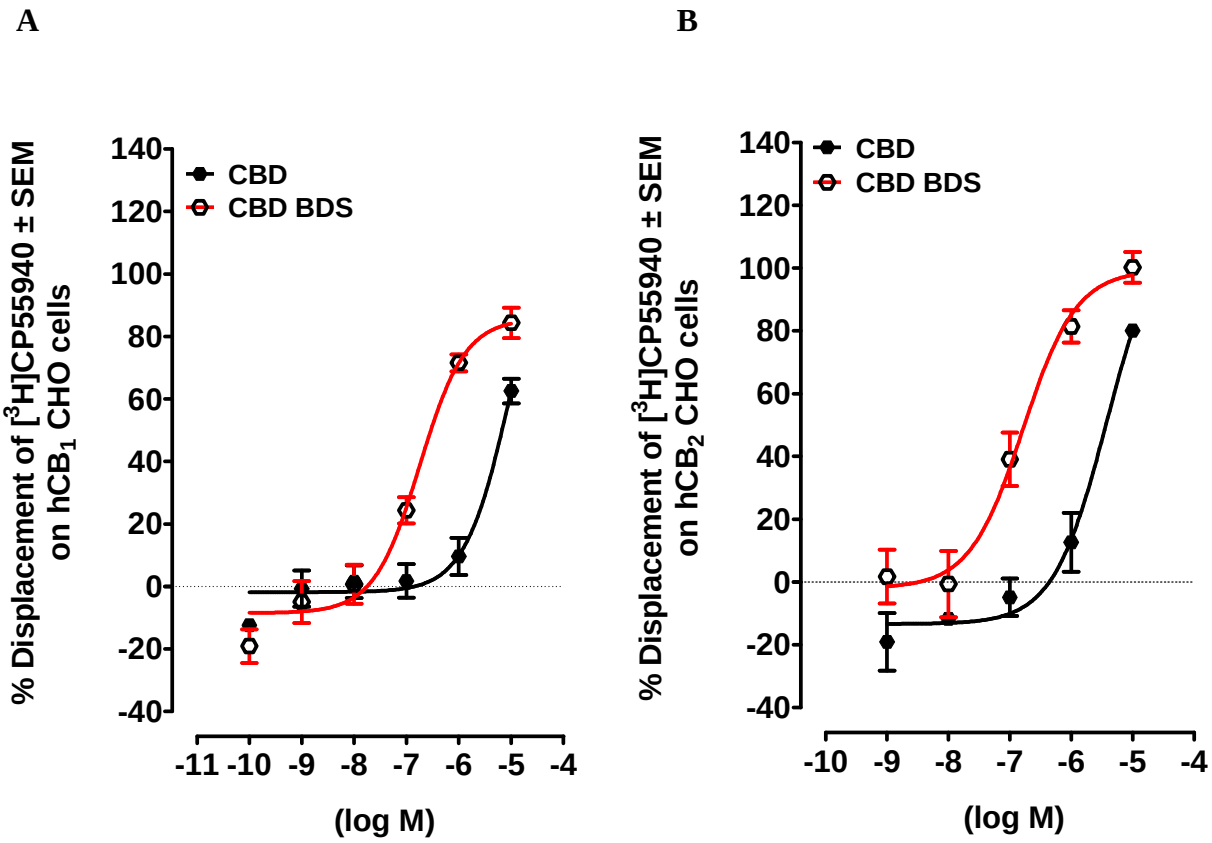

Figure 40. Displacement of [^{3}H]CP55940 by cannabidiol (CBD) and a *Cannabis sativa* extract with high content of CBD (CBD BDS) from specific binding sites on hCB_1-CHO cell membranes (A) and hCB_2-CHO cell membranes (B). Each symbol represents the mean percent displacement ± SEM (n=4).

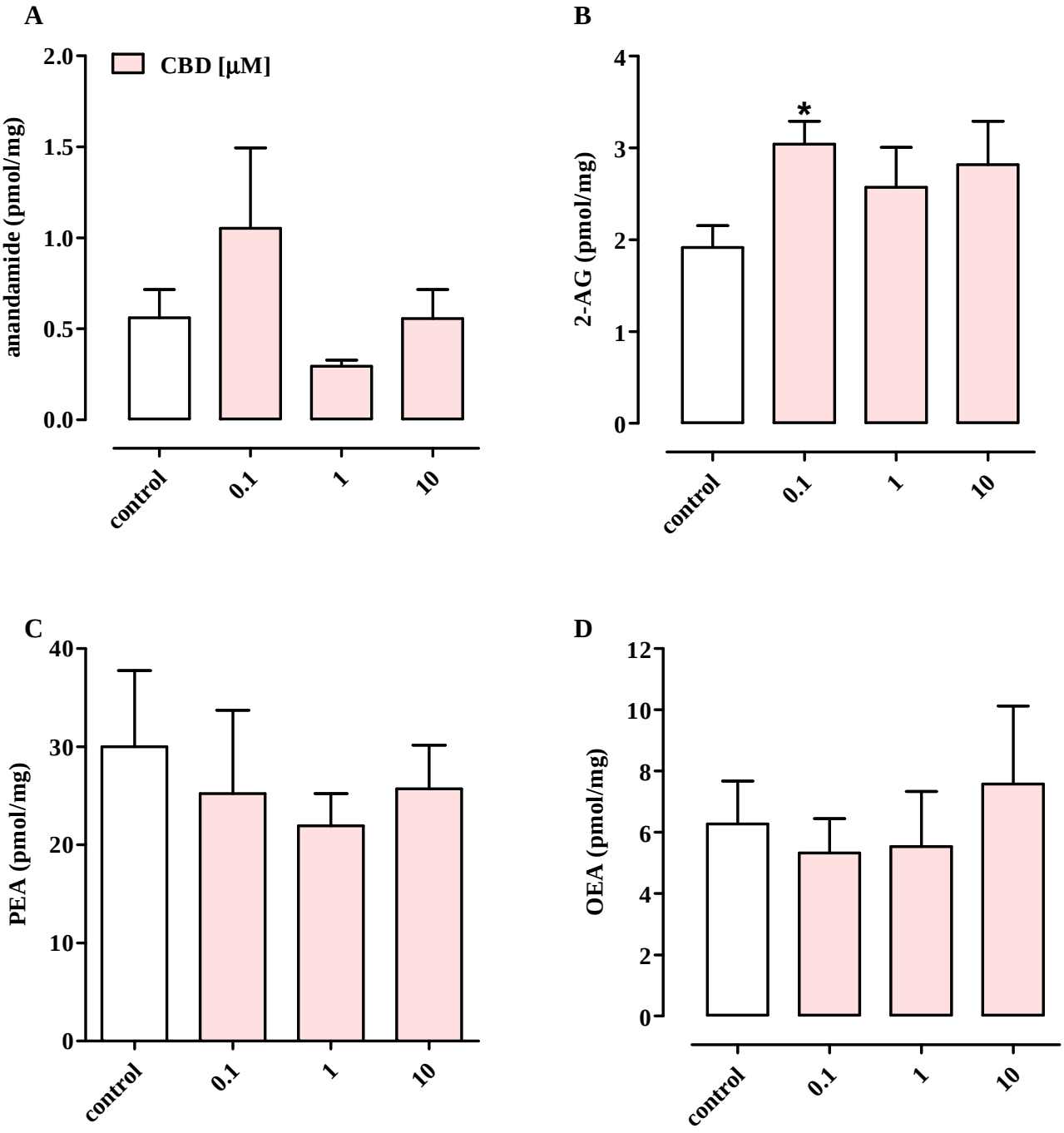

Figure 41. Levels of anandamide (A), 2-arachidonoylglycerol (2-AG, B),palmitoylethanolamide (PEA, C) and oleoylethanolamide (OEA, D) in Caco-2 cells exposed to cannabidiol (CBD, 0.1–10 μM, 24 h). Each bar represents the mean±SE mean of three independent experiments. $^{*}p<0.05$ vs control.

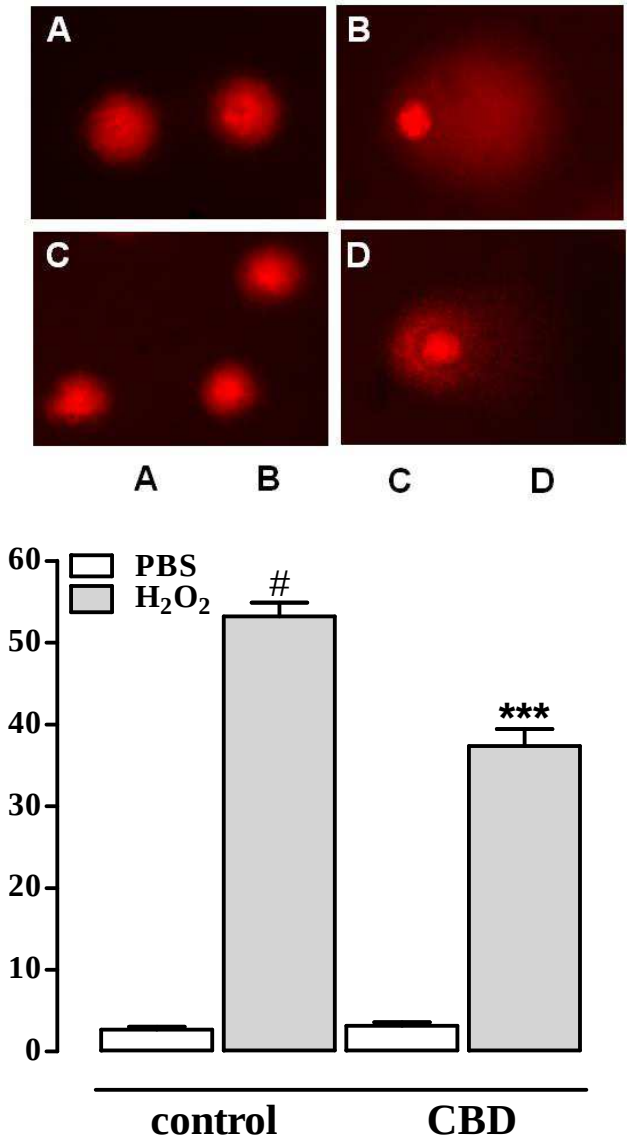

Figure 42. Effect of cannabidiol (CBD, 10 μM for 24 h) on hydrogenperoxide (H_2O_2)-induced DNA damage evaluated by the comet assay. The DNA damage was induced in Caco-2 cells by 75 μMH_2O_2 (B) and compared with PBS-treated (undamaged) cells (A). The effect of CBDwas studied in presence (D) or absence (C) ofH_2O_2. A–D Representative comets. Each bar represents the mean±SE mean of three independent experiments where at least 75 cells per gel in triplicate were scored. $^{\#}p<0.001$ *vs* undamaged cells (A, PBS) and $^{***}p<0.001$ *vs* damaged cells (B, H_2O_2). DNA damage, expressed as percentage of fluorescencein the comet tail (% DNA tail) was quantified using at least 75cells per gel were scored and each sample was evaluated in triplicate (n= independent experiments).

4.2.2 CANNABIGEROL (CBG)

4.2.2.1 Effect of CBG in azoxymethane (AOM) murine model of colon cancer

AOM treatment resulted in the formation of ACF, polyps and tumours (Figure 43B-D). Only foci with 4 or more crypts were analysed since it has been suggested that ACF (containing four or more crypts *per* focus) have higher risk for malignant tumor progression. Compared with the control group with AOM, CBG (1 and 5 mg/kg)-treated animals showed a reduced number of ACF (Figure 43B). Notably, at the 5 mg/kg dose, CBG completely suppressed the formation of ACF. CBG did not affect significantly polyp formation, but, at least at the 5 mg/kg dose, it reduced by one half the number of tumours (Figure 43C-D).

4.2.2.2 Effect of CBG in xenograft colorectal tumours mice model

We determined the potential *in vivo* antitumoural curative effect of CBG by inoculating subcutaneously colorectal cancer cells in athymic nude mice. Following intraperitoneal injection with CBG (1-10 mg/kg), a marked inhibition of the growth of the xenografted tumours was observed, the effect being significant for the 3 mg/kg and 10 mg/kg doses (Figure 43A). The differences in tumour volumes between the vehicle and the 3 mg/kg and 10 mg/kg CBG treatment groups were statistically significant from day 3^{th} of treatment to the end of the experiment. After 5 days of drug administration, the average tumour volume in the control group was 2500±414 mm^3, whereas the average tumour volume in the 3 mg/kg CBG-treated group was 1367±243, exhibiting a 45.3 % inhibition of tumour growth (Figure 43A).

4.2.2.3 CB_1, CB_2, TRPA1, TRPV1, TRPV2, TRPM8 and 5-HT_{1A} mRNA expression in colorectal carcinoma (Caco-2) cells and healthy human colonic epithelial cells (HCEC)

CBG has been shown to behave as a weak partial agonist at CB_1 and CB_2 receptors, a relatively potent and highly effective TRPA1 agonist, a weak agonist at TRPV1 and TRPV2, and a potent

TRPM8 and 5-HT_{1A} receptor antagonist. Thus, we analysed, by RT-PCR, the possible presence of such potential targets in Caco-2 cells as well as in HCEC. Results showed that all the investigated targets are expressed in Caco-2 cells, with TRPV1, CB_2, $5HT_{1A}$ more expressed than CB_1, TRPM8, TRPV2 and TRPA1 (Table 3). In HCEC, the rank order of expression was TRPV1>> CB_1, TRPA1 and TRPV2, with TRPM8, CB_2, $5HT_{1A}$ receptors very faintly expressed (expression values very close to background values) (Table 3).

4.2.2.4 Effect of CBG on colorectal cancer (Caco-2) cells viability

Because the effect of pCBs on tumoural cells viability is known to be increased with a low serum proteins concentration (De Petrocellis *et al.*, 2013), in the first series of experiments we evaluated the effect of CBG in Caco-2 cells incubated (3-48 hours) with 1% FBS. By using the MTT assay we found that CBG, in the presence of 1% FBS, three hours after its incubation, exerted a significant cytotoxic effect only at the highest concentration tested (30 µM), while after 48 h a significant inhibitory effect was achieved starting from the 3 µM concentration (Figure 44). A maximal inhibitory effect was achieved after 24-48 hours incubation [IC_{50}±SEM: 3.8±2.1 µM (24 h incubation); 1.3±2.2 µM (48 h incubation]. Further experiments were performed at the 24 h because at this time point: i) CBG displayed a well-defined concentration-related effect and ii) CBG displayed a submaximal IC_{50} value.

4.2.2.5 Effect of CBG on colorectal cancer HCT 116 and on healthy human colonic epithelial (HCEC) cells viability

Figure 45A shows that CBG also reduced viability in another colorectal cancer (*i.e.* HCT116) cell line, with a significant inhibitory effect starting from the 3 µM concentration. To investigate the selectivity of CBG effect in tumoral *vs* non-tumoral cells, various concentrations (from 1-30 µM) of CBG were tested in HCEC. CBG, at a concentration similar to its IC_{50}

values in colorectal cancer cells (3.8±2.1 µM), did not affect the vitality of HCEC (Figure 45B). Only at a concentration of 30 µM (*i.e.* a concentration that was 7.8 fold higher than the IC_{50} value), CBG exhibited a cytotoxic effect in these non-tumoral cells.

4.2.2.6 Effect of CBG on colorectal cancer (Caco-2) cells viability in presence of cannabinoids receptor antagonists

Since CBG is a constituent of *Cannabis*, we verified if its effect on cell viability on Caco-2 cells was affected by selective CB_1 and CB_2 receptor antagonists. We found that the CB_1 receptor antagonist AM251 did not modify CBG (10 µM)-induced changes in cell viability (Figure 46A). By contrast, the CB_2 receptor antagonist AM630 (1 µM) not only did not counteract but, instead, significantly enhanced the inhibitory effect of CBG (1 µM) on cell viability (Figure 46A).

4.2.2.7 Effect of CBG on colorectal cancer (Caco-2) cells viability in presence of a TRP channel antagonist

Ruthenium red is a non-selective TRP channel antagonists. Specifically, it blocks TRPA1 (IC_{50}< 1-3 µM), TRPV1 (IC_{50}: 0.09-0.22 µM) and TRPV2 (IC_{50}: 0.6 µM), being the TRPM8 insensitive to its action (Alexander *et al.,* 2013). We found that ruthenium red, at concentrations (10 µM and 25 µM) several fold higher than the IC_{50} able to block TRPA1, TRPV1 and TRPV2 channels (Alexander *et al*., 2013), did not modify significantly the inhibitory effect of CBG on cell viability (Figure 46B).

4.2.2.8 Effect of TRPM8 antagonists on colorectal cancer (Caco-2) cells viability

Because CBG is a potent TRPM8 antagonist (De Petrocellis *et al.,* 2011) in this series of experiments we verified if the effect of CBG was shared by well-established TRPM8 antagonists. We found that, similarly to CBG, the synthetic TRPM8 antagonist AMTB as well

as cannabidiol and cannabidivarin (two *Cannabis*-derived TRPM8 antagonists) inhibited, in a concentration-dependent manner, Caco-2 cells viability (Figure 47A-C). Cannabichromene, another phytocannabinoid without activity at the TRPM8 channel (De Petrocellis *et al.,* 2011), inhibited cell growth only at the highest concentration (30 µM) tested (Figure 47D).

4.2.2.9 Effect of a $5HT_{1A}$ antagonist on colorectal (Caco-2) cells viability

CBG is a moderately potent 5-HT_{1A} antagonist (Cascio *et al.,* 2010). In contrast to TRPM8 antagonists, the effect of CBG was not mimicked by the 5-HT_{1A} antagonist WAY100635 (up to 1 µM) (cell viability %: control 100±6.3; WAY100635 0.2 µM 97.2 ±6.2; WAY100635 1 µM 95.9±6.2; DMSO 20 % 47.9±3.8*; $^{*}p<0.001$ *vs* control, n=3 experiments including 8–10 replicates for each treatment), thus suggesting the lack of involvement of such receptor.

4.2.2.10 Effect of CBG on apoptosis and necrosis

To investigate whether the growth inhibitory effect of CBG was due to induction of apoptosis or necrosis, we examined Caco-2 cell death by eosin-haematoxylin staining. As shown in Figure 48A, compared to necrotic cells, the number of apoptotic cells was elevated after CBG treatment (CBG 10 µM: 72±11.0 % of apoptotic cells; 17.7±7.2 % of necrotic cells; n=3). Morphological assessment revealed absence of death in untreated cells and the presence of cells with a typical apoptotic morphology (*i.e.* reduced size, hypereosinophilic cytoplasm, hyperchromic nucleus, irregular nuclear membrane and nuclear material outside the nucleus) in cells incubated with CBG. The induction of apoptosis by CBG was confirmed by enzymatic assay, which indicated a 2.43 fold increase of caspase 3/7 activity in CBG treated Caco-2 cells compared to vehicle (Figure 48B).

4.2.2.11 Effect of CBG on reactive oxygen species (ROS) production in colorectal (Caco-2) and in healthy human colonic epithelial (HCEC) cells

To determine if the apoptotic action of CBG was associated to ROS production, we measured the levels of ROS generation by using the fluorescence sensitive probe DCFH-DA. We found that CBG 10 µM significantly increased ROS production in Caco-2 cells (Figure 49A) but not in HCEC (Figure 49B). Fenton's reagent (2 mM of H_2O_2/Fe^{+2}), used as a positive control, increased ROS production both in Caco-2 cells and in HCEC (data not shown).

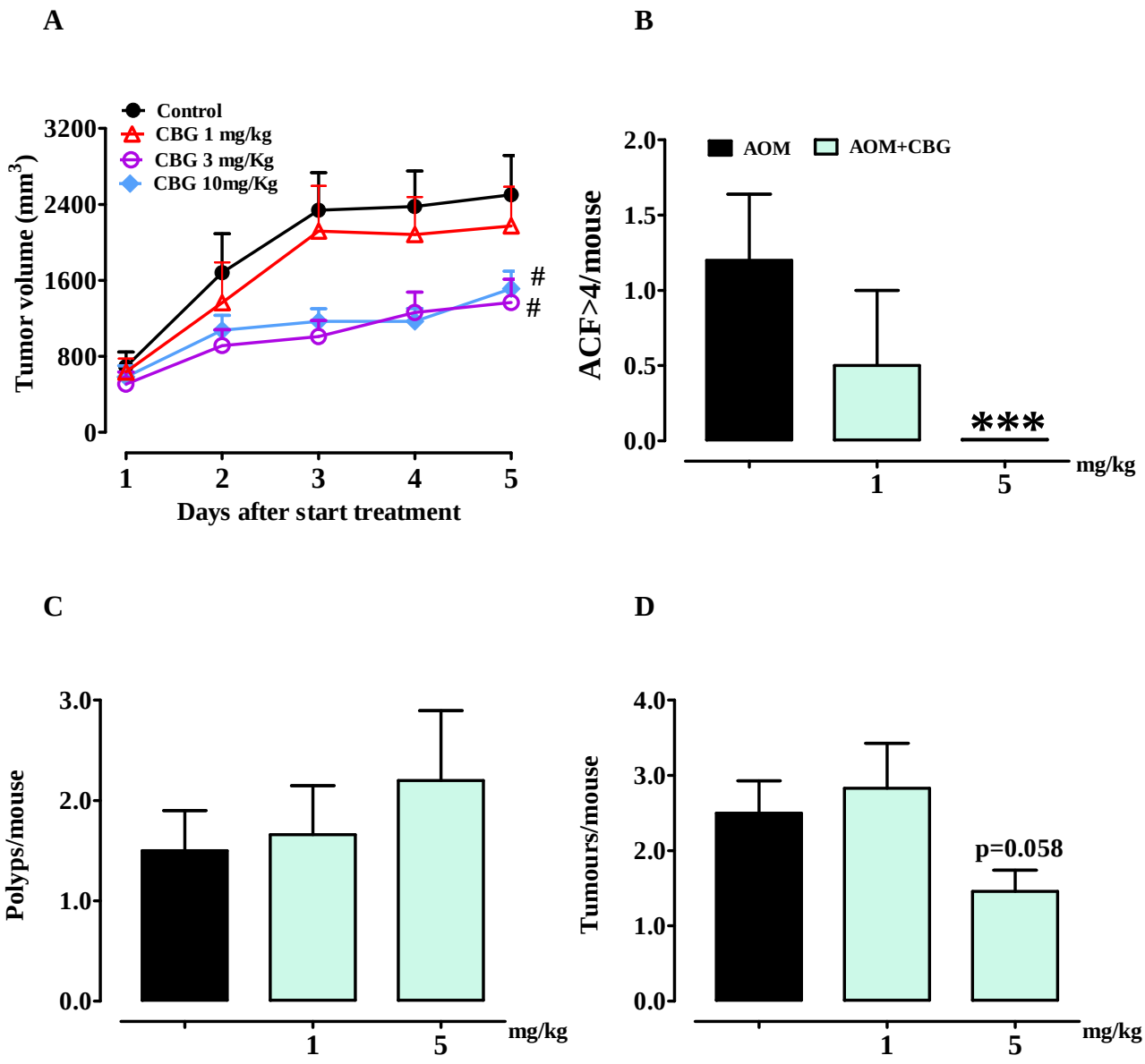

Figure 43. CBG reduces colon carcinogenesis *in vivo*. Figure 43A reports the inhibitory effect of cannabigerol (CBG, 1-10 mg/kg) on xenograft formation induced by subcutaneous injection of HCT 116 cells into the right flank of athymic female mice. Approximately, treatment started after 10 days of cell inoculation. Tumour size was measured every day by digital caliper measurements, and tumour volume was calculated. CBG (1-10 mg/kg, *ip*) was given every day for the whole duration of the experiment. Figure 43B-D report the inhibitory effect of CBG (1 and 5 mg/kg) on aberrant crypt foci with four or more crypts (ACF≥4/mouse) (B), polyps (C) and tumours (D) induced in the mouse colon by azoxymethane (AOM). CBG was given *ip* three times a week for the whole duration of the experiment starting 1 week before the first administration of AOM. Measurements were performed 3 months after the first injection of AOM.Each point for xenograft curve represents the mean ± SEM of 8 animals for each experimental group. $^{\#}p<0.001$; ANOVA CBG curves *vs* control curve. For AOM model, each bar represents the mean ± SEM of 9-11 mice. $p<0.058$ and $^{***}p<0.001$ *vs* AOM alone.

Table 3: Detection of CB_1, CB_2, TRPA1, TRPV1, TRPV2, TRPM8 and 5-HT_{1A} mRNA by quantitative (real-time) RT-PCR analysis in human colorectal carcinoma cells (Caco-2) and in healthy human colonic epithelial cells (HCEC).

Accession	Target	HCEC	Caco-2	Background
	Acronymous	Cq mean (SD)	Cq mean (SD)	Cq NTC (SD)
NM_016083	**CB_1**	33.12 (0.267) **VLE**	30.86 (0.217) **LE**	N/A (N/A)
NM_001841	**CB_2**	31.71 (0.136) **CtB**	29.89 (0.388) **ME**	36.50 (0.154)
NM_007332	**TRPA1**	34.37 (0.259) **VLE**	32.29 (0.227) **LE**	N/A (N/A)
AF196175	**TRPV1**	28.05 (0.091) **ME**	25.86 (0.100) **ME**	35.88 (0.483)
NM_016113	**TRPV2**	34.00 (0.500) **VLE**	30.19 (0.158) **LE**	N/A (N/A)
NM_024080	**TRPM8**	33.05 (0.519) **CtB**	30.06 (0.120) **LE**	36.88 (0.397)
NM_000524	**5HT1A**	31.64 (0.180) **CtB**	29.25 (0.149) **ME**	35.90 (0.310)

Cq, quantitative cycles; **SD**, standard deviation of quantitative cycles; **NTC**, negative control minus template; **N/A**, not applicable, no quantitative cycles detected within 40 repeats. **HE,** high expression; **ME** middle expression; **LE**, low expression; **VLE**, very low expression; **CtB**, close to background. Quality significance parameters: Δ (Cq_{mean}-Cq_{bkg}) $\geq$ 5; replicate samples CqStddev $\leq$ 0.500.

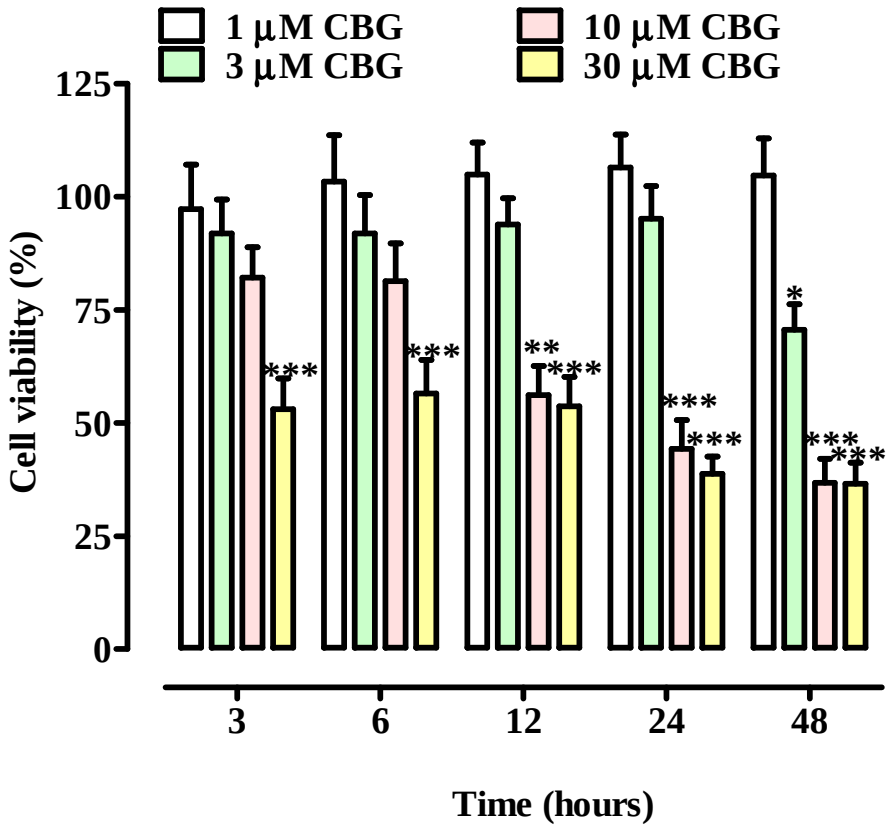

Figure 44. Cannabigerol (CBG) reduces cell viability, evaluated by the MTT assay, in human colorectal cancer (Caco-2) cells in a time- and concentration-dependent manner. Caco-2 cells were incubated with increasing concentration of CBG (1-30 µM) for 3, 6, 12, 24 and 48 hours in a medium containing 1% FBS. Each bar represents the mean±SEM of three independent experiments. $^{*}p<0.05$, $^{**}p<0.01$ and $^{***}p<0.001$ *vs* control (untreated cells).

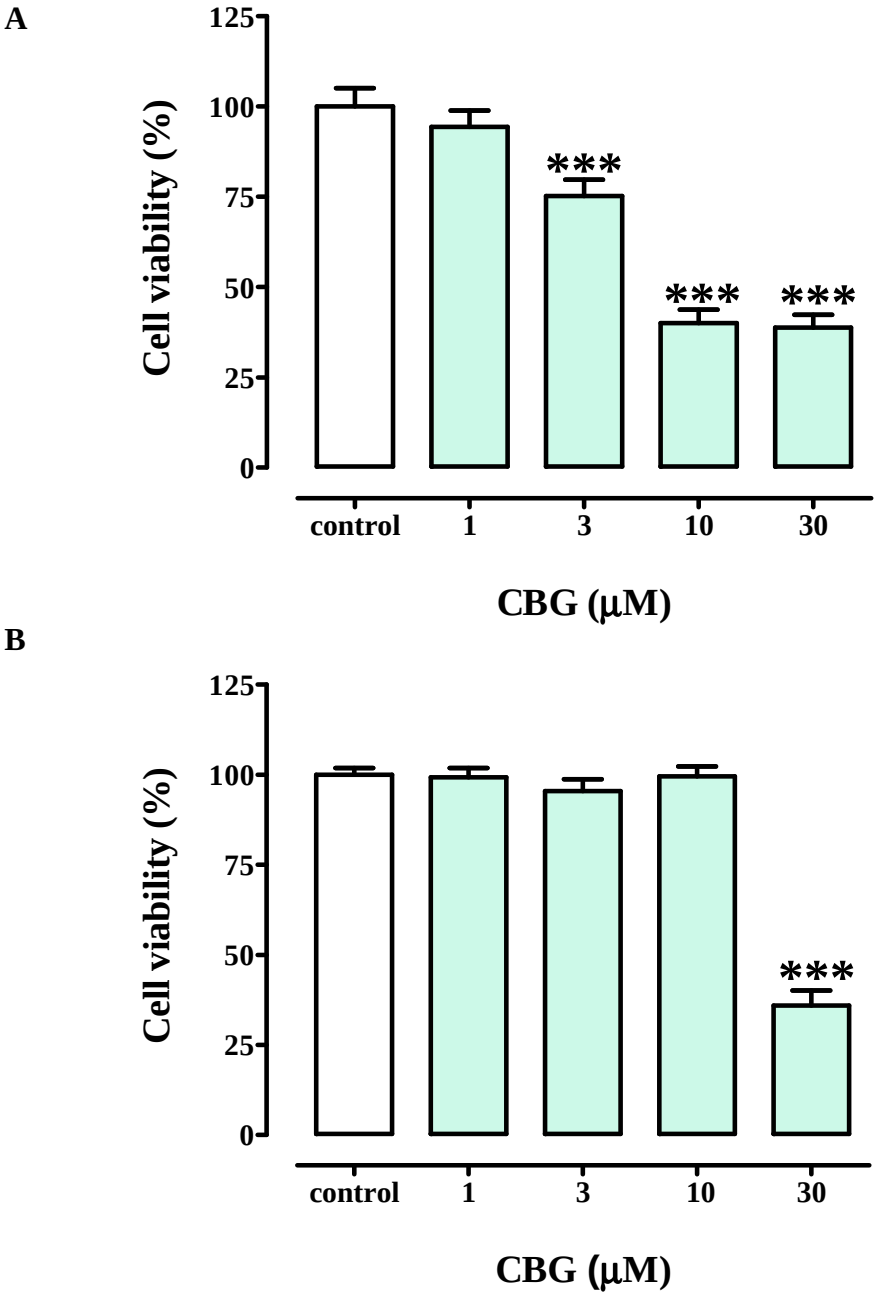

Figure 45. Inhibitory effect of cannabigerol (CBG), evaluated by the MTT assay, on cell viability in human colorectal cancer (HCT 116) cells (A) and in healthy human colonic epithelial cells (HCEC) (B). Both cell lines were incubated with increasing concentration of CBG (1-30 μM, 24 h exposure) in a medium containing 1% FBS. Each bar represents the mean ±SEM of three independent experiments. $^{***}p<0.001$ *vs* control (untreated cells).

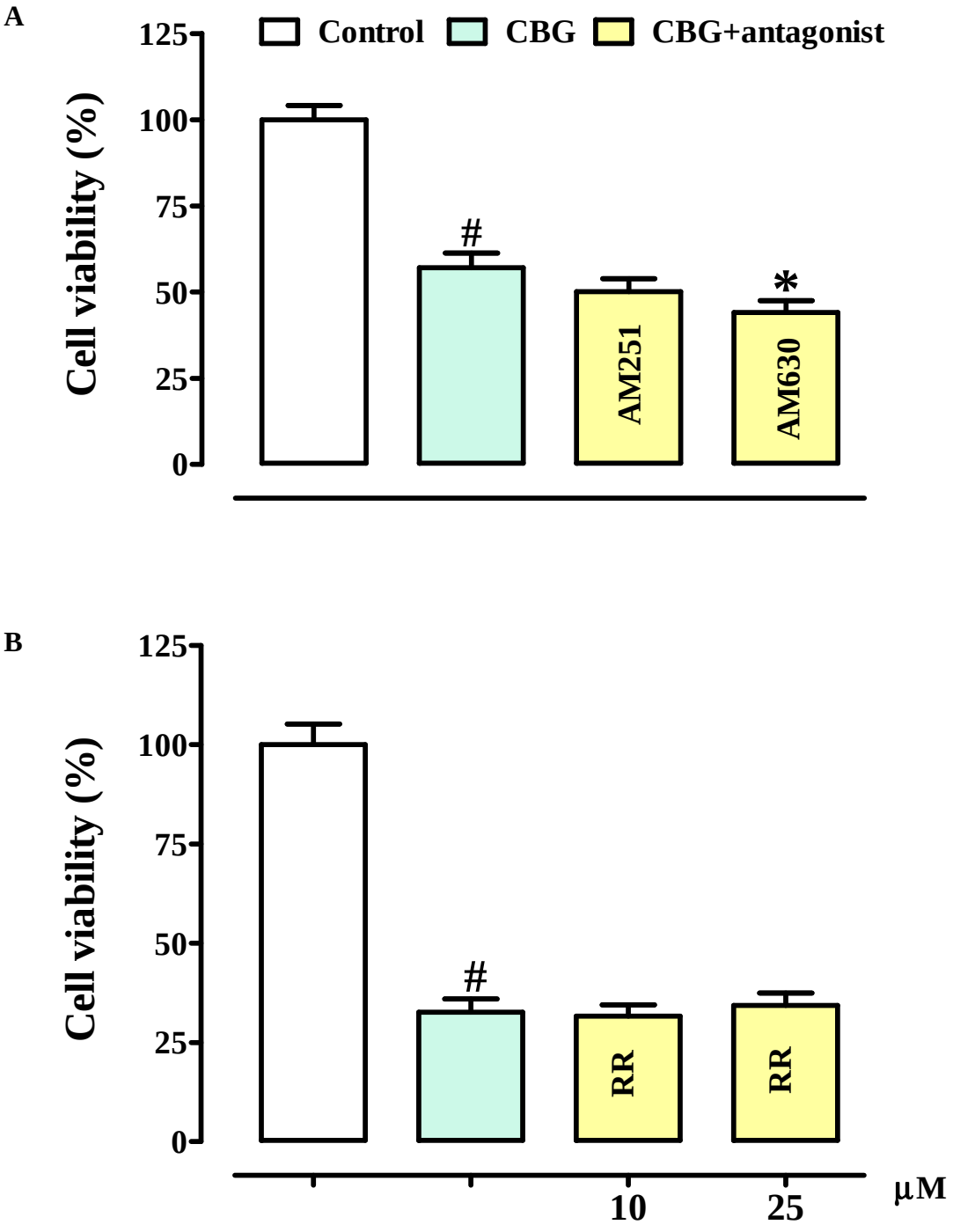

Figure 46. Cytotoxic effect of cannabigerol (CBG, 10 µM in a 1% FBS medium, 24 h exposure), evaluated by the MTT assay, alone or in the presence of (A) AM251 (1 µM, selective CB_1 receptor antagonist), AM630 (1 µM, selective CB_2 receptor antagonist) and (B) ruthenium red (RR, 10 and 25 µM, a non-selective TRP channels antagonist) in colorectal cancer (Caco-2) cells. The antagonists were incubated 30 min before CBG. Each bar represents the mean ± SEM of three independent experiments. $^{\#}p<0.001$*vs* control; $^{*}p<0.05$ *vs* CBG alone.

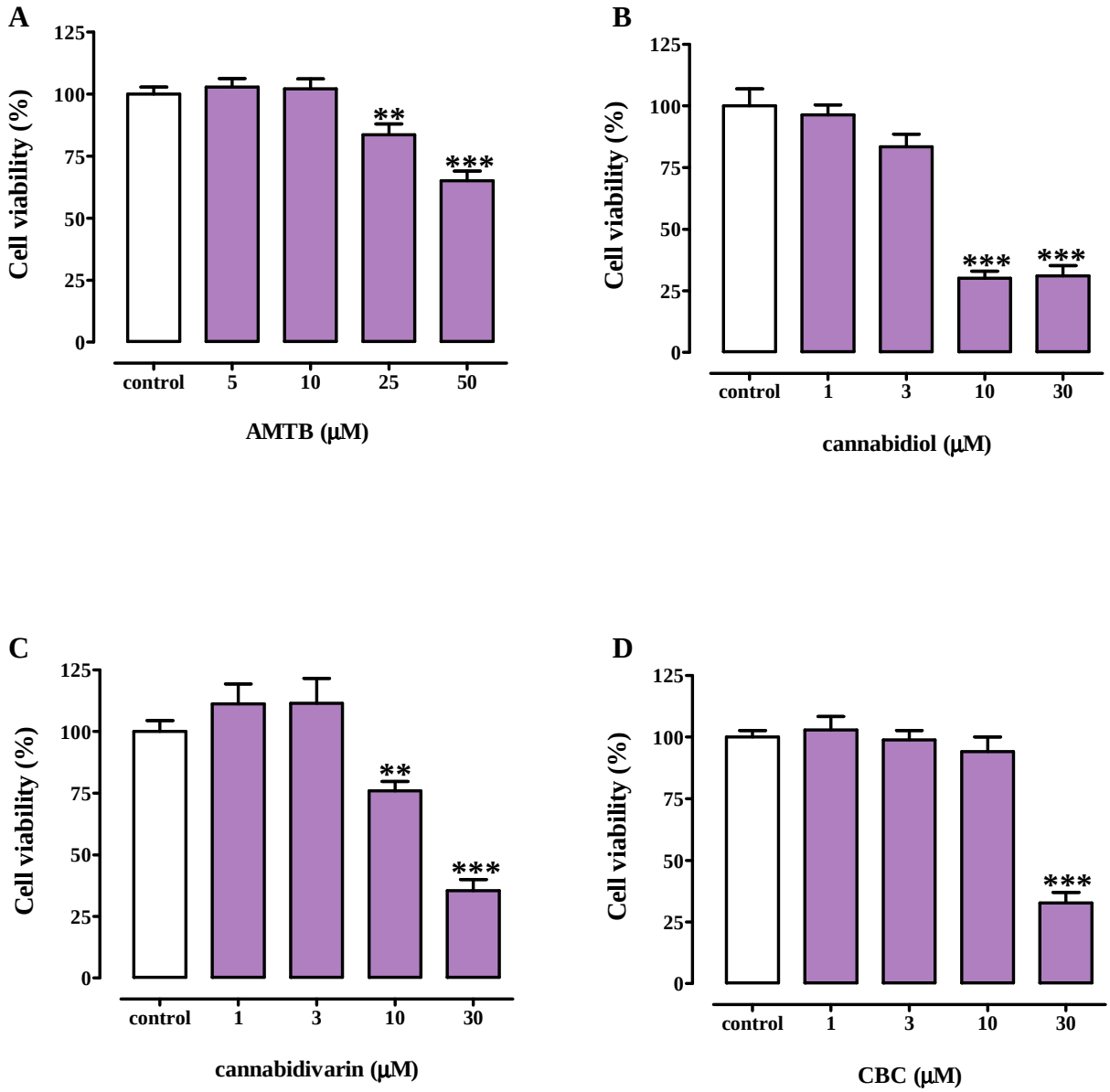

Figure 47. Effect of AMTB (5-50 µM, A), cannabidiol (CBD, 1-30 µM, B), cannabidivarin (CBDV, 1-30 µM, C) and cannabichromene (CBC, 1-30 µM, D) on cell viability, evaluated by the MTT assay, in colorectal cancer (Caco-2) cells. Cells were incubated with increasing concentration of compounds (24 h exposure in a 1% FBS medium). Each bar represents the mean ± SEM of three independent experiments. $^{**}p<0.01$ and $^{***}p<0.001$ *vs* control (untreated cells).

A **B**

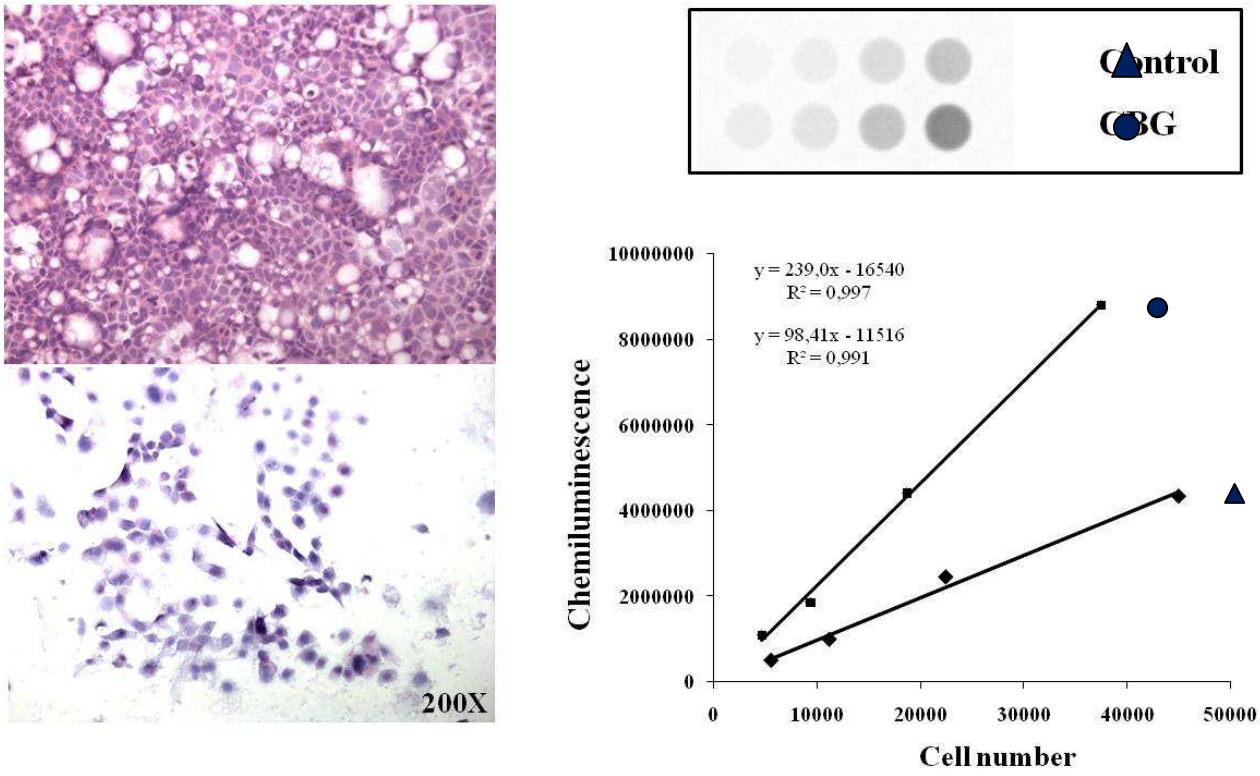

Figure 48. Cannabigerol (CBG) induces apoptosis in colorectal cancer (Caco-2) cells. (A) Morphological assessment of colorectal cancer (Caco-2 cells) evaluated by eosin-haematoxylin staining revealed the absence of death in untreated cells (upper pannel) and the presence of cells with a reduced size, showing an hypereosinophilic cytoplasm, hyperchromic nucleus, irregular nuclear membrane and nuclear material outside the nucleus in CBG-treated cells (10 µM, 24 h incubation in a 1% FBS, down pannel). Original magnification 200X. The figure is representative of 3 experiments. (B) Increase of caspase3/7 enzymatic activity evaluated by Caspase-Glo®3/7 assay. In the plot each point represents the mean of three independent determination (the mean standard error was not greater of 10% of the graphed value). In the insert panel a picture of part of the plate is shown. The cell amount in each dot increases from left to right as reported in the plot *abscissa*. The increase of caspase 3/7 enzymatic activity (2.43 fold) was calculated by the *ratio* of the curve slopes: 239.0 and 98.41 for CBG and vehicle treated cells, respectively.

A

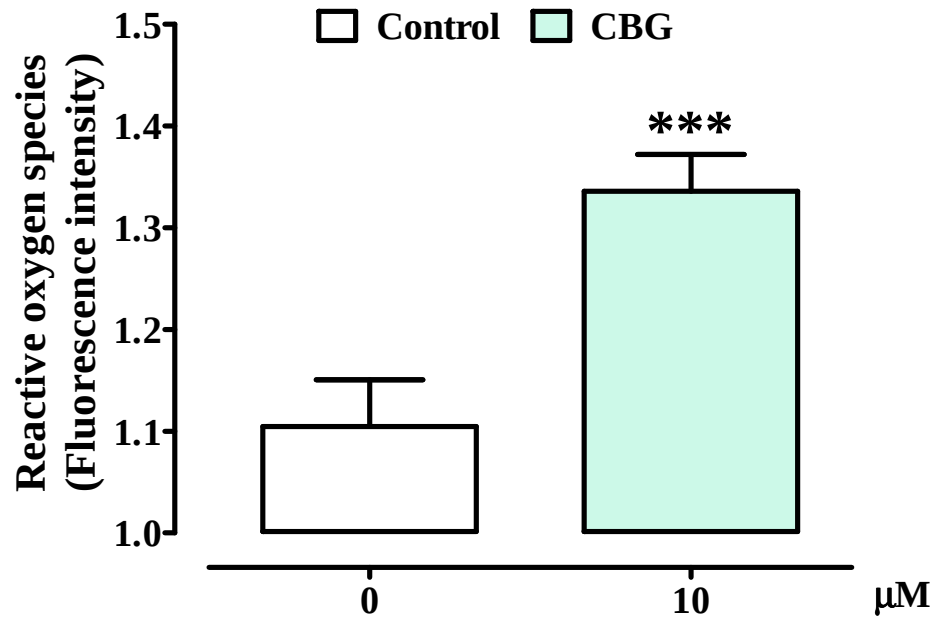

B

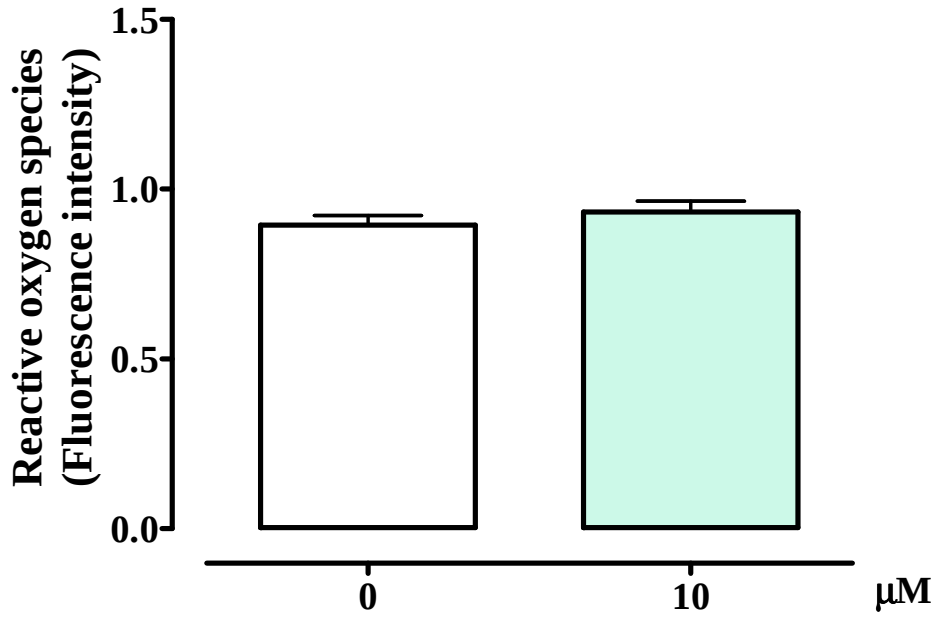

Figure 49. Effect of cannabigerol (CBG, 10μM in a 1% FBS medium, 24 h exposure) on reactive oxygen species production in colorectal carcinoma (Caco-2) cells (A) and healthy human colonic epithelia cells (B). Data represent mean ± SEM of 6 experiments. $^{***}p<0.001$ vs control.

5.0 DISCUSSION

Inflammatory bowel disease (IBD) and colorectal cancer (CRC) are widespread diseases which affect millions of persons worldwide. Despite the progress in pharmacotherapy, preventive measures and cures are still unsatisfactory. Thus, there is an urgent need for safe and effective innovative therapeutics. During the PhD work, a number of non-psychotropic cannabinoids from *Cannabis sativa* have been evaluated in experimental models of IBD and colon cancer. These include CBD, CBG, CBC and THCV. Additionally, a botanical extract with high content of CBD (here named CBD BDS) has been evaluated in experimental models of colon cancer. The *rationale* for studying pCBs both in intestinal inflammation and colon cancer lies in the observation that clinical IBD represents an example of a condition that greatly increases the risk of CRC.

5.1 Inflammatory bowel disease (IBD)

Preparations of *Cannabis* have been used since antiquity as medicinal agents to alleviate the symptoms of inflammation, including IBD (Zurier, 2003). Recently, clinical studies, by showing beneficial effects of *Cannabis* use in humans, seem to confirm such anecdotal reports (Naftali *et al.*, 2011; Lahat *et al.*, 2012; Lal *et al.*, 2011; Naftali *et al.*, 2013).The effect of Δ^9-THC and CBD, two main *Cannabis* constituents, on experimental models of IBD is well established and their effect on intestinal inflammation has been extensively reviewed (Alhouayek and Muccioli, 2012; Esposito *et al.*, 2013). However, the issue of whether other *Cannabis* constituents contribute to the anti-inflammatory effect of the plant is a matter of investigation. In the present work we have investigated the anti-inflammatory effects of three non-psychotropic phytocannabinoids, namely CBG, CBC and THCV.

5.1.1 Effect of CBG, CBC and THCV on experimental colitis

The potential anti-inflammatory effect of pCBs was verified by using the DNBS model of colitis. DNBS is dissolved in ethanol, which provokes the destruction of the mucosal barrier. DNBS evokes granulomas with infiltration of inflammatory cells in all layers of the intestine (Hibi *et al.*, 2002).

We have found that CBG, CBC and THCV reduced colon weight/colon length *ratio* of the inflamed colon, which is considered a reliable and sensitive indicator of the severity and extent of the inflammatory response (Gálvez *et al.*, 2000). Because the main goal in IBD is to cure rather than to prevent, all the phytocannabinoids tested were given after the inflammatory insult. CBG and CBC were studied more thoroughly and for such compounds histological analysis, immunoistochemistry, neutrophil infiltration and intestinal membrane integrity studies were performed. Additionally, the effect of CBG was evaluated on cytokine levels and enzymes (COX-2 and iNOS) expression.

Histological examination showed that CBG and CBC reduced the signs of colon injury; specifically, in the colon of phytocannabinoid-treated animals, the glands were regenerating, the *oedema* in *sub*-mucosa was reduced and the infiltration of granulocytes into the mucosa and *sub*-mucosa was reduced. The curative effect of both CBG and CBC was further supported by their capability to reduce or abrogate the increase in intestinal permeability induced by DNBS administration (notably, CBG restored completely the integrity of intestinal epithelium). Accordingly, neutrophil infiltration, revealed by measuring MPO activity (Krawisz *et al.*, 1984), was likewise reduced by both pCBs. Furthermore immunohistochemical analyses demonstrated that CBG and CBC limited the colonic diffusion of Ki-67, a useful marker for the evaluation of dysplasia in ulcerative colitis (Andersen *et al.*, 1998).

As stated above, CBG was investigated more in details and, for this phytocannabinoid we performed further *ex vivo* studies in the colon of DNBS-treated mice. Specifically, we measured some cytokines which are known to be involved in IBD (Madsen, 2002) such as IL-1β (a cytokine which plays an important pro-inflammatory role in the initiation and amplification of the intestinal inflammatory response) (Strober and Fuss, 2011), IL-10 (a regulatory cytokine which inhibits pro-inflammatory cytokine release, resulting in anti-inflammatory effects within the gut) (Barbara *et al.*, 2000) and IFN-γ, another pro-inflammatory cytokine that plays a crucial function in the initiation of experimental colitis (Strober and Fuss, 2011; Ito *et al.*, 2006). Also, we measured iNOS and COX-2 expression, two key enzymes that play a pivotal role in gut inflammation (Kolios *et al.*, 2004; Wallace and Devchand, 2005) and investigated the potential antioxidant effect of CBG. Consistent with previous studies, we observed that intracolonic administration of DNBS caused an increase in colonic IL-1β and interferon-γ as well as a decrease in IL-10 levels (Lamine *et al.*, 2004; Borrelli *et al.*, 2009). More importantly, we found that CBG counteracted the colonic variations of the three cytokines, thus suggesting the possible involvement of these cytokines in CBG-mediated anti-inflammatory effects. We also demonstrated here that the expression of both iNOS and COX-2 was increased in the colon of DNBS-treated mice and that CBG reduced the expression of the iNOS, but not COX-2 protein. Others have reported that CBG inhibits COX-2 activity in intestinal cells, but in a higher concentration range, and decreases prostaglandin production in the human colon adenocarcinoma (HT29) cell line (Ruhaak *et al.*, 2011). Finally, CBG was able to restore SOD activity, suggesting its potential antioxidant effects in the inflamed gut.

5.1.2 Experiments in peritoneal macrophages

In order to give some insights into the mode of action of the three pCBs, we investigated their effect on peritoneal macrophages. Macrophage targeting treatment ameliorates colonic inflammation in experimental colitis models and the regulation of abnormal responses of macrophages appears to be a promising therapeutic approach for the treatment of IBD (Yoshino *et al.*, 2010). When activated by inflammatory *stimuli* (for example LPS), macrophages express iNOS and consequently produce a large amount of NO (Moncada *et al.*, 1991). We thus evaluated the effect of the three pCBs on LPS-stimulated nitric oxide production in isolated peritoneal macrophages.

We found that CBG, CBC and THCV reduce the levels of nitrites, the stable metabolites of NO. The inhibitory effect of CBG and THCV on LPS-induced nitrite levels was associated to down-regulation of iNOS, suggesting that inhibition of induction of such enzyme is one of the mechanisms underlying the inhibition of NO production by the pCBs. Regarding CBC, it is unlikely that it affects the processes linked to the induction of iNOS since the phytocannabinoid: i) was pharmacologically active when given both 30 min before LPS as well as 15 h after the pro-inflammatory insult, *i.e.* once the enzyme had been already expressed and ii) did not affect iNOS mRNA and protein expression, as revealed by RT-PCR and western blot analyses. On the other hand, CBC reduced the levels of both IL-10 and IFN-γ, two cytokines which limit the inflammatory response in LPS-treated macrophages (Hawiger, 2001; Moore *et al.*, 2001). The ability of macrophages to overproduce IL-10 (an anti-inflammatory cytokine) in response to LPS has been previously documented (Brightbill *et al.*, 2000) and can be considered as an adaptive reaction of the macrophages aiming at counteracting the inflammatory insult.

In order to explore the molecular target of CBG, THCV and CBC action, we considered the possibility that such phytocannabinoids may affect the components of the so-called endogenous cannabinoid system. Specifically: i) CBG was shown to behave as a partial agonist of CB_1 and CB_2 receptors (Cascio *et al.*, 2010), although exhibiting low affinity for these receptors (Pollastro *et al.*, 2011), and to inhibit the reuptake of the endocannabinoid anandamide (De Petrocellis *et al.*, 2011); ii) CBC inhibits endocannabinoid re-uptake, and thus to potentially activate indirectly – *via* increased extracellular endocannabinoid levels – the cannabinoid receptors (Ligresti *et al.*, 2006; De Petrocellis *et al.*, 2011); iii) THCV behaves as a CB_1 antagonist and a CB_2 partial agonist (Pertwee, 2008).The possible involvement of cannabinoid receptors in CBG, CBC and THCV action was studied by evaluating: 1) the effect of selective CB_1 and CB_2 receptor antagonists on phytocannabinoids-induced inhibition of nitrite production, and 2) possible alterations in cannabinoid receptor mRNA produced by the phytocannabinoids in LPS-challenged macrophages.

Our results suggest that cannabinoid receptor antagonists can modulate the pharmacological action of the three pCBs, although in a different way. Specifically:

i) the inhibitory effect of THCV on nitrite levels was counteracted by SR 144528 (CB_2 receptor antagonist), but not by rimonabant (CB_1 receptor antagonist). Our data are consistent with the ability of this phytocannabinoid to activate CB_2 receptors in binding studies and decrease carrageenan-induced *oedema* in mice in a CB_2 receptor-sensitive way (Bolognini *et al.*, 2010). This result is of relevance considering that CB_2 receptors are up-regulated in inflammatory bowel conditions (Izzo, 2007) and CB_2 agonists ameliorate experimental colitis (Storr *et al.*, 2009). On the other hand, THCV reduced LPS-induced CB_1 receptor hyper-expression, a relevant information in the light of the observation that CB_1 receptor activation reduces nitrite production in LPS-challenged macrophages (Aviello *et al.*, 2011) as well as ameliorates experimental colitis (Storr *et*

al., 2010). Importantly, among the phytocannabinoids tested, THCV was the unique to counteract the elevation in IL-1β and COX-2 induced by LPS, which is relevant because IL-1β represents one of the main pro-inflammatory cytokines able to induce COX-2 expression in macrophages (Samad *et al.*, 2001; Liu *et al.*, 2003).

ii) The inhibitory effect of CBG on nitrite production was not modified by the CB_1 receptor antagonist rimonabant. By contrast, the CB_2 receptor antagonist SR 144528, at a concentration which was *per se* inactive, further augmented the inhibitory effect of CBG on nitrite production, suggesting a modulatory role of CB_2 receptors. In other words, our results suggest that an endogenous cannabinoid tone may exists, via CB_2 receptors, influencing negatively the anti-inflammatory effect of CBG signalling. Alternatively, it is possible that CBG can merely synergize with SR 144528, by unmasking the anti-inflammatory action of a *per se* inactive dose of this antagonist. Moreover, we found that CBG did not modify the effect of LPS on CB_1 and CB_2 receptor mRNA expression.

iii) The inhibitory effect of CBC was further increased by a *per se* inactive concentration of rimonabant. These results, which are similar to those observed for the modulation of CBG action by a CB_2 receptor antagonist described above, negate the possibility that CBC acts via CB_1 direct or indirect activation. This hypothesis is also supported by the results we obtained in the [^{35}S]GTPγS binding assay performed with hCB_1-CHO cell membranes. Thus, we found that CBC, at concentrations that included the one at which it significantly inhibits nitric oxide production (1 μM), did not induce any significant activation of cannabinoid CB_1 receptors. Moreover, using the same assay, we also found that when CBC was administered 30 min after 0.1μM rimonabant, it did not significantly affect the E_{max} of this compound for its inhibition of [^{35}S]GTPγS binding. It might be possible that an endogenous CB_1 tone exists, which may couple negatively

to the CBC signalling pathway and counteract CBC inhibition of nitrite production. Indeed, we found that LPS enhances anandamide levels in macrophages, and that CBC, instead, only elevates OEA levels. According to some Authors, also OEA, but not PEA (the levels of which were not elevated by CBC) is taken up by cells through the same mechanism responsible for anandamide uptake (Hillard *et al.*, 1997; Alhouayek and Muccioli, 2012). It is possible that CBC could not elevate anandamide levels because these were already maximally up-regulated by LPS. OEA, which is chemically-related to anandamide, was previously shown to produce anti-inflammatory effects (Lo Verme *et al*., 2005) and hence, it is possible that a part of the beneficial effect of CBC observed here in macrophages could be due to its ability to increase OEA levels. Finally, we found that CBC did not affect LPS-induced changes in CB_1 and CB_2 cannabinoid mRNA expression. These results rule against the possibility that this phytocannabinoid could exert anti-inflammatory actions in macrophages by altering cannabinoid mRNA receptor expression.

5.1.3 Conclusions

Our results show that the degree of intestinal inflammation caused by intracolonic administration of DNBS is substantially reduced by a curative treatment of mice with the *Cannabis*-derived ingredients CBG, CBC and THCV. More in depth *ex vivo* investigations on CBG showed that its anti-inflammatory action was associated to modulation of cytokine (IL-1β, IL-10 and interferon-γ) levels and down-regulation of iNOS expression.

Studies on peritoneal macrophages suggest that the three pCBs inhibited NO production, an effect associated to inhibition of iNOS expression (for CBG and THCV, but not for CBC). THCV was the unique among the phytocannabinoids to counteract the elevation in IL-1β and COX-2 induced by LPS. The effect of THCV, but not CBG or CBC, was mediated by CB_2

receptor activation, since its effect was abrogated by a CB_2 receptor antagonist. However, based on the observation that the CBC response on macrophages was augmented in the presence of CB_1 antagonists and the CBG response was likewise increased in the presence of a CB_2 antagonist, it is possible that an endogenous cannabinoid ‘‘tone’’ coupled at CB_1 and CB_2 receptors influences negatively the anti-inflammatory effect of CBC and CBG signalling, respectively.

5.2 Colorectal cancer (CRC)

Colorectal cancer (CRC) is an important health problem across the world. It is noteworthy that the CRC pathological process can develop spontaneously or can develop on the grounds of inflammatory bowel disease, thus suggesting a link between intestinal inflammation and cancer. Although significant progress has been made in understanding CRC development through epidemiological, laboratory and clinical studies, this type of cancer continues to be a major public health problem in the United States and many other parts of the world. Accordingly, novel therapeutic approaches, including chemopreventive measures, are urgently needed (Madka and Rao, 2013). *Cannabis* extracts and pCBs have demonstrated direct anti-tumoural effects and are also used in cancer patients to stimulate appetite as well as antiemetics (Fowler *et al.*, 2010; Carter *et al.*, 2011; Pertwee, 2012; Velasco *et al.*, 2012; Massi *et al.*, 2013).

We have investigated here the intestinal anti-tumoural effects of CBG and CBG as well as of a *Cannabis* extract with high content in CBD, here named CBD BDS. Relevant for the present investigation are the observation that both CBD and CBG: i) displayanti-inflammatory effects in the gut [Borrelli *et al.*, 2009; Jamontt *et al.*, 2010, (see also results reported above)], a pertinent observation in the light of the well-known association existing between intestinal inflammation and colorectal cancer (Terzić *et al.*, 2010); ii) inhibit the metabolism of

endocannabinoids (Izzo *et al.*, 2009; De Petrocellis *et al.*, 2011), which exert antitumoural effects in the gut (Izzo and Camilleri, 2009); iii) inhibit cell growth in a number of cell lines, including colorectal cancer cells (Ligresti *et al.*, 2006). Furthermore ,CBD BDS is one of the main components of Sativex (Nabiximols in the USA), a cannabinoid formulation which has been shown to provide a protection against chemotherapy-induced nausea and vomiting (Duran *et al.*, 2010) and has been proposed as a useful add-on analgesic for patients with opioid-refractory cancer pain (Johnson *et al.*, 2010; Portenoy *et al.*, 2012; Johnson *et al.*, 2013). In this work, we have demonstrated that CBD, CBD BDS and CBG exerted protective effects in experimental models of colon carcinogenesis.

5.2.1 Effect of CBD, CBD BDS and CBG on experimental colon carcinogenesis in vivo

We have evaluated the effect of the pCBs in two experimental models of colon cancer, *i.e.*, the AOM model, which is useful for the study of chemopreventive substances and the xenograft model, which is more appropriate for the evaluation of curative effects. AOM is a potent carcinogen causing a high incidence of colon cancer in rodents and its development closely mirrors the pattern seen in humans. The AOM colon cancer model is extensively used in the study of the underlying mechanisms of human sporadic colon cancer (Chen and Huang, 2009). The xenograft model of colon cancer used in the present work is generated by the implantation of colorectal cancer cells into nude mice.

We have shown here that CBD, CBD BDS and CBG exerted beneficial effects in AOM-treated mice. More specifically, we found that: i) CBD, at the dose of 1 mg/kg, exerted an optimal chemopreventive effect, being able to significantly reduce ACF, polyps and tumours. At the highest 5 mg/kg dose, it prevented the formation of polyps only; ii) CBD BDS (5 mg/kg) significantly reduced the formation of ACF and polyps; tumours formation was reduced by 40%, although a statistical significance was not achieved; iii) CBG, at the 5 mg/kg dose,

completely abrogated the formation of ACF and reduced by one half the number of tumours induced by AOM in mice. Furthermore, daily injection with pCBs resulted in a reduction of the tumour growth in the xenograft model of colon cancer. Collectively, such results highlight the potential chemopreventive and curative effect of the investigated pCBs.

CBD was evaluated more in depth. For this cannabinoid, we evaluated the *ex vivo* intestinal biochemical changes (*i.e.* caspase-3, phospho-Akt, iNOS, COX-2 evaluations) associated to its chemopreventive effect. We found that the protective effect of CBD on colon carcinogenesis was associated to up-regulation of the active fragment of caspase-3, *i.e.* one of the major final effectors of the apoptotic process (Kim, 2005). Proapoptotic mechanisms induced by CBD have been previously documented in human breast carcinoma and glioma cells (Ligresti *et al.*, 2006; Massi *et al.*, 2006).When we investigated the potential role of the phosphoinositide3-kinase (PI3K)/Akt pathway, which is crucial for the regulation of cell growth, migration, differentiation, and apoptosis (Sheng *et al.*, 2003; Wang *et al.*, 2001), we found that CBD counteracted AOM-induced up-regulation of the phosphorylated form of Akt protein. These data are suggestive of an involvement of the PI3K-Akt survival signalling cascade in CBD-induced protective effect. Interestingly, Greenhough and colleagues found that the psychotropic cannabinoid Δ^9-THC, *via* CB_1 activation, induced apoptosis in colorectal cancer cells and that its protective effect also involved inhibition of the PI3K-Akt survival signaling cascade. Finally, we found that CBD did not change the overexpression of COX-2 and iNOS, two key enzymes involved in colon carcinogenesis (Rao, 2004; Wu *et al.*, 2010). Likewise, the protective effect of CBD against glioma *in vivo* was not associated with changes in COX-2 activity in glioma tumour tissues (Kim, 2005). We have previously shown that the anti-inflammatory effect of CBD in the gut is associated with down-regulation ofiNOS, but not COX-2, expression (Borrelli *et al.*, 2009).

5.2.2 Effect of CBD, CBD BDS and CBG on colorectal cancer cell growth

In order to give further insights into the antitumoural actions observed *in vivo*, we investigated the effect of these phytocannabinoids on several colorectal carcinoma cell lines.

Cannabidiol (CBD)

CBD is known to exert antiproliferative effects in different tumour cell lines (Massi *et al.*, 2006; Ligresti *et al.*, 2006). In the present thesis, we have shown that this compound, at not-cytotoxic concentrations, exerts antiproliferative effects in three different colorectal carcinoma cell lines, *i.e.* Caco-2, HCT116 and DLD-1 cells. To evaluate the target(s) downstream the *in vitro* effect of CBD, we investigated, in Caco-2 cells, the potential involvement of: (1) cannabinoid receptors, because CBD may increase endocannabinoid levels (De Petrocellis *et al.*, 2011; Izzo and Camilleri, 2009), which, in turn, may exert antiproliferative effects *in vitro via* cannabinoid receptor activation (Ligresti *et al.*, 2003); (2) TRPV1, because CBD may directly activate this ion channel; in addition, anandamide, an endogenous TRPV1 ligand (De Petrocellis *et al.*, 2011), is elevated in the AOM model of colon cancer (Izzo *et al.*, 2008), as well as in biopsies of patients with colon cancer (Ligresti *et al.*, 2003); (3) PPARγ, because cannabidiol may activate PPARγ and PPARγ agonists exert protective effect in colon carcinogenesis (O'Sullivan *et al.*, 2009). Our data show that the antiproliferative effect of CBD was counteracted by rimonabant and AM251 (two CB_1 receptor antagonists), capsazepine (a TRPV1 receptor antagonist) and GW9662 (a PPARγ receptor antagonist), thus suggesting that this non-psychotropic phytocannabinoid may exert anti-cancer effects *in vitro* through multiple mechanisms. In line with our results, it has been demonstrated that CBD reduces intestinal permeability in Caco-2 cells in a CB_1 and TRPV1 antagonist-sensitive manner (Alhamoruni *et al.*, 2010). Because CBD does not bind CB_1 receptors with high affinity, the reversal by the CB_1 antagonists could be explained by indirect activation of such receptors, *e.g. via*

enhancement of endocannabinoid(s) in colorectal carcinoma cell lines. In support of this hypothesis, CBD increased 2-AG levels in Caco-2 cells. In addition, anandamide levels appeared to be increased with this concentration of CBD although in a non-statistically significant manner. Although FAAH is not the primary enzyme involved in 2-AG metabolism (Di Marzo, 2008), it has been previously demonstrated, in both Caco-2cells and colon of AOM-treated mice (Izzo *et al.*, 2008; Izzo and Camilleri, 2009), that arachidonoyl-serotonin, another FAAH inhibitor, increases the content of both anandamide and 2-AG.

Finally, using the single cell electrophoretic assay (Comet assay), a widely accepted tool for investigating DNA damage, we have demonstrated that CBD was unable to induce DNA damage and, more importantly, whereas it exerted protective effects against hydrogen peroxide induced DNA damage. These results are of interest because DNA mutation is a crucial step in carcinogenesis and oxidatively derived DNA lesions have been observed in many tumours, where they are strongly implicated in the etiology of colon cancer.

Cannabidiol botanical drug substance (CBD BDS)

CBD BDS is one of the main components of Sativex (Nabiximols in the USA), a cannabinoid formulation actually used for the treatment of pain and spasticity associated with multiple sclerosis. CBD BDS is a mixture containing many pCBs (mainly CBD) together with other pCBs, such as THC (see Figure 5). Because CBD, the main component of CBD BDS, exerts antiproliferative actions in colorectal cancer cells (see results discussed above), we compared the antiproliferative effect of CBD BDS and pure CBD in colorectal cancer cells, such as DLD-1 and HCT116 cells. As expected, both pure CBD and CBD BDS exerted antiproliferative effects. Importantly, the effect of both CBD BDS and CBD was selective for tumoural cells, as the phytocannabinoid and the *Cannabis extract* did not show antiproliferative effects in healthy human epithelial cells. In contrast to other assays (Comelli *et al.*, 2008; Capasso *et al.*, 2011),

there was no significant difference in potency and efficacy between CBD BDS and pure CBD. In agreement with the results obtained in Caco-2 cells (see above), we found that the antiproliferative effect of CBD in DLD-1 cells was counteracted by selective cannabinoid CB_1 - but not CB_2 - receptor antagonists, suggesting an involvement of CB_1 receptors *via* enhancement of endocannabinoids levels. When we evaluated the pharmacological effect of CBD BDS, we found that its action on cell proliferation was sensitive to both CB_1 and CB_2 receptor antagonists, thus suggesting that CBD and CBD BDS have a different mode of action. In order to give insights into the observed different mode of action, we compared the cannabinoid receptor binding of CBD BDS to that of pure CBD. In $hCB_1$and hCB_2 transfected CHO cells, we found that CBD BDS showed greater affinity than pure CBD for both CB_1 and CB_2 receptors. Pure CBD had little affinity for either CB_1 or CB_2 receptors, with only the concentration of 10 µM exhibiting any significant binding. Among the other pCBs contained in CBD BDS (see Figure 5 and Table 1), THC has been shown to be a potent CB_1 and CB_2 receptor agonist, CBN has a weak partial agonist activity at the CB_1 receptor and moderate partial agonist activity at the CB_2 receptor and CBG has been shown to be a weak ligand at both CB_1 or CB_2 receptors (Pertwee, 2005; Pertwee, 2008; Cascio *et al.*, 2010; Pollastro *et al.*, 2011). Together, these binding data suggest that the presence of both THC (contained in CBD BDS at a 2.4% concentration) and to a very less extent CBN (present in CBD BDS at a 0.1% concentration) could account for the ability of CBD BDS to displace [^{3}H]CP55940 with higher affinity than pure CBD. It is also noteworthy that CBD BDS most probably shares the ability of CBD to activate cannabinoid receptors indirectly by increasing the levels of endogenously released endocannabinoids, as showed above.

Cannabigerol (CBG)

To investigate the effect of CBG on colorectal cancer cell growth, we adopted a different approach, *i.e.* we compared the effect of this phytocannabinoid on cell growth on tumoural *vs* healthy cells. Experiments were performed in the presence of low serum concentrations, because there is evidence in the literature that the effect of phytocannabinoids on tumoural cells viability is increased with a low serum proteins concentration (De Petrocellis *et al.*, 2013). We found that CBG reduced viability in two colorectal carcinoma cell lines. Importantly, the effect of CBG was rather selective for colorectal carcinoma cells, showing that the phytocannabinoid has a very low inhibitory action on healthy human colonic epithelial cells. In order to investigate the mode of CBG action, we considered a number of receptors (*i.e.* cannabinoid receptors, TRPA1, TRPV1 and TRPV2 channels, and $5HT_{1A}$ receptors) which have been shown, based on pharmacodynamic studies, to be targeted by CBG. It is well established that CB_1 or CB_2 receptor activation results in inhibition of colorectal cell growth (Ligresti *et al.*, 2003; Izzo and Coutts, 2005; Izzo and Camilleri, 2009). CBG has been shown to behave as a weak partial agonist of CB_1 and CB_2 receptors (Cascio *et al.*, 2010). Furthermore, CBG inhibits the reuptake of endocannabinoids, which have been detected in Caco-2 cells (as reported above) and thus might indirectly activate – *via* increased extracellular endocannabinoid levels – the cannabinoid receptors. We have here observed that the inhibitory effect of CBG on cell viability was unaffected by the selective CB_1 receptor antagonist AM251 and further increased by the CB_2 receptor antagonist AM630. Such results negate the possibility that CBG acts *via* direct or indirect activation of cannabinoid receptors and rather suggest that an endogenous CB_2 tone exists, which may couple negatively to the CBG signalling pathway leading to the inhibition of cell viability. A similar result has been observed also in peritoneal macrophages (as discussed above), where the inhibitory effect of CBG on

LPS-stimulated nitrite production was further augmented by SR 144528, another CB_2 receptor antagonist.

TRP channels form a superfamily of proteins which affect several pathological processes, including the fate of cancer cells (Shapovalov *et al.*, 2001; Gkika and Prevarskaya, 2009; Santoni *et al.*, 2011). CBG has been shown to behave as a relatively potent and highly effective TRPA1 agonist and a weak agonist at TRPV1 and TRPV2 channels (De Petrocellis *et al*., 2011; De Petrocellis *et al.*, 2012). However, it is unlikely that CBG acts via activation of TRPA1 and/or TRPV2 channels since ruthenium red, a non-selective TRP channel antagonist, at concentrations which were several fold higher than the IC_{50} able to block TRPA1/TRPV1-2 channels, did not modify the effect of CBG on cell viability. It has been reported than CBG is an antagonist of TRPM8 (De Petrocellis *et al.*, 2011), which is involved in the regulation of cell proliferation/apoptosis (Prevarskaya *et al.*, 2007) and it is now considered as a promising target for cancer, particularly for prostate cancer. TRPM8 mRNA has been detected in a number of primary tumours, including colorectal cancer tissues (Tsavaler *et al.*, 2001). Our results showed that TRPM8 mRNA was expressed in colorectal cancer cells and, more importantly, that the effect of CBG on cell viability was mimicked by the synthetic TRPM8 antagonist AMTB, by cannabidiol and cannabidivarin (two phytocannabinoids which share the ability of CBG to block the TRPM8). By contrast, cannabichromene, a phytocannabinoid which does not block the TRPM8 (De Petrocellis *et al.*, 2011) had a negligible effect on colorectal cell viability. Additionally, CBG exerted a very weak cytotoxic effect in healthy human colonic epithelial cells, in which TRPM8 mRNA is faintly expressed. Collectively, such results suggest that TRPM8 might be involved in CBG-induced inhibition of colorectal cancer cell growth. Finally, it is very unlikely that the effect of CBG is due to the block of $5\text{-}HT_{1A}$, a receptor involved in

carcinogenesis (Dizeyi *et al.*, 2004), since CBG effect was not mimicked by a well-established selective 5-HT_{1A} antagonist.

Apoptosis and necrosis are the two major processes leading to cell death (Maghsoudi *et al.*, 2012). Previous investigators have shown that endogenous and plant cannabinoids can induce apoptosis in cancer cells (Galve-Roperh *et al.*, 2000; Jacobsson *et al.*, 2001). However, to date, no information for CBG exists. By using eosin-haematoxylin staining, we have shown that the inhibitory effect of CBG on cell growth was due to apoptosis induction rather than necrosis, a result which was confirmed by an enzymatic assay showing an increased activity of caspase 3 and 7, two cysteine proteases specifically involved in apoptosis (Kumar, 2009), in CBG treated cells. Finally, we investigated the possible involvement of ROS in CBG-induced inhibition of tumoural cell growth. ROS are highly reactive molecules, generally derived from the normal metabolism of oxygen, that are produced primarily in mitochondria. Although basal ROS levels are considered to be physiological regulators of cell proliferation and differentiation, in balance with biochemical antioxidants, high levels of ROS triggers a series of mitochondria-associated events leading to apoptosis (Li *et al.*, 2012; Matés *et al.*, 2012). The relationship between ROS and cancer has been also emphasized by the observation that many chemopreventive agents may be selectively toxic to tumor cells because they increase oxidant stress and enhance ROS generation, which in turn, causes apoptosis of cancer cells (Lee *et al.*, 2013). In the present study, we have shown that CBG, at the same concentration able to exert pro-apoptotic effects, selectively increased ROS production in colorectal cancer cells but not in healthy colonic cells, thus suggesting that ROS overproduction might be implicated in CBG-induced apoptosis.

5.2.3 Conclusions

Our data show that CBD, CBD BDS and CBG hinders the development and the growth of colon carcinogenesis *in vivo*, by exerting both chemopreventive (in the AOM model of colon cancer) and curative (*vs* tumours generated by xenograft injection of colorectal cancer cells) effects. Data on colorectal cancer cells suggest that CBD, CBD BDS and CBG inhibit cell growth in tumoural - but not in healthy - intestinal cells. CBD BDS and CBD exerted cannabinoid-mediated antiproliferative effects, with CBD being able to increase endocannabinoids levels. More in depth studies on CBD revealed that this phytocannabinoid protected DNA damage caused by an oxidative insult and exerted antiproliferative effects through multiple mechanisms, including involvement of CB_1 receptors, TRPV1 and PPAR-γ. CBG also inhibited the growth of colorectal cancer cells, but with a mechanism not involving activation of cannabinoid receptors, although CBG effect was further increased by a CB_2 receptor antagonist. CBG acted *via* a pro-apoptotic mechanism, and its effect on tumoural cell growth was associated to overproduction of ROS. Notably, the inhibitory effect of CBG on cell growth was mimicked by other TRPM8 antagonists, thus suggesting that such receptor might be, at least in part, involved in its actions

6.0 Conclusions

There is anecdotal evidence for the therapeutic benefit of *Cannabis* in a variety of human gastrointestinal disease conditions, that spans over many centuries. For example, some IBD patients anecdotally report that they experience relief by smoking marijuana. Additionally, *Cannabis* and isolated cannabinoids have been used in cancer patients to stimulate appetite and as antiemetics. Phytocannabinoids include about 100 phytocannabinoids, accumulated in tiny epidermal resinous glands of the *Cannabis* plant and characterized, in most instances, by specific and potent pharmacological activities. However, most of the cannabinoids in *Cannabis sativa* have not been fully evaluated for their pharmacological activity. The results reported in this work supports the notion that the *Cannabis* plant is a treasure trove of potentially novel therapeutic agents for gastrointestinal diseases, including IBD and colon cancer. Briefly, we have shown that:

1. The non-psychotropic *Cannabis* ingredient CBG, CBC and THCV exert protective effects in a murine experimental model of IBD. In peritoneal macrophages the three phytocannabinoids inhibited NO production, an effect associated to inhibition of iNOS expression for CBG and THCV (but not for CBC). Studies aiming at investigating the mode of action of the phytocannabinoids revealed that the effect of THCV involves direct activation of CB_2 receptors. By contrast, an endogenous cannabinoid ‘‘tone’’ at CB_1 and CB_2 receptors is likely coupled negatively to CBC and CBG anti-inflammatory actions, respectively.

2. CBD, CBD BDS (a *Cannabis* extract with high content in CBD) and CBG exert chemopreventive curative effects in experimental models of colon cancer. Importantly, the phytocannabinoids/extract under investigation inhibited cell growth in tumoural - but not in healthy intestinal - cells. CBD BDS and CBD exerted cannabinoid-mediated antiproliferative effects via cannabinoid-mediated mechanisms, with TRPV1 and PPAR-γ possibly involved in

the antiproliferative action of CBD. By contrast, CBG inhibited the growth of colorectal cancer cells, but with a mechanism not involving activation of cannabinoid receptors, although CBG effect, similarly to the action on macrophages, was negatively modulated by cannabinoid CB_2 receptors. Notably, the inhibitory effect of CBG on cell growth was mimicked by other TRPM8 antagonists, thus suggesting that such receptor might be, at least in part, involved in its actions.

On the whole, these results could provide a pharmacological basis to explain, at least in part, the beneficial effects of *Cannabis* preparations observed in IBD and possibly in cancer patients. In a therapeutic prospective, the use of non-psychoactive plant cannabinoids appears to be a promising approach because their use is not associated to the unwanted side effects derived from activation of brain CB1 receptors. In the light of their safety records, it is believed that the non-psychotropic phytocannabinoids evaluated in this work might be considered as good candidates to be clinically evaluated for the prevention and/or treatment of IBD and colon cancer.

7.0 REFERENCES

Abraham C, Cho JH. Inflammatory bowel disease. N Engl J Med. 2009;361:2066-2078.

Alexander SP, Benson HE, Faccenda E, Pawson AJ, Sharman JL, Catterall WA, Spedding M, Peters JA, Harmar AJ; CGTP Collaborators. The Concise Guide to PHARMACOLOGY 2013/14: ion channels. Br J Pharmacol. 2013;170:1607-51.

Alhamoruni A, Lee AC, Wright KL, Larvin M, O'Sullivan SE. Pharmacological effects of cannabinoids on the Caco-2 cell culture model of intestinal permeability. J Pharmacol Exp Ther. 2010;335:92–102.

Alhamoruni A, Wright KL, Larvin M, O'Sullivan SE. Cannabinoids mediate opposing effects on inflammation-induced intestinal permeability. Br J Pharmacol. 2012;165:2598-2610.

Alhouayek M, Muccioli GG. The endocannabinoid system in inflammatory bowel diseases: from pathophysiology to therapeutic opportunity. Trends Mol Med. 2012;18:615-625.

Andersen SN, Rognum TO, Bakka O, Clausen OP. Ki-67: a useful marker for the evaluation of dysplasia in ulcerative colitis. Mol Pathol. 1998;51:327-332.

Aviello G, Rowland I, Gill CI, Acquaviva AM, Capasso F, McCann M, Capasso R, Izzo AA, Borrelli F. Antiproliferative effect of rhein, an anthraquinone isolated from Cassia species, on Caco-2 human adenocarcinoma cells. J Cell Mol Med. 2010;14:2006–2014.

Aviello G, Borrelli F, Guida F, Romano B, Lewellyn K, De Chiaro M, Luongo L, Zjawiony JK, Maione S, Izzo AA, Capasso R. Ultrapotent effects of salvinorin A, a hallucinogenic compound from Salvia divinorum, on LPS-stimulated murine macrophages and its anti-inflammatory action in vivo. J Mol Med (Berl). 2011;89:891-902.

Baek SH, Kim YO, Kwag JS, Choi KE, Jung WY, Han DS. Boron trifluoride etherate on silica-A modified Lewis acid reagent (VII). Antitumor activity of cannabigerol against human oral epitheloid carcinoma cells. Arch Pharm Res. 1998;21:353-356.

Barbara G, Xing Z, Hogaboam CM, Gauldie J, SM Collins. Interleukin 10 gene transfer prevents experimental colitis in rats. Gut. 2000;46:344-349.

Blonski W, Buchner AM, Lichtenstein GR. Inflammatory bowel disease therapy: current state-of-the-art. Curr Opin Gastroenterol. 2011;27:346-357.

Bolognini D, Costa B, Maione S, Comelli F, Marini P, Di Marzo V, Parolaro D, Ross RA, Gauson LA, Cascio MG, Pertwee RG. The plant cannabinoid Delta9-tetrahydrocannabivarin can decrease signs of inflammation and inflammatory pain in mice. Br J Pharmacol. 2010;160:677-687.

Borrelli F, Aviello G, Romano B, Orlando P, Capasso R, Maiello F, Guadagno F, Petrosino S, Capasso F, Di Marzo V, Izzo AA. Cannabidiol, a safe and non-psychotropic ingredient of the marijuana plant Cannabis sativa, is protective in a murine model of colitis. J Mol Med (Berl). 2009;87:1111-1121.

Brightbill HD, Plevy SE, Modlin RL, Smale ST (2000). A prominent role for Sp1 during lipopolysaccharide-mediated induction of the IL-10 promoter in macrophages. J Immunol. 2000;164:1940–1951.

Brizzi A, Brizzi V, Cascio MG, Bisogno T, Siriani R, Di Marzo V. Design, synthesis, and binding studies of new potent ligands of cannabinoid receptors J Med Chem. 2005;48:7343–7350.

Brown I, Cascio MG, Wahle KW, Smoum R, Mechoulam R, Ross RA , Pertwee RG, Heys SD. Cannabinoid receptor-dependent and -independent anti-proliferative effects of omega-3 ethanolamides in androgen receptor-positive and -negative prostate cancer cell lines. Carcinogenesis. 2010;31:1584-1591.

Burisch J, Munkholm P. Inflammatory bowel disease epidemiology. Curr Opin Gastroenterol. 2013;29:357-362.

Burstein SH, Zurier RB. Cannabinoids, endocannabinoids, and related analogs in inflammation. AAPS J. 2009;11:109-119.

Capasso R, Borrelli F, Aviello G, Romano B, Scalisi C, Capasso F, Izzo AA. Cannabidiol, extracted from Cannabis sativa, selectively inhibits inflammatory hypermotility in mice. Br J Pharmacol. 2008;154:1001-1008.

Capasso R, Aviello G, Borrelli F, Romano B, Ferro M, Castaldo L, Montanaro V, Altieri V, Izzo AA. Inhibitory effect of standardized cannabis sativa extract and its ingredient cannabidiol on rat and human bladder contractility. Urology. 2011;77:1006.e9-1006.e15.

Carter GT, Flanagan AM, Earleywine M, Abrams DI, Aggarwal SK, Grinspoon L. Cannabis in palliative medicine: improving care and reducing opioid-related morbidity. Am J Hosp Palliat Care. 2011;28:297-303.

Cascio MG, Gauson LA, Stevenson LA, Ross RA, Pertwee RG. Evidence that the plant cannabinoid cannabigerol is a highly potent alpha2-adrenoceptor agonist and moderately potent 5HT1A receptor antagonist. Br J Pharmacol. 2010;159:129-141.

Chen J, Huang XF. The signal pathways in azoxymethane-induced colon cancer and preventive implications. Cancer Biol Ther. 2009;8:1313-1317.

Cianchi F, Papucci L, Schiavone N, Lulli M, Magnelli L, Vinci MC, Messerini L, Manera C, Ronconi E, Romagnani P, Donnini M, Perigli G, Trallori G, Tanganelli E, Capaccioli S, Masini E. Cannabinoid receptor activation induces apoptosis through tumor necrosis factor alpha-mediated ceramide de novo synthesis in colon cancer cells. Clin Cancer Res. 2008;14:7691-7700.

Cluny NL, Naylor RJ, Whittle BA, Javid FA. The effects of cannabidiolic acid and cannabidiol on contractility of the gastrointestinal tract of Suncus murinus. Arch Pharm Res. 2011;34:1509-1517.

Comelli F, Giagnoni G, Bettoni I, Colleoni M, Costa B. Antihyperalgesic effect of a Cannabis sativa extract in a rat model of neuropathic pain: mechanisms involved. Phytother Res. 2008;22:1017-1024.

Cosnes J, Gower-Rousseau C, Seksik P, Cortot A. Epidemiology and natural history of inflammatory bowel diseases. Gastroenterology. 2011;140:1785-1794.

Cunningham D, Atkin W, Lenz HJ, Lynch HT, Minsky B, Nordlinger B, Starling N. Colorectal cancer. Lancet. 2010;375:1030-1047.

D'Argenio G, Valenti M, Scaglione G, Cosenza V, Sorrentini I, Di Marzo V. Up-regulation of anandamide levels as an endogenous mechanism and a pharmacological strategy to limit colon inflammation. FASEB J. 2006;20:568–570.

Danese S, Fiocchi C. Etiopathogenesis of inflammatory bowel diseases. World J Gastroenterol. 2006;12:4807-4812

De Filippis D, Esposito G, Cirillo C, Cipriano M, De Winter BY, Scuderi C, Sarnelli G, Cuomo R, Steardo L, De Man JG, Iuvone T. Cannabidiol reduces intestinal inflammation through the control of neuroimmune axis. PLoS One. 2011;6:e28159.

de Meijer EP, Bagatta M, Carboni A, Crucitti P, Moliterni VM, Ranalli P, Mandolino G. The inheritance of chemical phenotype in Cannabis sativa L. Genetics. 2003;163:335-346.

de Meijer EPM, Hammond KM. The inheritance of chemical phenotype in Cannabis sativa L. (II): cannabigerol predominant plants. Euphytica. 2005;145:189–198.

de Meijer EPM, Hammond KM, Sutton A. The inheritance of chemical phenotype in Cannabis sativa L. (IV): cannabinoid-free plants. Euphytica. 2009;168:95–112.

De Petrocellis L, Vellani V, Schiano-Moriello A, Marini P, Magherini PC, Orlando P, Di Marzo V. Plant-derived cannabinoids modulate the activity of transient receptor potential channels of ankyrin type-1 and melastatin type-8. J Pharmacol Exp Ther. 2008;325:1007-1015.

De Petrocellis L, Ligresti A, Moriello AS, Allarà M, Bisogno T, Petrosino S, Stott CG, Di Marzo V. Effects of cannabinoids and cannabinoid-enriched Cannabis extracts on TRP channels and endocannabinoid metabolic enzymes. Br J Pharmacol. 2011;163:1479-1494.

De Petrocellis L, Orlando P, Moriello AS, Aviello G, Stott C, Izzo AA, Di Marzo V. Cannabinoid actions at TRPV channels: effects on TRPV3 and TRPV4 and their potential relevance to gastrointestinal inflammation. Acta Physiol (Oxf). 2012;204:255-266.

De Petrocellis L, Ligresti A, Schiano Moriello A, Iappelli M, Verde R, Stott CG, Cristino L, Orlando P, Di Marzo V. Non-THC cannabinoids inhibit prostate carcinoma growth in vitro and in vivo: pro-apoptotic effects and underlying mechanisms. Br J Pharmacol. 2013;168:79-102.

DeLong GT, Wolf CE, Poklis A, Lichtman AH. Pharmacological evaluation of the natural constituent of Cannabis sativa, cannabichromene and its modulation by Δ(9)-tetrahydrocannabinol. Drug Alcohol Depend. 2010;112:126-133.

Di Marzo V. Targeting the endocannabinoid system: to enhance or reduce? Nat Rev Drug Discov. 2008;7:438–455.

Di Marzo V, Capasso R, Matias I, Aviello G, Petrosino S, Borrelli F, Romano B, Orlando P, Capasso F, Izzo AA. The role of endocannabinoids in the regulation of gastric emptying: alterations in mice fed a high-fat diet. Br J Pharmacol. 2008;153:1272-1280.

Dizeyi N, Bjartell A, Nilsson E, Hansson J, Gadaleanu V, Cross N, Abrahamsson PA. Expression of serotonin receptors and role of serotonin in human prostate cancer tissue and cell lines. Prostate. 2004;59:328-336.

Dunn EF, Iida M, Myers RA, Campbell DA, Hintz KA, Armstrong EA, Li C, Wheeler DL. Dasatinib sensitizes KRAS mutant colorectal tumors to cetuximab. Oncogene. 2011;30:561-574.

Duran M, Pérez E, Abanades S, Vidal X, Saura C, Majem M, Arriola E, Rabanal M, Pastor A, Farré M, Rams N, Laporte JR, Capellà D. Preliminary efficacy and safety of an oromucosal standardized cannabis extract in chemotherapy-induced nausea and vomiting. Br J Clin Pharmacol. 2010;70:656-663.

Ekbom A, Helmick C, Zack M, Adami HO. Ulcerative colitis and colorectal cancer. A population-based study. N Engl J Med. 1990;323:1228-1233.

Engel MA, Kellermann CA, Burnat G, Hahn EG, Rau T, Konturek PC. Mice lacking cannabinoid CB1-, CB2-receptors or both receptors show increased susceptibility to trinitrobenzene sulfonic acid (TNBS)-induced colitis. J Physiol Pharmacol. 2010;61:89-97.

Esposito G, Filippis DD, Cirillo C, Iuvone T, Capoccia E, Scuderi C, Steardo A, Cuomo R, Steardo L. Cannabidiol in inflammatory bowel diseases: a brief overview. Phytother Res. 2013;27:633-636.

Evans FJ. Cannabinoids: the separation of central from peripheral effects on a structural basis. Planta Med. 1991;57:S60-S67.

Ferlay J, Parkin DM, Steliarova-Foucher E. Estimates of cancer incidence and mortality in Europe in 2008. Eur J Cancer. 2010;46:765-81.

Fowler CJ, Gustafsson SB, Chung SC, Persson E, Jacobsson SO, Bergh A. Targeting the endocannabinoid system for the treatment of cancer--a practical view. Curr Top Med Chem. 2010;10: 814-827.

Fukuyama R, Niculaita R, Ng KP, Obusez E, Sanchez J, Kalady M, Aung PP, Casey G, Sizemore N. Mutated in colorectal cancer, a putative tumor suppressor for serrated colorectal cancer, selectively represses beta-catenin-dependent transcription. Oncogene. 2008;27:6044-6055.

Galve-Roperh I, Sánchez C, Cortés ML, Gómez del Pulgar T, Izquierdo M, Guzmán M. Anti-tumoral action of cannabinoids: involvement of sustained ceramide accumulation and extracellular signal-regulated kinase activation. Nat Med. 2000;6:313-319.

Gálvez J, Garrido M, Merlos M, Torres MI, Zarzuelo A. Intestinal anti-inflammatory activity of UR-12746, a novel 5-ASA conjugate, on acute and chronic experimental colitis in the rat. Br J Pharmacol. 2000;130:1949-1959.

Gkika D, Prevarskaya N. Molecular mechanisms of TRP regulation in tumor growth and metastasis. Biochim Biophys Acta. 2009;1793:953-958.

Goldblum SE, Wu KM, Jay M. Lung myeloperoxidase as a measure of pulmonary leukostasis in rabbits. J Appl Physiol. 1985;59:1978-1985.

Greenhough A, Patsos HA, Williams AC, Paraskeva C. The cannabinoid delta(9)-tetrahydrocannabinol inhibits RAS-MAPK and PI3K-AKT survival signalling and induces BAD-mediated apoptosis in colorectal cancer cells. Int J Cancer. 2007;121:2172-2180.

Guo J, Zhou AW, Fu YC, Verma UN, Tripathy D, Frenkel EP, Becerra CR. Efficacy of sequential treatment of HCT116 colon cancer monolayers and xenografts with docetaxel, flavopiridol, and 5-fluorouracil. Acta Pharmacol Sin. 2006;27:1375-1381.

Guzman M. Cannabinoids: potential anticancer agents. Nat Rev Cancer. 2003;3:745-755.

Half E, Arber N. Colon cancer: preventive agents and the present status of chemoprevention. Expert Opin Pharmacother. 2009;10:211-219.

Hawiger J. Innate immunity and inflammation: a transcriptional paradigm. Immunol Res. 2001;23:99–109.

Hermanson DJ, Marnett LJ. Cannabinoids, endocannabinoids, and cancer. Cancer Metastasis Rev. 2011;30:599-612.

Hibi T, Ogata H, Sakuraba A. Animal models of inflammatory bowel disease. J Gastroenterol. 2002;37:409-417.

Hill AJ, Williams CM, Whalley BJ, Stephens GJ. Phytocannabinoids as novel therapeutic agents in CNS disorders. Pharmacol Ther. 2012;133:79-97.

Hillard CJ, Edgemond WS, Jarrahian A, Campbell WB. Accumulation of N-arachidonoylethanolamine (anandamide) into cerebellar granule cells occurs via facilitated diffusion. J Neurochem. 1997;69:631-638.

Holley JH, Hadley KW, Turner CE. Constituents of Cannabis sativa L. XI: Cannabidiol and cannabichromene in samples of known geographical origin. J Pharm Sci. 1975;64:892-894.

Ihenetu K, Molleman A, Parsons M, Whelan C. Pharmacological characterization of cannabinoid receptors inhibiting interleukin 2 release from human peripheral blood mononuclear cells. Eur J Pharmacol. 2003;464:207-215.

Ito R, Shin-Ya M, Kishida T, Urano A, Takada R, Sakagami J, Imanishi J, Kita M, Ueda Y, Iwakura Y, Kataoka K, Okanoue T, Mazda O. Interferon-gamma is causatively involved in experimental inflammatory bowel disease in mice. Clin Exp Immunol. 2006;146:330-338.

Izzo AA, Coutts AA. Cannabinoids and the digestive tract. Handb Exp Pharmacol. 2005;168:573-598.

Izzo AA. The cannabinoid CB(2) receptor: a good friend in the gut. Neurogastroenterol Motil. 2007;19:704-708.

Izzo AA, Aviello G, Petrosino S, Orlando P, Marsicano G, Lutz B, Borrelli F,Capasso R, Nigam S, Capasso F, Di Marzo V. Endocannabinoid Research Group. Increased endocannabinoid levels reduce the development of precancerous lesions in the mouse colon. J Mol Med (Berl). 2008;86:89-98.

Izzo AA, Borrelli F, Capasso R, Di Marzo V, Mechoulam R. Non-psychotropic plant cannabinoids: new therapeutic opportunities from an ancient herb. Trends Pharmacol Sci. 2009;30:515-527.

Izzo AA, Camilleri M. Cannabinoids in intestinal inflammation and cancer. Pharmacol Res. 2009;60:117-125.

Izzo AA, Sharkey KA. Cannabinoids and the gut: new developments and emerging concepts. Pharmacol Ther. 2010;126:21-38.

Jacobsson SO, Wallin T, Fowler CJ. Inhibition of rat C6 glioma cell proliferation by endogenous and synthetic cannabinoids. Relative involvement of cannabinoid and vanilloid receptors. J Pharmacol Exp Ther. 2001;299:951-959.

Jamontt JM, Molleman A, Pertwee RG, Parsons ME. The effects of delta-tetrahydrocannabinol and cannabidiol alone and in combination on damage, inflammation and in vitro motility disturbances in rat colitis. Br J Pharmaco. 2010;160:712–723.

Johnson JR, Burnell-Nugent M, Lossignol D, Ganae-Motan ED, Potts R, Fallon MT. Multicenter, double-blind, randomized, placebo-controlled, parallel-group study of the efficacy, safety, and tolerability of THC:CBD extract and THC extract in patients with intractable cancer-related pain. J Pain Symptom Manage. 2010;39:167-179.

Johnson JR, Lossignol D, Burnell-Nugent M, Fallon MT. An open-label extension study to investigate the long-term safety and tolerability of THC/CBD oromucosal spray and oromucosal THC spray in patients with terminal cancer-related pain refractory to strong opioid analgesics. J Pain Symptom Manage. 2013;46:207-218.

Jones NP, Siegle GJ, Proud L, Silk JS, Hardy D, Keljo DJ, Dahl RE, Szigethy E. Impact of inflammatory bowel disease and high-dose steroid exposure on pupillary responses to negative information in pediatric depression. Psychosom Med. 2011;73:151-157.

Kaneko Y, Szallasi A. Transient Receptor Potential (TRP) channels: a clinical perspective. Br J Pharmacol. 2013 (*in press*)

Kargl J, Haybaeck J, Stančić A, Andersen L, Marsche G, Heinemann A, Schicho R. O-1602, an atypical cannabinoid, inhibits tumor growth in colitis-associated colon cancer through multiple mechanisms. J Mol Med (Berl). 2013;91:449-458.

Kim R. Recent advances in understanding the cell death pathways activated by anticancer therapy. Cancer. 2005;103:1551–1560

Klaunig JE, Wang Z, Pu X, Zhou S. Oxidative stress and oxidative damage in chemical carcinogenesis. Toxicol Appl Pharmacol. 2011;254:86-99.

Ko Y, Butcher R, Leong RW. Epidemiological studies of migration and environmental risk factors in the inflammatory bowel diseases. World J Gastroenterol. 2014;20:1238-1247.

Kolios G, Valatas V, Ward SG. Nitric oxide in inflammatory bowel disease: a universal messenger in an unsolved puzzle. Immunology. 2004;113:427-437.

Krawisz JE, Sharon P, Stenson WF. Quantitative assay for acute intestinal inflammation based on myeloperoxidase activity. Assessment of inflammation in rat and hamster models. Gastroenterology. 1984; 87:1344-1350.

Kumar S. Caspase 2 in apoptosis, the DNA damage response and tumour suppression: enigma no more? Nat Rev Cancer. 2009;9:897-903.

Kuthan H, Haussmann HJ, Werringloer J. A spectrophotometric assay for superoxide dismutase activities in crude tissue fractions. Biochem J. 1986;237:175–180.

Lahat A, Lang A, Ben-Horin S. Impact of cannabis treatment on the quality of life, weight and clinical disease activity in inflammatory bowel disease patients: a pilot prospective study. Digestion. 2012;85:1-8.

Lal S, Prasad N, Ryan M, Tangri S, Silverberg MS, Gordon A, Steinhart H. Cannabis use amongst patients with inflammatory bowel disease. Eur J Gastroenterol Hepatol. 2011;23:891-896.

Lamine F, Eutamène H, Fioramonti J, Buéno L, Théodorou V. Colonic responses to Lactobacillus farciminis treatment in trinitrobenzene sulphonic acid-induced colitis in rats. Scandinavian Journal of Gastroenterology. 2004;39:1250-1258.

Lee JH, Khor TO, Shu L, Su ZY, Fuentes F, Kong AN. Dietary phytochemicals and cancer prevention: Nrf2 signaling, epigenetics, and cell death mechanisms in blocking cancer initiation and progression. Pharmacol Ther. 2013;137:153-171.

Li L, Ishdorj G, Gibson SB. Reactive oxygen species regulation of autophagy in cancer: implications for cancer treatment. Free Radic Biol Med. 2012;53:1399-1410.

Ligresti A, Bisogno T, Matias I, De Petrocellis L, Cascio MG, Cosenza V, D'argenio G, Scaglione G, Bifulco M, Sorrentini I, Di Marzo V. Possible endocannabinoid control of colorectal cancer growth. Gastroenterology. 2003;125:677-687.

Ligresti A, Moriello AS, Starowicz K, Matias I, Pisanti S, De Petrocellis L, Laezza C, Portella G, Bifulco M, Di Marzo V. Antitumor activity of plant cannabinoids with emphasis on the effect of cannabidiol on human breast carcinoma. J Pharmacol Exp Ther. 2006;318:1375-1387.

Liu W, Reinmuth N, Stoeltzing O, Parikh AA, Tellez C, Williams S, Jung YD, Fan F, Takeda A, Akagi M, Bar-Eli M, Gallick GE, Ellis LM. Cyclooxygenase-2 is up-regulated by interleukin-1 beta in human colorectal cancer cells via multiple signaling pathways. Cancer Res. 2003;63:3632-3636.

Lo Verme J, Fu J, Astarita G, La Rana G, Russo R, Calignano A, Piomelli D. The nuclear receptor peroxisome proliferator-activated receptor-alpha mediates the anti-inflammatory actions of palmitoylethanolamide. Mol Pharmacol. 2005;67:15-19.

Madka V, Rao CV. Anti-inflammatory phytochemicals for chemoprevention of colon cancer. Curr Cancer Drug Targets. 2013;13:542-557.

Madsen K. Combining T cells and IL-10: a new therapy for Crohn's disease? Gastroenterology. 2002;123: 2140-2144.

Maghsoudi N, Zakeri Z, Lockshin RA. Programmed cell death and apoptosis—where it came from and where it is going: from Elie Metchnikoff to the control of caspases. Exp Oncol. 2012;34:146-152.

Markowitz SD, Bertagnolli MM. Molecular origins of cancer: molecular basis of colorectal cancer. N Engl J Med. 2009;361:2449–2460.

Massa F, Marsicano G, Hermann H, Cannich A, Monory K, Cravatt BF, Ferri GL, Sibaev A, Storr M, Lutz B. The endogenous cannabinoid system protects against colonic inflammation. J Clin Invest. 2004;113:1202-1209.

Massi P, Vaccani A, Bianchessi S, Costa B, Macchi P, Parolaro D. The non-psychoactive cannabidiol triggers caspase activation and oxidative stress in human glioma cells. Cell Mol Life Sci. 2006;63:2057–2066.

Massi P, Solinas M, Cinquina V, Parolaro D. Cannabidiol as potential anticancer drug. Br J Clin Pharmacol. 2013;75:303-312.

Matés JM, Segura JA, Alonso FJ, Márquez J. Oxidative stress in apoptosis and cancer: an update. Arch Toxicol. 2012;86:1649-1665.

McMahon SB, Wood JN. Increasingly irritable and close to tears: TRPA1 in inflammatory pain. Cell. 2006;124:1123-1125.

Mehmedic Z, Chandra S, Slade D, Denham H, Foster S, Patel AS, Ross SA, Khan IA, ElSohly MA. Potency trends of Δ^9-THC and other cannabinoids in confiscated cannabis preparations from 1993 to 2008. J Forensic Sci. 2010;55:1209-1217.

Moncada S, Palmer RM, Higgs EA. Nitric oxide: physiology, pathophysiology, and pharmacology. Pharmacol Rev. 1991;43:109-142.

Moore KW, de Waal MR, Coffman RL, O'Garra A. Interleukin-10 and the interleukin-10 receptor. Annu Rev Immunol. 2001;19:683–765.

Mosmann T. Rapid colorimetric assay for cellular growth and survival: application to proliferation and cytotoxicity assays. J. Immunol. Methods. 1983;65:55-63.

Naftali T, Lev LB, Yablecovitch D, Half E, Konikoff FM. Treatment of Crohn's disease with cannabis: an observational study. Isr Med Assoc J. 2011;13:455-458.

Naftali T, Bar-Lev Schleider L, Dotan I, Lansky EP, Sklerovsky Benjaminov F, Konikoff FM. Cannabis induces a clinical response in patients with Crohn's disease: a prospective placebo-controlled study. Clin Gastroenterol Hepatol. 2013;11:1276-1280.

Neurath MF, Fuss I, Kelsall BL, Stüber E, Strober W. Antibodies to interleukin 12 abrogate established experimental colitis in mice. J Exp Med. 1995;182:1281-1290.

Osanai M, Nishikiori N, Murata M, Chiba H, Kojima T, Sawada N. Cellular retinoic acid bioavailability determines epithelial integrity: Role of retinoic acid receptor alpha agonists in colitis. Mol Pharmacol. 2007;71:250-258

O'Sullivan SE, Sun Y, Bennett AJ, Randall MD, Kendall DA. Time-dependent vascular actions of cannabidiol in the rat aorta. Eur J Pharmacol. 2009;612:61–68.

Pertwee RG, 2005. Pharmacological actions of cannabinoids. Handb Exp Pharmacol. 2005;168:1-51.

Pertwee RG. The diverse CB1 and CB2 receptor pharmacology of three plant cannabinoids: delta9-tetrahydrocannabinol, cannabidiol and delta9-tetrahydrocannabivarin. Br J Pharmacol. 2008;153:199-215.

Pertwee RG. Targeting the endocannabinoid system with cannabinoid receptor agonists: pharmacological strategies and therapeutic possibilities. Philos Trans R Soc Lond B Biol Sci. 2012;367:3353-3363.

Podolsky DK. Inflammatory bowel disease. N Engl J Med. 2002;347: 417-429.

Pollastro F, Taglialatela-Scafati O, Allarà M, Muñoz E, Di Marzo V, De Petrocellis L, Appendino G. Bioactive prenylogous cannabinoid from fiber hemp (Cannabis sativa). J Nat Prod. 2011;74:2019-2022.

Portenoy RK, Ganae-Motan ED, Allende S, Yanagihara R, Shaiova L, Weinstein S, McQuade R, Wright S, Fallon MT. Nabiximols for opioid-treated cancer patients with poorly-controlled chronic pain: a randomized, placebo-controlled, graded-dose trial. J Pain. 2012;13:438-449.

Prevarskaya N, Zhang L, Barritt G. TRP channels in cancer. Biochim Biophys Acta. 2007;1772:937-946.

Quimby MW. Botany of cannabis sativa. Arch Invest Med (Mex). 1974;5:127-134.

Rao CV. Nitric oxide signaling in colon cancer chemoprevention. Mutat Res. 2004;555:107–119.

Rodrigues NR, Rowan A, Smith ME, Kerr IB, Bodmer WF, Gannon JV, Lane DP. p53 mutations in colorectal cancer. Proc Natl Acad Sci U S A. 1990;87:7555-7559.

Ross RA, Brockie HC, Pertwee RG. Inhibition of nitric oxide production in RAW264.7 macrophages by cannabinoids and palmitoylethanolamide. Eur J Pharmacol. 2000;401:121-130.

Ruhaak LR, Felth J, Karlsson PC, Rafter JJ, Verpoorte R, Bohlin L. Evaluation of the cyclooxygenase inhibiting effects of six major cannabinoids isolated from Cannabis sativa. Biol Pharm Bull. 2011;34: 774-778.

Russo EB. Taming THC: potential cannabis synergy and phytocannabinoid-terpenoid entourage effects. Br J Pharmacol. 2011;163:1344-1364.

Samad TA, Moore KA, Sapirstein A, Billet S, Allchorne A, Poole S, Bonventre JV, Woolf CJ. Interleukin-1beta-mediated induction of Cox-2 in the CNS contributes to inflammatory pain hypersensitivity. Nature. 2011;410:471–475.

Santoni G, Farfariello V, Amantini C. TRPV channels in tumor growth and progression. Adv Exp Med Biol. 2011;704:947-967.

Sargent DJ, Patiyil S, Yothers G, Haller DG, Gray R, Benedetti J, Buyse M, Labianca R, Seitz JF, O'Callaghan CJ, Francini G, Grothey A, O'Connell M, Catalano PJ, Kerr D, Green E, Wieand HS, Goldberg RM, de Gramont A; ACCENT Group. End points for colon cancer adjuvant trials: observations and recommendations based on individual patient data from 20,898 patients enrolled onto 18 randomized trials from the ACCENT Group. J Clin Oncol. 2007;25:4569-4574.

Schicho R, Storr M. Topical and systemic cannabidiol improves trinitrobenzene sulfonic acid colitis in mice. Pharmacology. 2012;89:149-155.

Sewell JL, Inadomi JM, Yee HF Jr. Race and inflammatory bowel disease in an urban healthcare system. Dig Dis Sci. 2010;55:3479-3487.

Shapovalov G, Lehen'kyi V, Skryma R, Prevarskaya N. TRP channels in cell survival and cell death in normal and transformed cells. Cell Calcium. 2011;50:295-302.

Sheng H, Shao J, Townsend CM Jr, Evers BM. Phosphatidylinositol 3-kinase mediates proliferative signals in intestinal epithelial cells. Gut. 2003;52:1472–1478.

Siegel R, Ma J, Zou Z, Jemal A. Cancer statistics, 2014. CA Cancer J Clin. 2014;64:9-29.

Sreevalsan S, Joseph S, Jutooru I, Chadalapaka G, Safe SH. Induction of apoptosis by cannabinoids in prostate and colon cancer cells is phosphatase dependent. Anticancer Res. 2011;31:3799-3807.

Storr MA, Keenan CM, Zhang H, Patel KD, Makriyannis A, Sharkey KA. Activation of the cannabinoid 2 receptor (CB2) protects against experimental colitis. Inflamm Bowel Dis. 2009;15:1678-1685.

Storr M, Emmerdinger D, Diegelmann J, Pfennig S, Ochsenkühn T, Göke B, Lohse P, Brand S. The cannabinoid 1 receptor (CNR1) 1359 G/A polymorphism modulates susceptibility to ulcerative colitis and the phenotype in Crohn's disease. PLoSOne. 2010;5:e9453.

Strober W, Fuss IJ. Proinflammatory cytokines in the pathogenesis of inflammatory bowel diseases. Gastroenterology. 2011;140:1756-1767.

Takahashi M, Wakabayashi K. Gene mutations and altered gene expression in azoxymethane-induced colon carcinogenesis in rodents. Cancer Sci. 2004;95:475-480.

Terzić J, Grivennikov S, Karin E, Karin M. Inflammation and colon cancer. Gastroenterology. 2010;138:2101–2114.

Thapa D, Kang Y, Park PH, Noh SK, Lee YR, Han SS, Ku SK, Jung Y, Kim JA. Anti-tumor activity of the novel hexahydrocannabinol analog LYR-8 in Human colorectal tumor xenograft is mediated through the inhibition of Akt and hypoxia-inducible factor-1α activation. Biol Pharm Bull. 2012;35:924-932.

Tsavaler L, Shapero MH, Morkowski S, Laus R. Trp-p8, a novel prostate-specific gene, is up-regulated in prostate cancer and other malignancies and shares high homology with transient receptor potential calcium channel proteins. Cancer Res. 2001;61:3760-3769.

Turner CE, Elsohly MA. Biological activity of cannabichromene, its homologs and isomers. J Clin Pharmacol. 1981;21:283S-291S.

Velasco G, Sánchez C, Guzmán M. Towards the use of cannabinoids as antitumour agents. Nat Rev Cancer. 2012;12:436-444.

Voskoglou-Nomikos T, Pater JL, Seymour L. Clinical predictive value of the in vitro cell line, human xenograft, and mouse allograft preclinical cancer models. Clin Cancer Res. 2003;9:4227-4239.

Wallace JL, Devchand PR. Emerging roles for cyclooxygenase-2 in gastrointestinal mucosal defense. Br J Pharmacol. 2005;145: 275-282.

Wang Q, Wang X, Hernandez A, Kim S, Evers BM. Inhibition of the phosphatidylinositol 3-kinase pathway contributes to HT29 and Caco-2 intestinal cell differentiation. Gastroenterology. 2001;120:1381–1392.

Wang D, Wang H, Ning W, Backlund MG, Dey SK, DuBois RN. Loss of cannabinoid receptor 1 accelerates intestinal tumor growth. Cancer Res. 2008;68:6468-6476.

Wilkinson JD, Williamson EM. Cannabinoids inhibit human keratinocyte proliferation through a non-CB1/CB2 mechanism and have a potential therapeutic value in the treatment of psoriasis. J Dermatol Sci. 2007;45:87-92.

Wirth PW, Watson ES, ElSohly M, Turner CE, Murphy JC. Anti-inflammatory properties of cannabichromene. Life Sci. 1980;26:1991-1995.

Wolpin BM, Mayer RJ. Systemic treatment of colorectal cancer. Gastroenterology. 2008;134:1296-1310.

Wright KL, Duncan M, Sharkey KA. Cannabinoid CB2 receptors in the gastrointestinal tract: a regulatory system in states of inflammation. Br J Pharmacol. 2008;153:263-270.

Wu WK, Sung JJ, Lee CW, Yu J, Cho CH. Cyclooxygenase-2 in tumorigenesis of gastrointestinal cancers: an update on the molecular mechanisms. Cancer Lett. 2010;295:7–16.

Yoshino T, Nakase H, Honzawa Y, Matsumura K, Yamamoto S, Takeda Y, Ueno S, Uza N, Masuda S, Inui K, Chiba T. Immunosuppressive effects of tacrolimus on macrophages ameliorate experimental colitis. Inflamm Bowel Dis. 2010;16:2022-2033.

Zhang X, Goncalves R, Mosser DM. The isolation and characterization of murine macrophages. Curr Protoc Immunol. 2008;chapter 14:Unit 14.1.

Zoppi S, Madrigal JL, Pérez-Nievas BG, Marín-Jiménez I, Caso JR, Alou L, García-Bueno B, Colón A, Manzanares J, Gómez-Lus ML, Menchén L, Leza JC. Endogenous cannabinoid system regulates intestinal barrier function in vivo through cannabinoid type 1 receptor activation. Am J Physiol Gastrointest Liver Physiol. 2012;302:G565-71.

Zurier RB. Prospects for cannabinoids as anti-inflammatory agents. J Cell Biochem. 2003;88:462-466.